Additive Manufacturing of Shape Memory Polymers: Effects of Print Orientation and Infill Percentage on Mechanical and Shape Memory Recovery Properties

By

Jorge Fernando Villacres

A thesis submitted in partial fulfillment of the requirements for the degree of

Master of Science

Department of Mechanical Engineering

University of Alberta

ABSTRACT

Material Extrusion Additive Manufacturing (MEAM), also known as Fused Deposition Modeling (FDM), is a manufacturing technique in which three-dimensional objects are built. These objects are built by repeatedly extruding thin layers of molten materials through a nozzle in different paths and depositing these layers until the desired object is formed. The shapes are defined by a computer aided design file. This manufacturing technique has become more user friendly and more available over the last decade, thus its uses and applications have risen exponentially. Shape Memory Polymers (SMP) are stimulus responsive materials which have the ability to recover their permanent form after being deformed to a temporary form. In order to induce its shape memory recovery, an external stimulus - such as heat - is needed. The manufacturing of SMP objects through a MEAM process has a vast potential for different applications; however, the mechanical and shape recovery properties of these objects need to be analyzed in detail before any practical application can be developed. As such, this project investigates and reports on the production and characterization of a shape memory polymer (SMP) material filament that is manufactured to print SMP objects using MEAM. To achieve consistent manufactured SMP filament, different parameters of the raw materials were analyzed and a production line for SMP filaments was established. Having a defined filament production line facilitated the manufacture of SMP filaments with consistent characteristics. Additionally, the effects of major printing parameters, such as print orientation and infill percentage, on the mechanical (elastic modulus, ultimate tensile strength and maximum strain) and shape recovery properties of MEAM-produced SMP samples were investigated and outlined. The analyzed shape recovery properties were: recovery force, recovery speed and time elapsed before activation. Results show that print angle and infill percentage do have a significant impact on the mechanical and shape recovery properties of the

manufactured test sample. For elastic modulus, ultimate tensile strength, maximum strain, shape recovery time and shape recovery force an increase in infill percentage increases their value. On the contrary, increasing infill percentage decreases shape recovery speed. Moreover, an increase in print angle decreases elastic modulus and ultimate tensile strength. In contrast, maximum strain shape recovery speed and shape recovery force increased when increasing print angle. Shape recovery time didn't seem affected the change in print angle. Findings can significantly influence the tailored design and manufacturing of smart structures using SMP and MEAM.

Keyword: Fused deposition modelling, Layered manufacturing, Mechanical properties, shape memory polyurethanes, smart materials, Additive manufacturing

ACKNOWLEDGEMENTS

Working in this thesis has been a wonderful as well as challenging experience, which would not have been possible without the guidance and support of many different people around me.

First of all, I would like to thank my supervisors Dr. Cagri Ayranci and Dr. David Nobes for their mentorship throughout this project, for being patient with me and for trusting my abilities to overcome any challenges that appeared through this project.

I would like to thank Irina Garces, Nicolas Olmedo, Coleen Eiman and Kento Osuga for their unconditional moral support and being my family away from home.

I would like to thank my family for always being there for me and always finding the way to make me feel close to home. They are the inspiration behind all my work

Finally, I would like to thank god for all the blessings and lessons he puts in my path.

TABLE OF CONTENTS

LIST OF TABLES

LIST OF FIGURES

1 INTRODUCTION

1.1 Motivation

Additive manufacturing is a manufacturing technique in which three dimensional objects are built by continuously adding and/or fusing layers of materials [1]. Material Extrusion Additive Manufacturing (MEAM), or also known as Fused Deposition Modeling (FDM), is the most common of the additive manufacturing technologies, in which the objects are built by extruding molten polymeric materials through a nozzle onto a platform in different paths and layers defined by a computer aided design (CAD) data file [1, 2]. By using this technology, different parts can be manufactured in a shorter time and with less cost compared to traditional manufacturing processes [1]. Generally, MEAM processes utilize thermoplastic materials. Acrylonitrile butadiene styrene (ABS) and polylactic acid (PLA) are the two most commonly used materials.

Shape Memory Materials (SMM) are characterized by having the ability to recover their original shape after being subject to a deformation. In order to recover their original shape, an external stimulus such as heat need to be applied to the material [3, 4]. Shape memory polymers (SMP) and shape memory alloys (SMA) are the most common types of SMM.

Although there are different SMP with different activation triggers, most SMP activate when heated over its glass transition temperature (Tg) [3 - 6]. The unstrained (permanent) shape of the material can be set by conventional polymer manufacture techniques, such as extrusion or injection molding, and this process can be repeated many times [3, 7]. SMP possesses the advantages of being moldable, lightweight, economical and have a high shape recovery ratio [3, 8]. Given all these characteristics, SMP are currently under extensive research for potential applications such

as light modulator display devices or orthodontic archwires. SMP are transparent, therefore arch wires made from this material are more esthetically pleasing and may provide a suitable alternative to traditional metal archwires [9].

Producing SMP parts by MEAM has great potential for producing different components with shape recovery properties with a broad range of applications, for example SMP stents for biomedical use or micro-aerial vehicles manufactured from SMP. MEAM allows the components to be produced quickly and without the need to additionally produce costly molds. Nevertheless, this process and the mechanical properties of the produced components need to be characterized first in order to obtain reliable and consistent results. This project reports on the production process for creating printed SMP samples and investigates the print parameters' effects on the elastic, mechanical and shape memory recovery properties of the produced materials.

1.2 Thesis Objectives

The main objective of this thesis is to produce consistent SMP samples through MEAM and analyze the influence of print orientation and infill percentage on the mechanical and shape memory recovery properties of these samples. In order to obtain reliable results, the specimens were tested at 3 different infill percentage levels 50%, 75% and 100%, while print angle were tested at 0°, 30°, 60° and 90°. The mechanical properties examined were elastic modulus, ultimate tensile strength and maximum strain. The shape memory recovery properties analyzed were shape memory recovery speed, recovery activation time and shape memory recovery force. In order to determine whether the change in infill percentage and print angle effect the analyzed properties in a statistically significant matter, t-tests at 95% confidence factor were implemented and executed between all levels.

1.3 Thesis Outline

The thesis is organized into five different chapters. In chapter 2, a brief background information on materials and methods regarding additive manufacturing, fused deposition modeling, shape memory polymer, and filament extrusion are presented. In chapter 3, the influence of print orientation and infill percentage on the mechanical properties is presented. In chapter 4, the influence of print orientation and infill percentage on the shape memory recovery properties is presented. In chapter 5, conclusions from the entire thesis are presented.

1.4 References

[1] O. Mohamed, S. Masood and J. Bhowmik, "Optimization of fused deposition modeling process parameters:," Advanced Manufacture, pp. 42-53, 2015.

[2] B. Wendel, D. Rietzel, F. Kuhnlein and R. Feulner, "Additive Processing of Polymers".

[3] A. Lendlein and S. Kelch, "Shape Memory Polymer," in Shape Memory Effect, Teltow, Wiley, 2002, pp. 2034-2037.

[4] J. Guo, Z. Wang, L. Tong, H. Lv and W. Liang, "Shape memory and thermo-mechanical properties of shape memory," Composites, pp. 162-165, 2015.

[5] H. Tamagawa, "Thermo-responsive two-way shape changeable polymeric laminate," Materials Letters, pp. 749-751, 2010.

[6] M. Hager, S. Bode, C. Weber and U. S. Schubert, "Shape memory polymers: Past, present and future," Progress in Polymer Science, pp. 3-33, 2015.

[7] J. Raasch, M. Ivey, D. Aldrich, D. S. Nobes and C. Ayranci, "Characterization of polyurethane shape memory polymer processed," Additive Manufacturing, pp. 132-141, 2015.

[8] C.-S. Zhang and Q.-Q. Ni, "Bending behavior of shape memory polymer based laminates," composite structures, pp. 153-156, 2005.

[9] H. Meng and G. Li, "A review of stimuli-responsive shape memory polymer composites," Polymer, pp. 2199-2221, 2013.

2 BACKGROUND

2.1 Additive Manufacturing

2.1.1 Description

Additive manufacturing (AM) is the formal name given to the manufacturing technique most commonly known as 3D Printing [1]. The first form of this technique was developed in the 1980's for creating models and prototype parts. The major advantages that this process offers to product manufacturing are the time and cost reduction, human interaction, and the ability to crate customizable and intricate parts [2] This technology was developed as a result of the increase use of 3D computer aided design (CAD) modeling which had been becoming more prevalent and easy to use every day.

The term rapid prototyping (RP) was employed by different industries to refer to AM. However, this term only defined a process through which a prototype of a product could be quickly produced for it to be displayed as a basic representation of a model from which further models and eventually the final product will be derived [1]. Nonetheless, today this term is considered inadequate and does not effectively describe more recent applications of the AM technology. Developments in the quality of the output new AM technologies produce parts which have a much closer link to the final product, therefore these parts can no longer be referred to as prototypes. The major advances that this process has presented through time are: reduced manufacturing time and cost reduction, less human interaction, and higher quality resultant parts [3]. In 2009, American Society for Testing and Materials (ASTM) F42 Technical Committee has agreed that new terminology should be adopted [1]. ASTM consensus standards now use the term additive manufacturing.

2.1.2 Additive Manufacturing Steps

Figure 2-1 shows the sequence and steps taken in AM in order to produce a part [1].

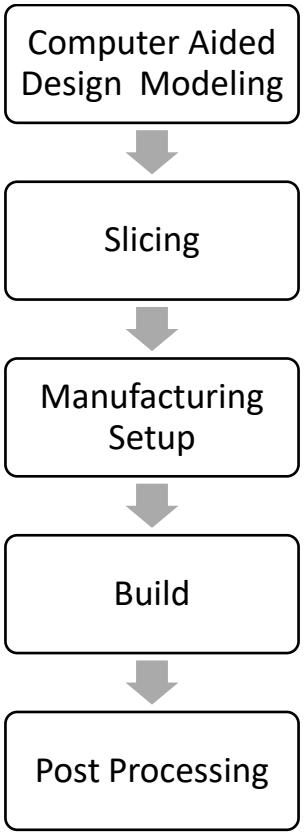

Figure 2-1 Additive Manufacturing Process

2.1.2.1 Computer Aided Design Modeling

The first step to create a manufactured part is to digitally design it. Currently, numerous CAD programs are available to design mechanical and artistical 3D figures [3]. The designed part should be converted to a STL file format. The STL file format describes and external closed surface

version of the original CAD file which is the basis for performing the slicing sequence described in the next step. Nowadays, every CAD system can output such a file format [1].

2.1.2.2 Slicing

To be able to manufacture these digital models through AM, these need to be divided into thin layers of material in a horizontal plane each layer is a thin cross-section of the part derived from the original CAD data [1]. These layers are indexed upwards until all have been combined together and the part is complete. [3] This process is known as 'slicing' and there exist numerous programs available which can perform this task. The thickness of the layers depends on the AM machine capabilities. The thinner each layer is, the closer the final part will be to the original [3]. In Figure 2-2 a dogbone specimen sliced for AM fabrication can be observed.

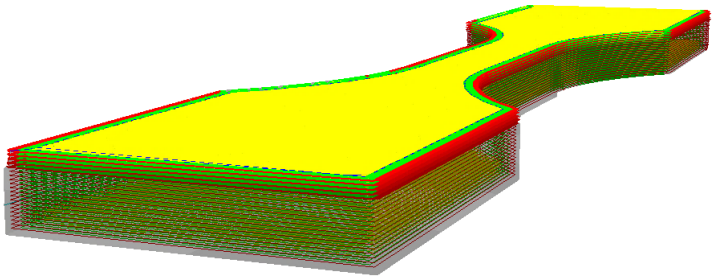

Figure 2-2 Sliced Dogbone Sample

2.1.2.3 Manufacturing setup

There exist different AM methods such as fused deposition modelling (FDM), stereolithography, material jetting among many others. The main difference between these AM technologies is how the layers are created and bonded to each other. The AM technology used can determine factors like the accuracy of the final, employed material, manufacturing speed, the size of the AM machine used cost of the machine and process [1]. Depending on the AM technology used different manufacturing parameters need to be set up. However, there are some common set-up parameters

which all AM technologies have such as: Layer height, infill percentage, printing speed and print material [3].

2.1.2.4 Build

This step consists of the automated process the machine performs to build the parts. For this step only superficial monitoring of the machine is required to avoid any errors [1].

2.1.2.5 Post-Processing

This step often requires time and experienced manual handling. Depending on the employed AM technology, parts may require additional cleaning before they are ready for use. Parts may also be hot or weak and require time to cool off or have supporting features that must be removed [1].

2.2 Fused Deposition Modeling

2.2.1 Description

Fused deposition modeling (FDM) is one type of AM techniques and is the one employed in this project. FDM is by far the most used AM technology. Currently, there are more FDM machines than any other AM machine type in the world [1]. FDM uses filaments of polymeric material which are pushed into a heating chamber by a gear arrangement [1,2]. The heating chamber melts the polymer that is fed into the system. The polymer is then pushed by the incoming filament and extruded through a nozzle that is typically made out of a 0.4 mm opening at its end. The nozzle is attached to a movable mechanism, which travels as the material is being extruded and builds the previously designed layers of material. These layers are added on top of each other and fuse together to build the designed part [1,2,4]. Figure 2-3 displays the different components of the

FDM machine used for this project (Ultimaker 2+) and Table 2-1 presents the general specifications/limitations of this machine.

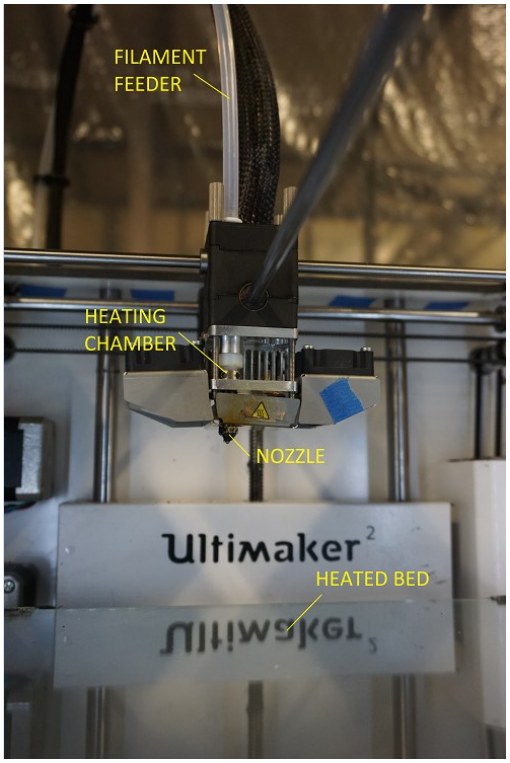

Figure 2-3 FDM Machine Components

Table 2-1 FDM Machine Characteristics [5]

Build Volume	x=223 [mm]; y=223[mm]; z=205 [mm]
Printer Head Travel Speed	30 [mm/s] to 300 [mm/s]
Layer Resolution	0.2 [mm] to 0.02 [mm]
Nozzle Diameter	0.4[mm]
Heat Chamber Power	35 [W]
Nozzle temperature	180 °C to 260 °C

2.2.2 Materials

MEAM processes predominantly employ amorphous polymers because they have no distinct melting point. Furthermore, the material increasingly softens and viscosity lowers with increasing temperatures [1]. Therefore, these polymers can be extruded in the form of a viscous paste. This allows the material to maintain its shape after extrusion, solidify quickly and at the same time bond with the additional layers of material. Additionally, highly crystalline polymers are suitable for powder bed fusion processes [1]. The most common materials used for FDM are polylactic acid (PLA), polycarbonate (PC), acrylonitrile butadiene styrene (ABS) and semi-aromatic polyamides. (Nylon) [2,4].

The main advantages of FDM are:

- Economical machinery and material resulting in a cost-effective process [2]
- No resins to cure and little to none chemical post-processing required [1]
- Strong mechanical properties. Parts made using FDM are among the strongest for any polymer-based additive manufacturing process [4].
- Numerous options of thermoplastic materials can be employed [3].

The main disadvantages of FDM are:

- Resolution on the *z*-axis is low compared to other additive manufacturing process. Thus, if a highly smooth surface is required, post-processing such as the use of solvents that lightly melt the part surface or coatings to achieve the right color and finish on a part are required [2].

- Slow built speed compared to other polymer manufacturing process. As previously described, the system operates with a moving nozzle which needs to provide a low inertia to the material for the material to be accurately positioned. Thus, the speed at which the nozzle can travel is limited [1].
- Nozzles are circular. Hence, sharp corners or edges cannot be manufactured. The minimal radius a corner or an edge can have, is equivalent to the radius of the nozzle [1]
- Manufactured pieces possess anisotropic characteristics. Strength in the *z*-direction is less than the strength in the *x*–*y* plane. Additionally, depending on the type of infill of the manufactured part the strength in the *x* and *y* direction can vary too [1,4].

2.3 Shape Memory Polymer

Shape memory materials possess the main characteristic of having the ability to recover an original preset shape after being subject to a deformation. In order to recover their original shape, an external stimulus, such as heat, magnetic field, UV, or humidity need to be applied to the material [6,7]. This shape recovery movement is associated with deformation stored during deformation [8,9]. Shape memory polymers (SMP) and shape memory alloys (SMA) are the most common types of SMM. SMP which start their shape recovering movement after being heated over its glass transition temperature (Tg) are called thermo-responsive [6,7,10,11].

The preset shape of the material can be established by manufacture techniques, such as extrusion, injection molding or AM and this process can be repeated many times if the chosen polymer is thermoplastic. [9,6,12].

When compared to SMA, SMP has the advantages of being moldable, lightweight, and economical [6,13]. Additionally, SMA have a limit recoverable strains of less than 8% [8] whereas SMP can

reach in excess of 300% strains that can be recoverable. For of all its characteristics, SMP are currently under extensive research for potential applications such as in sensors, actuators, biomedical devices, and the like [8].

2.3.1 Material Specifications and Preprocessing

The raw material used for this work is a semi crystalline thermoplastic polyurethane shape memory polymer (MM4520) that was purchased from SMP Technologies, Japan. The manufacturer specifications show the glass transition temperature (T_g) as 45°C [14]. Table 2-2 presents the material characteristics provided by the manufacturer.

Table 2-2 MM4520 Characteristics [14]

Density (g/cm^3)	1.2
Specific Gravity	1.25
Glass transition temperature Tg (°C)	45
Hardness below Tg (HDD)	76
Hardness above Tg (HDD)	30
Tensile strength below Tg (MPa)	55
Tensile strength above Tg (MPa)	10

The raw material was received in the form of pellets, which needed to be extruded into filaments in order to be fed into the MEAM machine The pellets were dried in a vacuum oven (Thermo Scientific, Lindberg Blue M) prior to the extrusion to form filaments, and their drying characteristics were documented. Drying the pellets before extrusion prevents bubbles from forming inside the filament. Figure 2-4 displays a filament produced without drying the pellets (left) and a filament produced with previously dried pellets. The filaments require to have a diameter of 3mm in order to be processed by the MEAM machine.

Figure 2-4 Filament without material preprocessing (left)/ Filament with material preprocessing (right)

2.4 Filament Extrusion

2.4.1 Description

Polymer extrusion is a manufacturing process in which raw polymer is melted and reshaped into a continuous form with a constant cross section [15].The manufacturing process of polymer filaments through filament extrusion consists of 5 principal stages**.** Feeding, melting, shaping, cooling and winding [15]. Figure 2-5 shows the schematic manufacturing set-up.

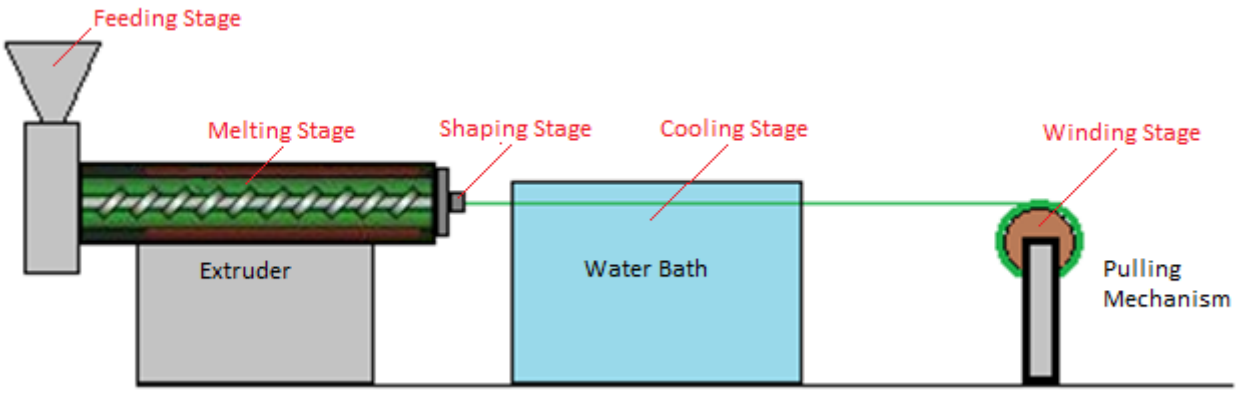

Figure 2-5 Filament manufacturing process

In the first stage, polymer material is placed in a hopper which feeds the barrel of the extruder machine. The raw polymer in the hopper is usually obtained in the form of powders flakes or pellets. [15]

In the melting stage, the polymer is introduced into the barrel. This barrel contains different independently controlled sequential heating zones. The polymer is then pushed by rotating screw at a constant rate through these zones. The heat and the screw rotation gradually melt and advance the polymer down the barrel [15]. In the shaping stage, the molten polymer is forced through a die. The cross section of the exit of the die gives the profile shape of the filament. For the purposes of this work a 3mm diameter die was used. The material that is exiting the die, extrudate, enters the cooling stage. In the cooling stage, the material can be put through different cooling mechanisms. The most common cooling mechanisms used in the industry are temperature controlled water baths, forced air cooling and cooling rolls [16].

In the last stage, the filament is wound on a roller through a pulling mechanism. The pulling mechanism provides a constant take-up speed to the filament that ensures the consistency of the diameter of the filament and avoids any air bubble formation before complete cooling.

2.4.2 Material Extrusion Settings

For this project, dried MM4520 pellets were used in a single screw extruder (Brabender, ATR Plasti-Corder) along with a water bath and a pulling/winding mechanism. The extruder has a 19-mm diameter screw and ran at a rate of 20 rpm. Figure 2-6 displays the extruding machine and its components.

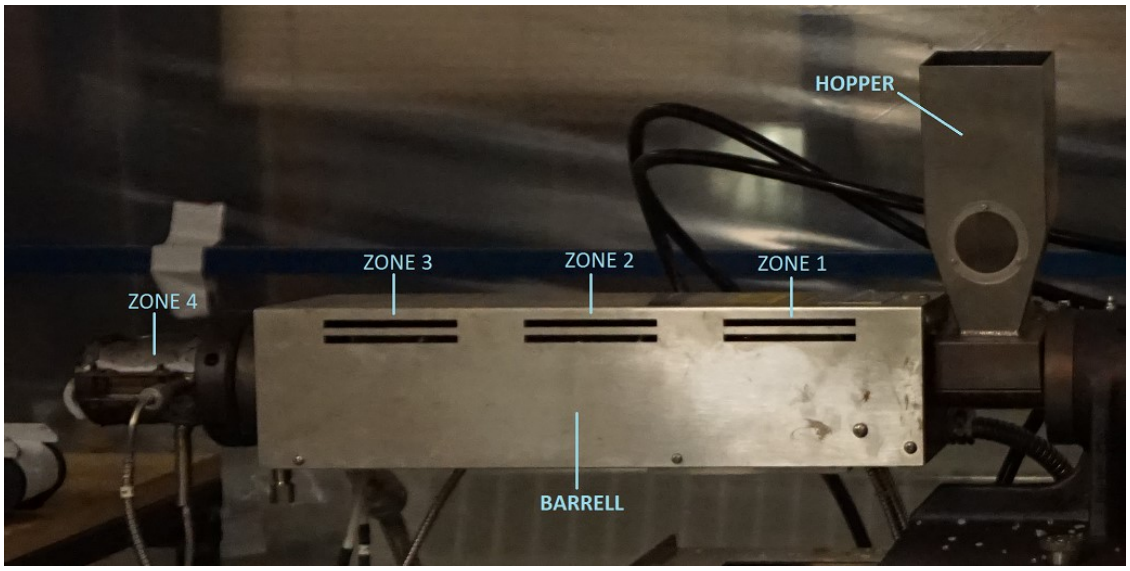

Figure 2-6 Brabender, ATR Plasti-Corder Components

The temperatures of the four chambers of the extruder were set at 170 °C, 180 °C, 190 °C and 195 °°C during the extrusion as it can be seen on Figure 2-7. In this figure, numbers in green represent the set points for the temperature at the 4 different heating zones and the speed of the rotating screw. Similarly, numbers in yellow represent the measured values of the temperature at the 4 different heating zones and the speed of the rotating screw.

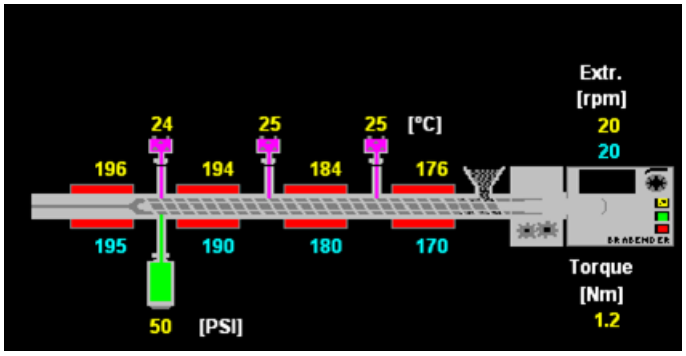

Figure 2-7 Extruder Settings

The extrudate that left the extruder's die was put through a water bath at 15°C to cool it down. This allowed the filament to be wound without sticking together after coming out of the water bath. The winding mechanism helps pulling the filament at a variable speed. While the pulling mechanism is winding the filament, the amount of filament stacked on the spool becomes larger. This increases the diameter of the winding mechanism. Therefore, the winding mechanism needs to rotate at a variable rate to maintain the linear pulling speed constant. In order to achieve this, the rolls pulling the filament stop every time they feel tension. This process keeps the 3-mm diameter constant with a standard deviation of +/-0.15 mm. Additionally, the filament diameter was measured consistently for quality control.

2.5 Material Testing

2.5.1 Tensile Test

This test method is designed according to ASTM D638 – 14 standards [17]. This test is designed to obtain the tensile properties of the tested plastic materials. In this test, specimen is subjected to a controlled strain until failure. For this test to be successful the following factors must be carefully controlled as described in the ASTM D638 standard [17].

- Specimen: The specimen must be a dogbone shaped specimen. Dimensions of this type of specimen can be found in the ASTM D638 standard [17]. For this project type V dogbones were used.

2.6 Statistical Testing: T-Test

The t-test is statistical test which compares two sets of data and defines whether they are significantly different from each other [18]. T-tests take into account the average and the standard deviation of each set of data and compares it to a normal statistical distribution. This statistical distribution varies depending on the confidence level of the analysis. The output value of the t-test comparison is called the p-value [18]. The α value comes from subtracting 1 from the confidence level [18]. For example, for a 95% confidence level t-test the α value would be:

$$\alpha = 1 - 0.95 = 0.05 \qquad \textit{Equation 2-1}$$

To determine whether the two sets of data are statistically different from each other, the resultant p-value needs to be lower than the determined alpha value. In this case, if the resultant p-value is lower than 0.05 we can conclude that the two compared levels are statistically different between each other [18].

2.7 Specimen Analysis Process

The previously defined background information is employed for analyzing the influence of printing angle and infill percentage in the mechanical and shape recovery properties of the SMP specimens. There are two different procedures we can follow when analyzing these specimens, one for analyzing the mechanical properties of the material and one for analyzing the shape memory recovery properties. Figure 2-8 presents the different steps of the specimen analysis

process. Each step has been explained throughout this chapter. Nonetheless, the settings and specifications of every step are covered in the upcoming chapters.

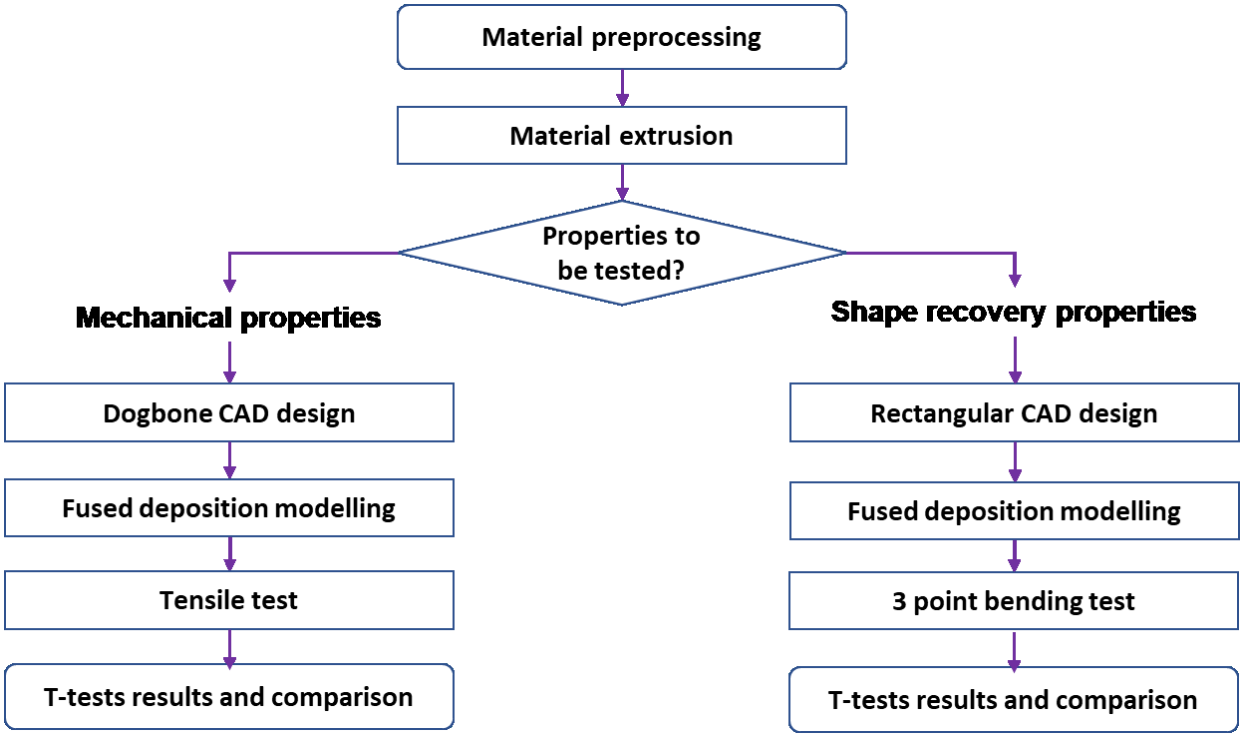

Figure 2-8 Specimen Analysis Steps State of the Art

2.8 State of the Art

Previous work similar in some aspects to the one presented in this thesis has been researched. B.M Tymrak et al [19] analyzed the variation on elastic modulus of ABS and PLA MEAM samples under two different print angles [0/90], [45/-45], and 3 different Layer heights 0.4, 0.3 and 0.2. Results from this research displayed no significant change in elastic modulus when employing different layer heights or print angles for ABS. Nonetheless, for PLA MEAM samples, elastic modulus did show a significant variation. However, these results do not obey a specific trend and

all of the analyzed angles form balanced laminates. Moreover, no statistical analysis or standard deviation of the results is presented either.

Wenzheng Wu et al [20] presents a very similar analysis to Tymrak et al [19]. The analyzed materials in this paper are ABS and PEEK. The elastic modulus of ABS and PEEK samples produced with injection molding is also found in this research. Results showed a variation in elastic modulus when employing different layer heights or print angles for ABS and PEEK. Nevertheless, these results do not obey a specific trend and all of the analyzed angles form a balanced laminate. When comparing the elastic modulus from MEAM and injection molding manufactured samples, ABS samples displayed no difference in elastic modulus. However, PEEK samples manufactured through injection molding displayed a much higher elastic modulus than MEAM PEEK samples. Nonetheless, no statistical analysis or standard deviation of any result is presented.

Yang et al [21]reports on the process of producing SMP filaments. These filaments are extruded under different temperature settings and fed to a MEAM machine. SMP samples are manufactured with these filaments and the quality of the prints is measured by testing surface roughness and density of the parts. Later these parts are deformed and activated but no shape recovery properties are recorded other than pictures of the samples before and after activation.

The main difference of the work presented in this thesis from other previously performed research, relies in the fact that a much deeper analysis of the mechanical and shape recovery properties of the samples is being performed. Additionally, shape recovery properties are tested recorded and compared for all designed levels. Finally, a statistical analysis is performed between every analyzed level and the standard deviation of the results is taken into account. This allows a more reliable analysis of the results and conclusions.

2.9 Conclusions

In this chapter, required background information regarding additive manufacturing was presented and its different steps for producing three-dimensional parts were defined. The additive manufacturing method employed in this thesis is fused deposition modeling. Thus, fused deposition modeling general settings employed for this project were displayed. Furthermore, the general handling methods and performance of shape memory polymers were presented and specific data of the shape memory polymer used for this project (MM4520) was displayed as well. Given that the shape memory polymer was acquired in the form of pellets, a filament extrusion process needed to be designed. The different manufacturing stages in the filament extrusion process were defined as well and the settings used at every stage. Finally, the different experimentation steps used in this project was explained and displayed in a flowchart.

.

2.10 References

[1] I. Gibson, D. Rosen and B. Stucker, Additive Manufacturing Technologies, New York: Springer, 2015.

[2] K. Wong and A. Hernandez, "A Review of Additive Manufacturing," ISRN Mechanical Engineering, vol. 2012, p. 10, 2012.

[3] I. Gibson, "The changing face of additive manufacturing," Journal of Manufacturing Technology Management, vol. 28, no. 1, pp. 10-17, 2017.

[4] H. Chia and B. Wu, "Recent advances in 3D printing of biomaterials," Journal of Biological Engineering, pp. 2-14, 2015.

[5] Ultimaker, "Ultimaker 2+ Specifications," [Online]. [Accessed 06 2016].

[6] A. Lendlein and S. Kelch, "Shape Memory Polymer," in Shape Memory Effect, Teltow, Wiley, 2002, pp. 2034-2037.

[7] J. Guo, Z. Wang, L. Tong, H. Lv and W. Liang, "Shape memory and thermo-mechanical properties of shape memory," Composites, pp. 162-165, 2015.

[8] C. Liu, H. Qin and P. Mather, "Review of progress in shape-memory polymers," Journal of Materials Chemistry, vol. 17, pp. 1543-1558, 2007.

[9] Z. X. Khoo, J. E. M. Teoh, Y. Liu, C. K. Chua, S. Yang, J. An, K. F. Leong and W. Y. Yeong, "3D printing of smart materials: A review on recent progresses in 4D printing," Virtual and Physical Prototyping, vol. 10, no. 3, pp. 103-122, 2015.

[10] H. Tamagawa, "Thermo-responsive two-way shape changeable polymeric laminate," Materials Letters, pp. 749-751, 2010.

[11] M. Hager, S. Bode, C. Weber and U. S. Schubert, "Shape memory polymers: Past, present and future," Progress in Polymer Science, pp. 3-33, 2015.

[12] J. Raasch, M. Ivey, D. Aldrich, D. S. Nobes and C. Ayranci, "Characterization of polyurethane shape memory polymer processed," Additive Manufacturing, pp. 132-141, 2015.

[13] C.-S. Zhang and Q.-Q. Ni, "Bending behavior of shape memory polymer based laminates," composite structures, pp. 153-156, 2005.

[14] SMP Technologies, "Shape Memory Polymer," 2012. [Online]. Available: http://www2.smptechno.com/en/smp/. [Accessed February 2016].

[15] C. Rauwendaal, Polymer Extrusion, Munich: Hanser, 2014.

[16] Z. Tadmor and C. Gogos, Principles of Polymer Processing, Hoboken : Wiley, 2006.

[17] ASTM, "Standard Test Method for Tensile Properties of Plastics," DESIGNATION: D638 - 14, 2015.

[18] D. Montgomery, Design and Analysis of Experiments, Tempe: Wiley, 2013.

[19] B. Tymrak, M. Kreiger and J.M.Pearce, "Mechanical Properties of Components fabricated with open source 3-D printers under realistic environmental conditions," Materials and Design, vol. 58, pp. 242-246, 2014.

[20] W. Wu, P. Geng, G. Li, D. Z. H. Z. and J. Zhao, "Influence of Layer Thickness and Raster Angle on the Mechanical Properties of 3D-Printed PEEK and a Comparative Mechanical Study between PEEK and ABS," Open Access Materials, vol. 8, pp. 5835-5846, 2015.

[21] Y. Yang, Y. Chen, Y. Wei and Y. Li, "3D printing of shape memory polymer for functional part fabrication," Advanced Manufacturing Technologies, 2015.

3 TENSILE PROPERTIES ANALYSIS (*)

(*) A version of this chapter was submitted to Rapid Prototyping Journal as a journal paper with the authors: J. Villacres, D. Nobes, C. Ayranci.

3.1 Introduction

Shape Memory Materials (SMM) are stimulus responsive materials that have the ability to return to an original shape from a programmed temporary shape upon the application of an external stimulus; such as heat, light, electric or magnetic fields [1,2]. The most common materials that have shape memory effects are shape memory alloys (SMA), shape memory ceramics (SMC) and shape memory polymers (SMP) [1,2]. In contrast with other SMM types, SMP have advantageous characteristics such as high shape recovery, lightweight, superior molding properties and lower cost [1,3]. Thermo-responsive SMP activate when it is heated to or above its transition temperature [1,2,4,5]. SMP can be assigned a temporary shape and its permanent shape can be recalled using a simple programming schedule. This process can be repeated many times [1,6]. Due to these novel and tailorable properties, SMP (and their composites) have a broad range of potential applications such as temperature sensors and microfluidic devices, and they are currently under extensive research for potential applications in the medical and aviation fields [7].

Additive manufacturing is a manufacturing technique in which three dimensional objects are built by continuously adding and/or fusing layers of materials [8]. Material Extrusion Additive Manufacturing (MEAM), or also known as Fused Deposition Modeling (FDM), is the most common of the additive manufacturing technologies, in which the objects are built by extruding molten polymeric materials through a nozzle onto a platform in different paths and layers defined by a computer aided design (CAD) data file [8,9]. By using this technology different parts can be

manufactured in a shorter time and with less cost compared to traditional manufacturing processes [8]. Generally, MEAM processes utilize thermoplastic materials. Acrylonitrile butadiene styrene (ABS) and polylactic acid (PLA) are the two most commonly used materials.

3.2 Sample Manufacturing

3.2.1 Sample Modeling and G-Code generation

The produced SMP filaments were fed into a commercial desktop printer (Ultimaker 2+), which extrudes the material through a 0.4 mm nozzle onto a heated glass bed and can reach layer heights down to 20 µm. There are numerous parameters that need to be fixed during a MEAM process and any change in these parameters may affect print quality and properties of the printed materials [10]. Thus, for the current work the printing parameters presented in Table 3-1 were used for every specimen. Additionally, the heat of the bed was shut down after the second layer of the material was constructed. This prevents variations between layers caused by the temperature gradient the heat bed produces.

Table 3-1MEAM Parameters

Nozzle Temperature	220° C
Bed Temperature	40° C
Layer Height	0.1mm
Shell Thickness	0.4 mm
Outline Direction	Inside Out
Printing Speed	1200 mm/min
Outline Underspeed	50%

A commercial software, Solidworks, facilitated the construction of the CAD data of the specimens. The specimens were prepared according to Type V dogbone specimens following ASTM D638

[11]; however, the thickness of the specimens were chosen as 2 mm to be able to stay below the maximum load capacity the load cell of the tensile testing apparatus.

For the purpose of analyzing the effects of the print angle and the infill percentage on the tensile properties of the specimens, a full factorial experiment design was used with 4 levels of print angle and 3 levels of infill percentage repeated five times. Table 3-2 presents the level distribution for the different SMP printed samples.

Table 3-2 Level distribution for test samples

Print angle	Infill Percentage	Number of prints
0°	50%	5
	75%	5
	100%	5
30°	50%	5
	75%	5
	100%	5
60°	50%	5
	75%	5
	100%	5
90°	50%	5
	75%	5
	100%	5
	Total # of samples	60

The CAD generated data file needed to be modeled by a slicing program. This program divided each layer of the designed piece in order to create a numerical control program. The numerical control program then set the paths and amount of extruded materials the printing machine will use while manufacturing the different samples. All these were achieved by the use of a commercial digital tool (Simplify 3D). Figure 3-1 shows an example of the samples prepared by Simplify 3D at different angles (30° and 90° angles with respect to the longitudinal direction). The 30° angle

piece has its extrusion path aligned at 30° to the longitudinal direction of the specimen, while the 90° angle one has its extrusion path set transversally.

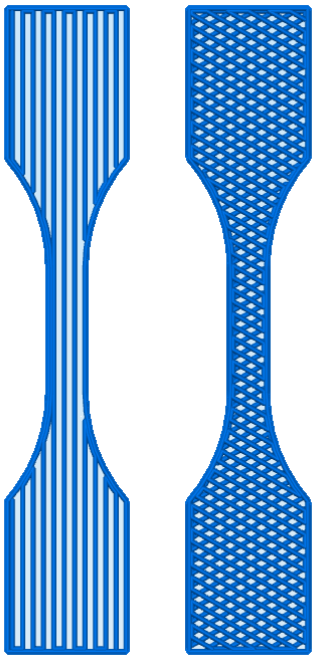

Figure 3-1 Test sample printed at 0° angle (left) and 60%-60° angle (right)

In this study, also the infill percentage of the specimens was changed to outline its effect on mechanical properties. At each different infill percentage level, the amount of material used in every specimen varied, thus the density of every sample also varied as well. The average weight and density of all the different pieces is displayed in Table 3-3.

Table 3-3 Weight and density averages of the printed specimens

Infill Percentage	Weight Average (grams)	Density Average (gr/cm^3)	
50%	0.70	1.01	0°
75%	0.86	1.24	
100%	0.99	1.44	
50%	0.72	1.04	30°
75%	0.84	1.22	
100%	0.96	1.39	
50%	0.72	1.05	60°
75%	0.85	1.23	
100%	0.96	1.39	
50%	0.71	1.03	90°
75%	0.86	1.25	
100%	0.98	1.42	

Prior to testing all samples were placed in a vacuum oven at 40°C for 14 hours to be dried. Once the samples were dried they were kept in vacuum sealed packages to avoid the SMP to absorb humidity from the surrounding environment.

3.2.2 Tensile Testing

Tensile tests were conducted using a ElectroForce 3200 system manufactured by BOSE. The system is equipped with a load cell that is capable of applying a maximum 450 N load. The strain in the specimens were measured using an in-house developed Optical Strain Measuring (OSM) system. A deformation rate of 4mm/min was used during the tests. Additionally, both the upper and lower clamps were tightened to a constant torque of 1700 N.mm for every sample using a torque wrench. Figure 3-2 presents a representative figure for the tests.

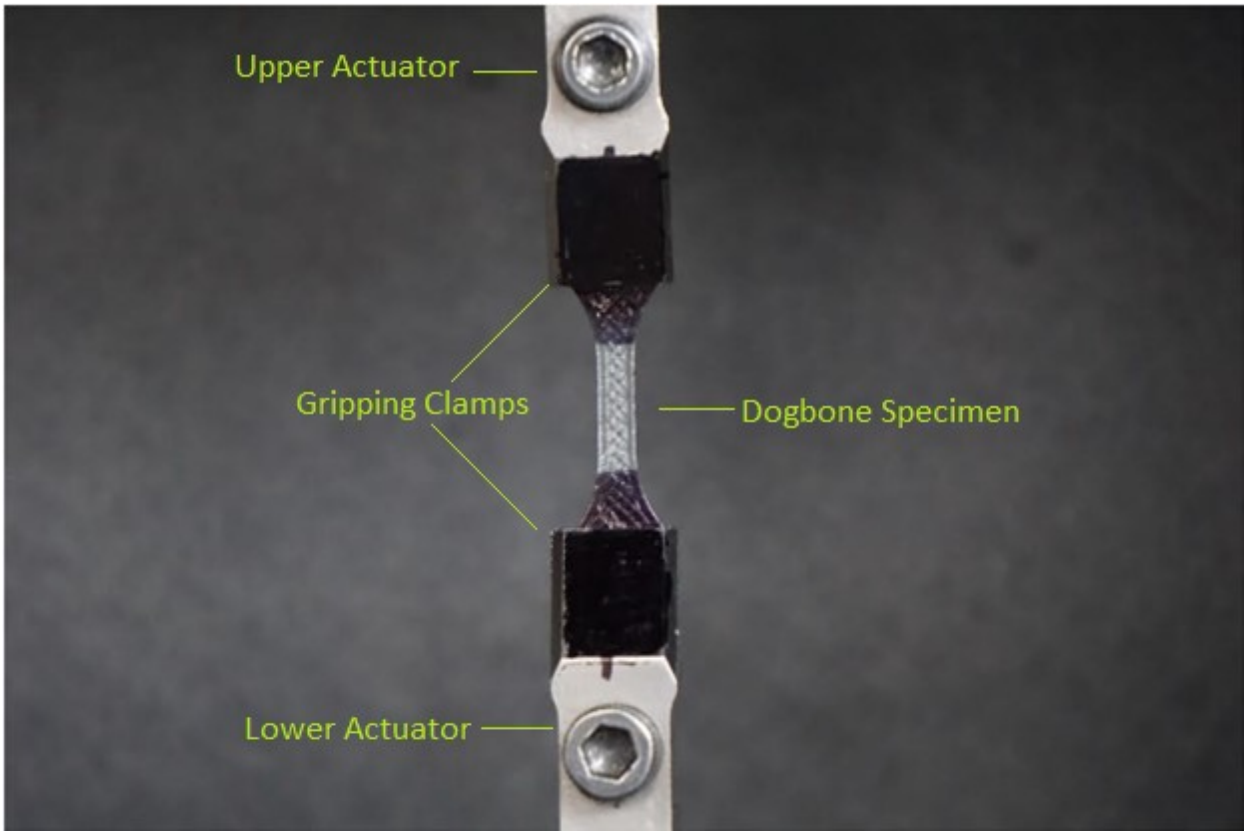

Figure 3-2 Type V Dogbone 30° angle/ 100% infill tensile test

3.3 Results and Discussion

3.3.1 Raw Material Pre-processing

The SMP pellets had to be dried before extruding. This prevents bubbles from forming inside the filament while extruding. Bubbles cause voids in the printed pieces and deteriorate the filament with time. Moreover, they can cause inconsistent mechanical properties between the specimens. T To avoid this, the pellets were heated in a vacuum oven at 80°C and were weighted every hour to define the sufficient drying time. As shown in Figure 3-3, the pellets weight stabilized after being dried for 10 hours. Hence, for this work the pellets were dried for 12 hours before being extruded. Additionally, filaments had a diameter of 3mm with a standard deviation of +/- 0.15 mm.

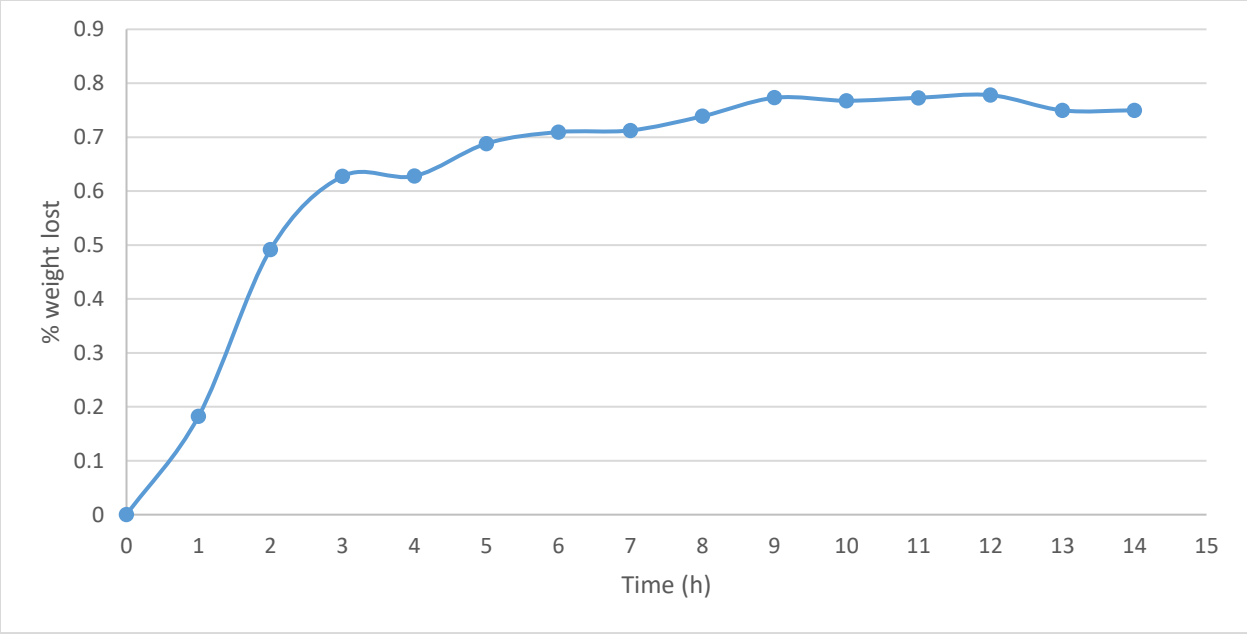

Figure 3-3 Pellets % weight loss in hours

Figure 3-4 shows the DSC curve for the polymer. As a result of this analysis the glass transition temperature range was found between 37.82 and 46.75 which confirms the manufacturer's Tg value of 45°C. Tm was found at 158.45°C.

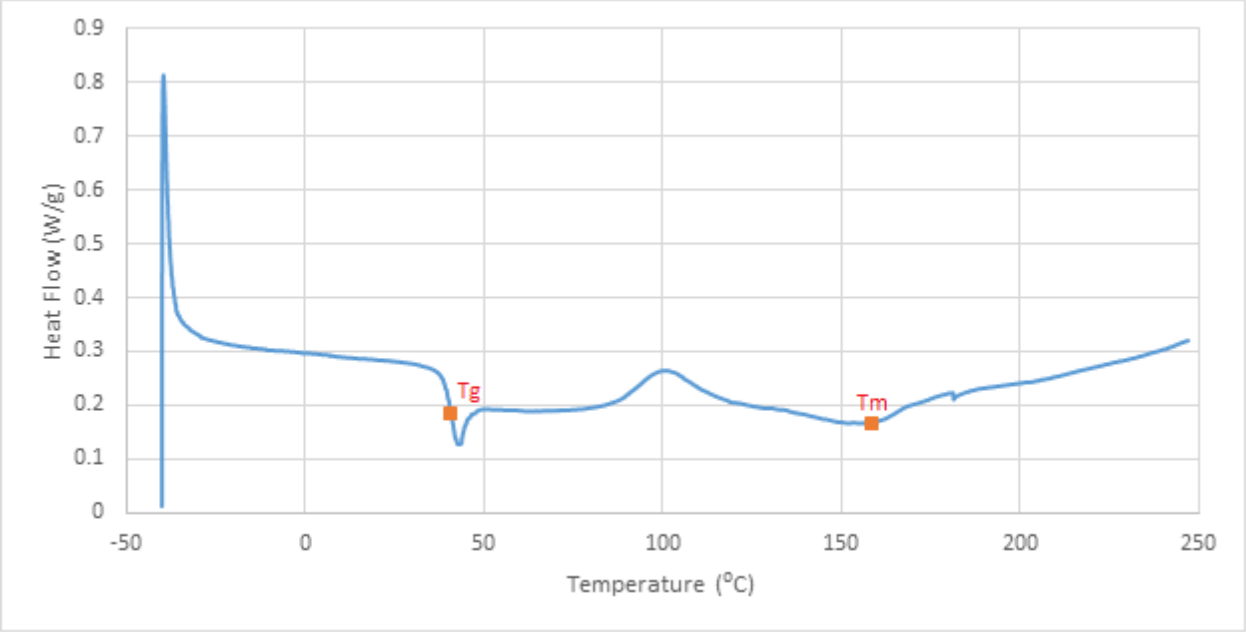

Figure 3-4 DSC of MM4520 obtained from a printed sample.

3.3.2 Tensile tests:

The three parameters examined were the elastic modulus, ultimate tensile strength (UTS) and strain at failure. As aforementioned, the investigated parameters were three different levels of infill percentage (100%, 75% and 50%) and four different levels of print angle (0°, 30°/-30°, 60°/-60° and 90°). A t-test with a 95% confidence level was also performed to assess results' statistical significance.

Figure 3-5 shows the representative stress-strain curves of the tested samples printed at a 0° using different infill percentages. This figure displays a particular breaking pattern for samples printed at 0° and 50% infill percentage. Samples printed at other print angles and infill percentages stretched uniformly and then broke as a uniform body. In contrast, the infill material of samples

printed at this particular level separated into different aligned fibers which broke independently from one another. This printing pattern appeared only in samples printed at this angle and infill percentage.

Figure 3-6 shows the representative stress-strain curves of tested samples printed at 50% infill but at different print angles.

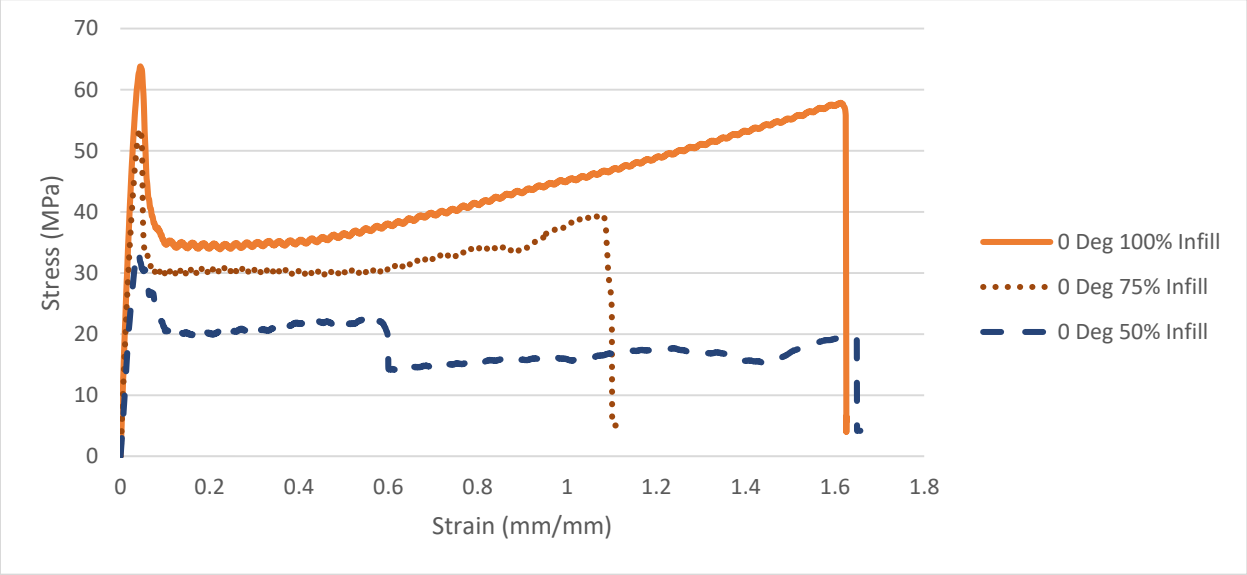

Figure 3-5 Representative stress-strain curve for specimens printed at the same angle but different infill percentages

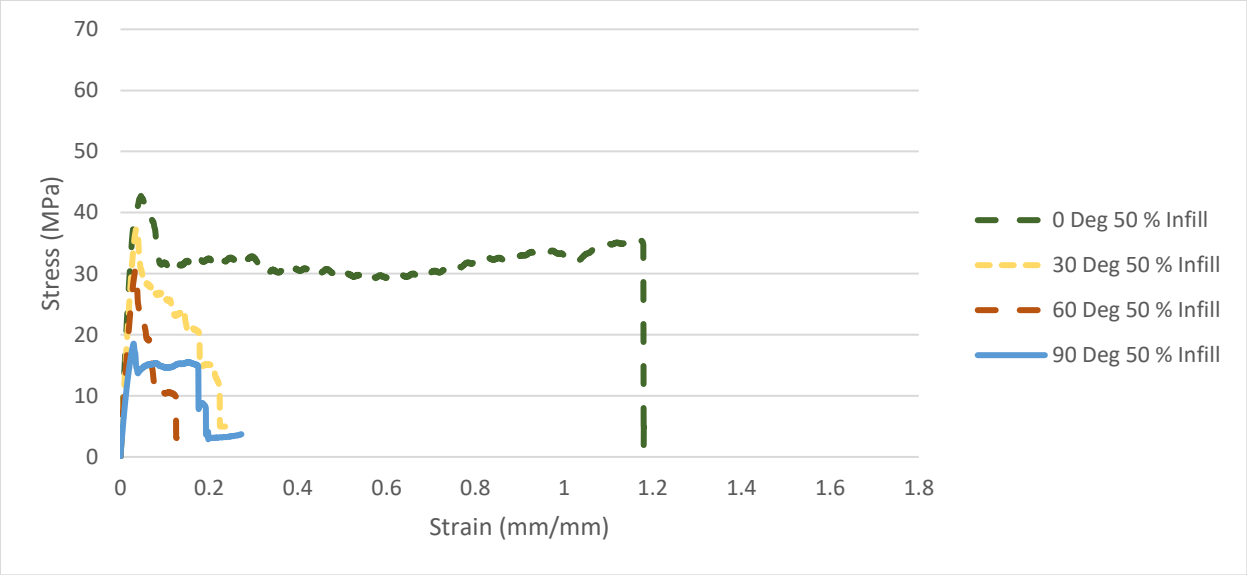

Figure 3-6 Representative stress-strain curves for specimens printed using the same infill percentages but different print angles

3.3.3 Elastic Modulus:

Figure 3-7 shows the change in Elastic Modulus (and the Standard Deviations) with respect to print angles and % infills, the data is grouped under different print angles for ease of observation. Table 3-4 outlines the numerical values used to plot this figure. In Figure 3-7, by only considering the average results, it can be seen that some trends have been developed when different parameters are used. At every print angle, an increase in the infill percentage always resulted in an increase in the elastic modulus. Similarly, a decreasing trend for the elastic moduli is observed for the same infill ratio but different print angles. Nevertheless, when the t-tests results (Table 3-5) are taken into account, the results show that a variation between 75% and 100% infill does not make a statistically significant impact on the elastic modulus. However, a variation between 50% and 100% infill does make a statistical difference and the same occurs between 75% infill and 100% infill. Moreover, the difference in time required to manufacture a sample is also presented in this table. This is an important characteristic to take into account when manufacturing a part for a

determined application. However, printing time cannot be analyzed or compared through statistical analysis given that it does not present any standard deviation since it is an automated process.

The percentage difference in the average results of the extreme cases is outlined, at 0° print angle there appears to be 31% difference between 50 % and 100 % infill printing. This number increases to 58.02 % difference for 90° print angle (Table 3-4). This highlights the tailorability of elastic modulus properties for the same raw material.

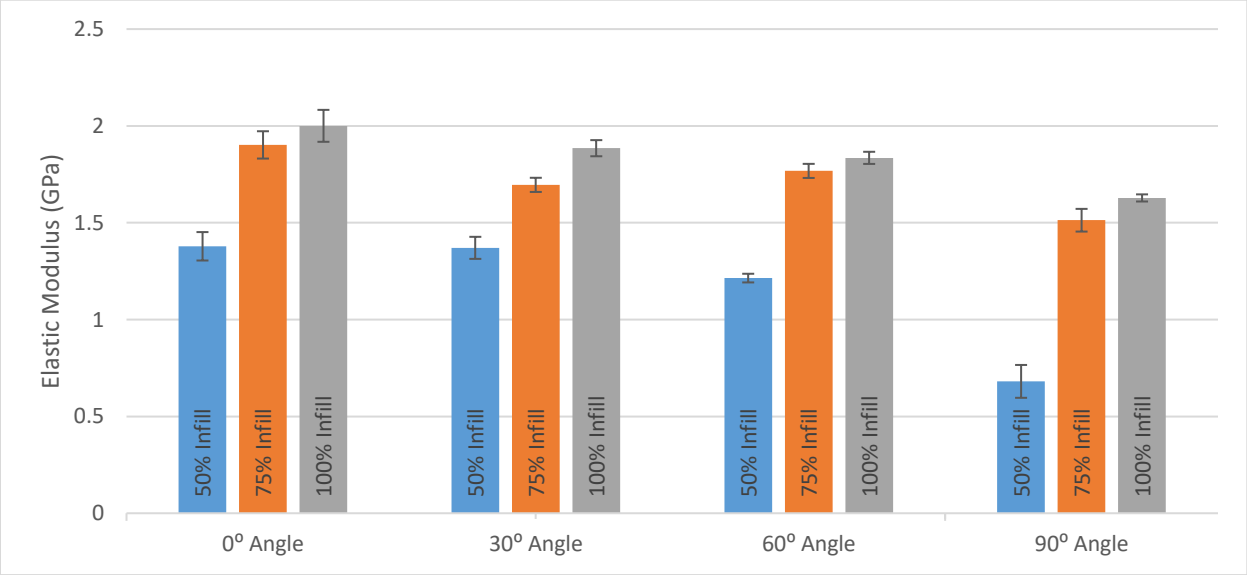

Figure 3-7 Elastic Moduli grouped under different print angles

Table 3-4 Average Elastic Modulus (+/- Standard Deviation) Results (GPa)

	50% Infill	75% Infill	100% Infill	Percentage difference between average Elastic Moduli values of 50% and 100 % infill	Time difference in printing specimens with 50% and 100 % infill (s)
0° Angle	1.38 (+/-0.07)	1.90 (+/-0.07)	2.00 (+/-0.06)	31%	67.35
30° Angle	1.37 (+/-0.05)	1.66 (+/-0.04)	1.89 (+/-0.04)	27.51%	64.73
60° Angle	1.21 (+/-0.02)	1.77 (+/-0.03)	1.84 (+/-0.03)	34.23%	65.03
90° Angle	0.68 (+/-0.08)	1.51 (+/-0.16)	1.62 (+/-0.01)	58.02%	64.95

Table 3-5 T-tests (95% confidence) results for Elastic Moduli compared between different infill percentages grouped under different print angles

Infill	50%	75%	100%	Angles
50%	-----			0°
75%	4.31E-04	-----		
100%	1.03E-04	0.28	-----	
50%	-----			30°
75%	1.13E-03	-----		
100%	6.27E-05	0.01	-----	
50%	-----			60°
75%	2.81E-06	-----		
100%	9.05E-06	0.18	-----	
50%	-----			90°
75%	0.01	-----		
100%	1.38E-04	0.54	-----	

Figure 3-8 is plotted using the same values of Figure 3-7; however, the values were grouped under different infills for ease of observation in discussing the influence of the print angle has on the elastic modulus. It is seen that for samples printed at 100% and 75% infill, the only print angles that are statistically different from each other are 0° and 90°. Nonetheless, when printing at 50% infill, almost all the variations of print angle do have a statistically significant impact in resultant

elastic moduli. The only angle variation at 50% infill that did not prove to be statistically different with a 95% confidence factor was between 0° and 30°. The t-test values are presented in Table 3-7.

In Table 3-6 the percentage comparison between printing angle extreme cases is presented, 0° and 90°. It is seen that for 50% infill percentage the difference between these extreme cases is 50.72% while for 100% infill percentage this difference is 19%. This demonstrates when printing at lower infill percentages, the influence the printing angle has on the elastic moduli of the material increases.

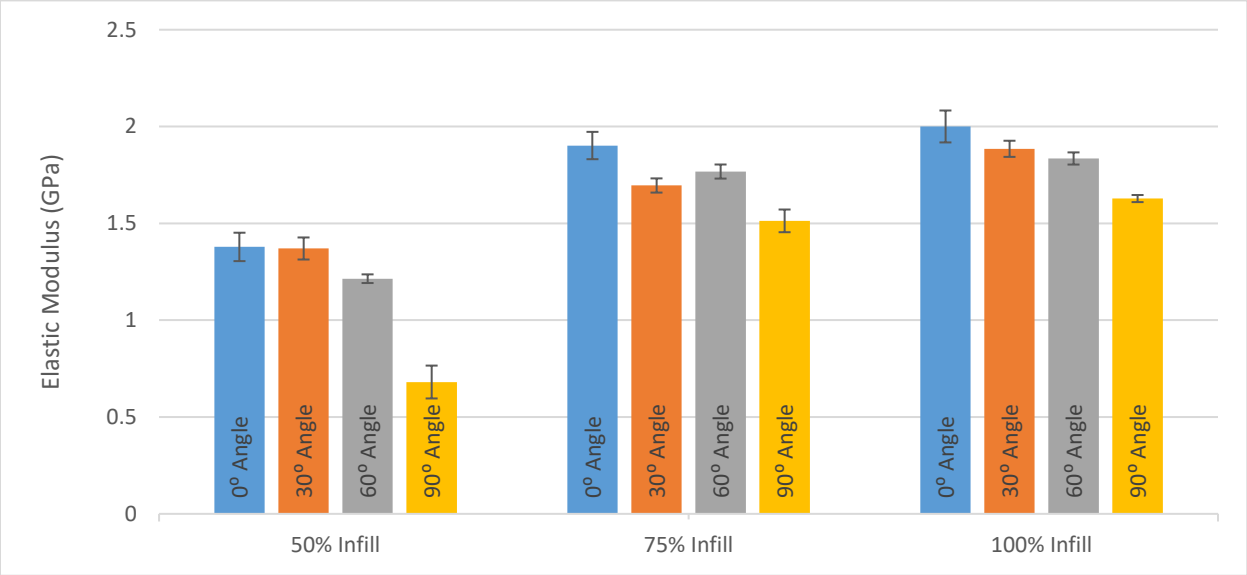

Figure 3-8 Elastic Moduli grouped under different % infills

Table 3-6 Percentage comparison between extreme angle cases for Elastic Moduli and printing time

	Percentage difference between average Elastic Moduli values of 0° and 90° print angle	Time difference in printing specimens with of 0° and 90° print angle (s)
50%	50.72%	4.95
75%	20.53%	3.5
100%	19%	2.55

Table 3-7 T-tests results for Elastic Moduli compared between different angles grouped under different infill percentages

Angles	0	30	60	90	Infill
0	-----				50%
30	0.92	-----			
60	0.03	0.03	-----		
90	1.30E-04	1.32E-04	1.51E-03	----	
0	-----				75%
30	0.03	-----			
60	0.06	0.16	-----		
90	0.10	0.36	0.03	----	
0	-----				100%
30	0.13	-----			
60	0.06	0.34	-----		
90	1.64E-03	9.78E-04	2.59E-03	----	

3.3.4 Ultimate Tensile Strength:

Figure 3-9 shows the change in Elastic Modulus (and the Standard Deviations) with respect to print angles and % infills, the data is grouped under different print angles for ease of observation. ***Error! Reference source not found.*** outlines the numerical values used to plot Figure 3-9, and similarly, the t-test results are included in Table 3-9. Additionally, in the last column of **Error! Reference source not found.**, the comparison of the percent difference in the average results of the extreme cases of infill percentage is displayed for all printing angles. For a 0° angle this difference is 37.78%. and for a 90° angle it comes up to 67.92%.

In Figure 3-9, similar trends to that of elastic moduli findings were observed in UTS values. The higher the infill percentage the higher the UTS, and the lower the print angle the higher the UTS values were observed. Similarly, a variation between 75% and 100% infill did not seem to make a statistically significant impact on the UTS of the samples. However, printing at 50% infill does have a statistically significant impact in the UTS of the printed samples when comparing it to 75% or 100% infill.

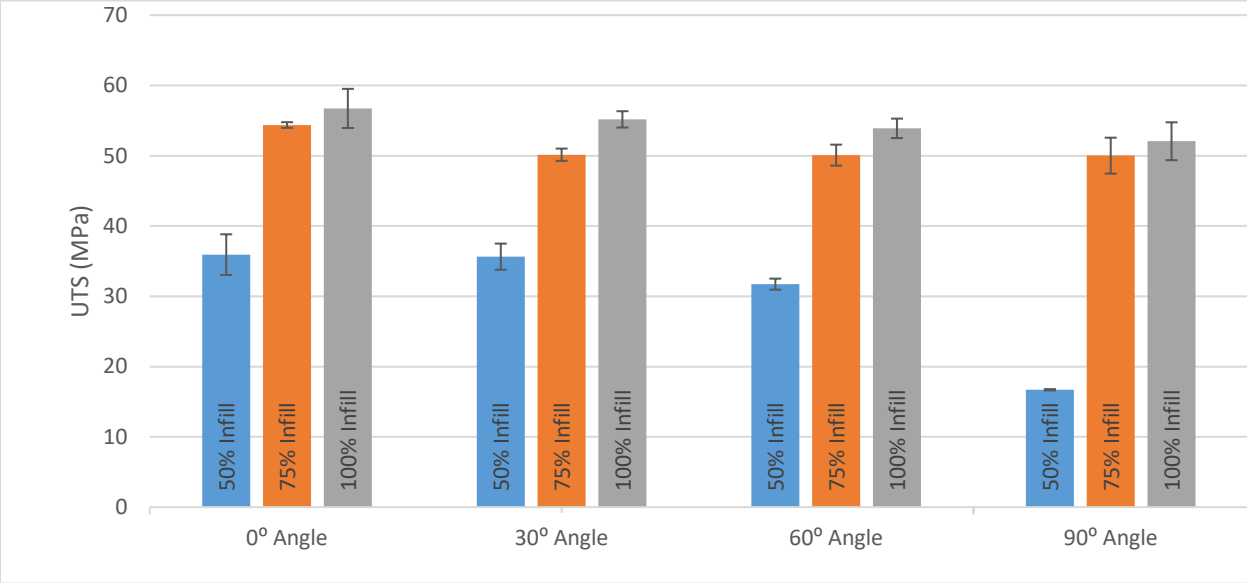

Figure 3-9 UTS at Different at Infill Percentage Comparison

Table 3-8 UTS (+/- Standard Deviation) Average Results (MPa)

	50% Infill	75% Infill	100% Infill	Percentage difference between average UTS values of 50% and 100 % infill
0° Angle	35.92 (+/-2.89)	54.37 (+/-0.4)	57.73 (+/-2.79)	37.78%
30° Angle	35.34 (+/-1.86)	50.14 (+/-0.88)	55.17 (+/-1.16)	35.94%
60° Angle	31.72 (+/-0.79)	50.08 (+/-1.5)	53.89 (+/-1.39)	41.14%
90° Angle	16.7 (+/-0.1)	50.01 (+/-2.56)	52.06 (+/-2.69)	67.92%

Table 3-9 T-tests results for UTS compared between different infill percentages grouped under different angles

Infill	50%	75%	100%	Angles
50%	-----			0
75%	8.67E-03	-----		
100%	2.19E-02	0.72	-----	
50%	-----			30
75%	1.73E-03	-----		
100%	6.49E-04	0.14	-----	
50%	-----			60
75%	1.66E-04	-----		
100%	3.11E-01	0.31	-----	
50%	-----			90
75%	2.54E-03	-----		
100%	6.68E-01	0.67	-----	

Figure 3-10 is plotted using the same values of Figure 3-9; however, the values were grouped under different infills for ease of observation in discussing the influence of the print angle on the UTS. It can be seen from the figure that the print angle has minimal effect on the UTS of the specimens if the % infill is kept constant for samples printed at 100% and 75% infill. Nevertheless, for specimens printed at 50% infill, results show that almost all the variations of print angle do have a statistically significant impact in resultant UTS. The only angle variation at 50% infill that did not prove to be statistically significant is between 0° and 30°. This trend is even more pronounced when comparing the extreme cases of printing angles for each infill percentage setting on Table 3-10. For 100% infill, we obtain a difference of 9.82%. In contrast, for a 50% printed sample the difference of extreme cases is 53.5%. This accentuates the tailorable capabilities of the material. The t-test results of the analysis are provided in

Table 3-11.

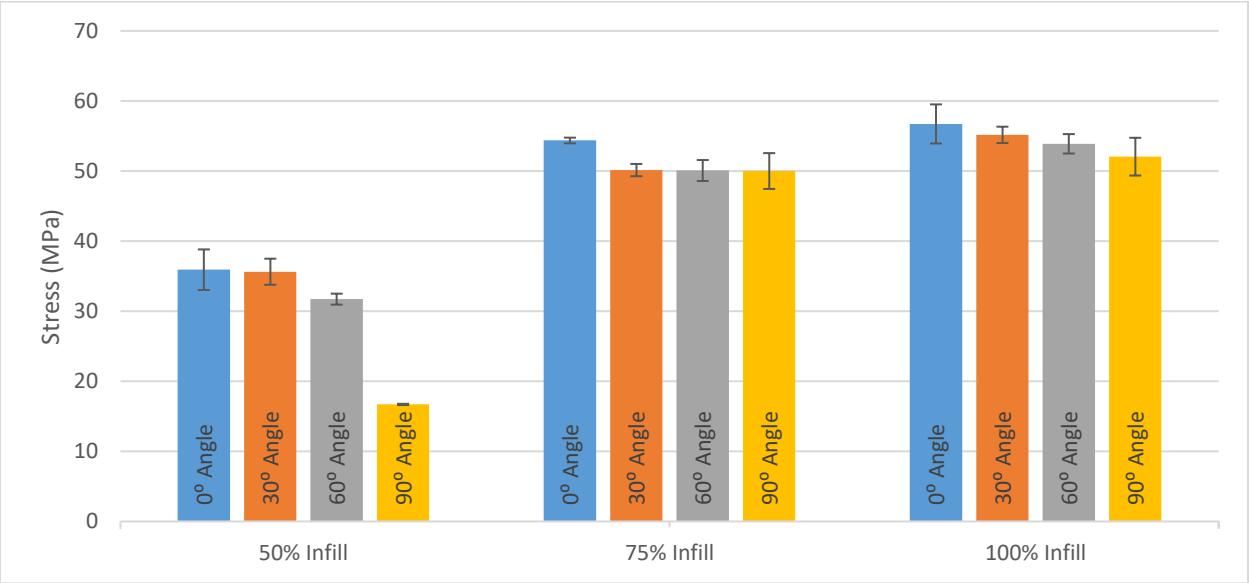

Figure 3-10 UTS at Different Print Angles Comparison

Table 3-10 Percentage comparison between extreme angle cases for UTS

	Percentage difference between average UTS values of 0° and 90° print angle
50%	53.5%
75%	8.02%
100%	9.82%

Table 3-11 T-tests results for UTS compared between different angles grouped under different infill percentages

Angles	0	30	60	90	Infill
0	-----				50%

30	0.83	-----			
60	0.33	0.25	-----		
90	4.13E-03	1.86E-03	9.78E-03	----	
0	-----				75%
30	0.02	-----			
60	0.06	0.89	-----		
90	0.47	0.85	0.80	----	
0	-----				100%
30	0.84	-----			
60	0.41	0.59	-----		
90	0.62	0.65	0.98	----	

3.3.5 Maximum Strain at Failure:

In Table 3-12, the average result of the maximum strain before failure for each tested level is presented. These results show a new trend. This time the higher the infill percentage the higher the maximum strain, except for 0° angle. Moreover, the lower the angle the higher the maximum strain except for 100% infill specimens.

Table 3-12 Maximum Strain at failure (+/- Standard Deviation) Average Results (mm/mm)

	50% Infill	75% Infill	100% Infill	Percentage difference between average Max Strain values of 50% and 100 % infill
0° Angle	1.54(+/-0.29)	1.01(+/-0.09)	1.46(+/-0.11)	5.48%
30° Angle	0.12(+/-0.03)	0.54(+/-0.25)	1.70(+/-0.1)	92.94%
60° Angle	0.11(+/-9*10^-3)	0.48(+/-0.25)	1.80(+/-0.05)	93.89%
90° Angle	0.09(+/-0.03)	0.11(+/-0.02)	1.65(+/-0.24)	94.55%

Table 3-13 displays the percent difference between extreme angle cases at every infill percentage level. We can observe that for a 50% infill, the difference between 90° and 0° is 94.16% while for 100% infill percentage this difference is 13.01%

Following the same procedure already used for examining previous parameters. The results for the analysis of the impact that infill percentage has regarding maximum strain show that 100% infill printed samples have a statistically significant difference on maximum strain when compared to 50% or 75% infill printed specimens for every angle except 0° Whereas the difference between 50% and 75% printed sample infill on maximum strain proved to be statistically different with the exception of 90°. Additionally, when comparing the extreme cases of infill percentage for every level, it can be observed in the last row of Table 3-12 that for level there exists a remarkable difference. For example, for a 90° angle the difference between 100% and 50% infill is 94.55%. This is similar for all levels except 0°. This level presents a low difference of 5.78%.

The results obtained by performing the t-test can be seen in Table 3-14.

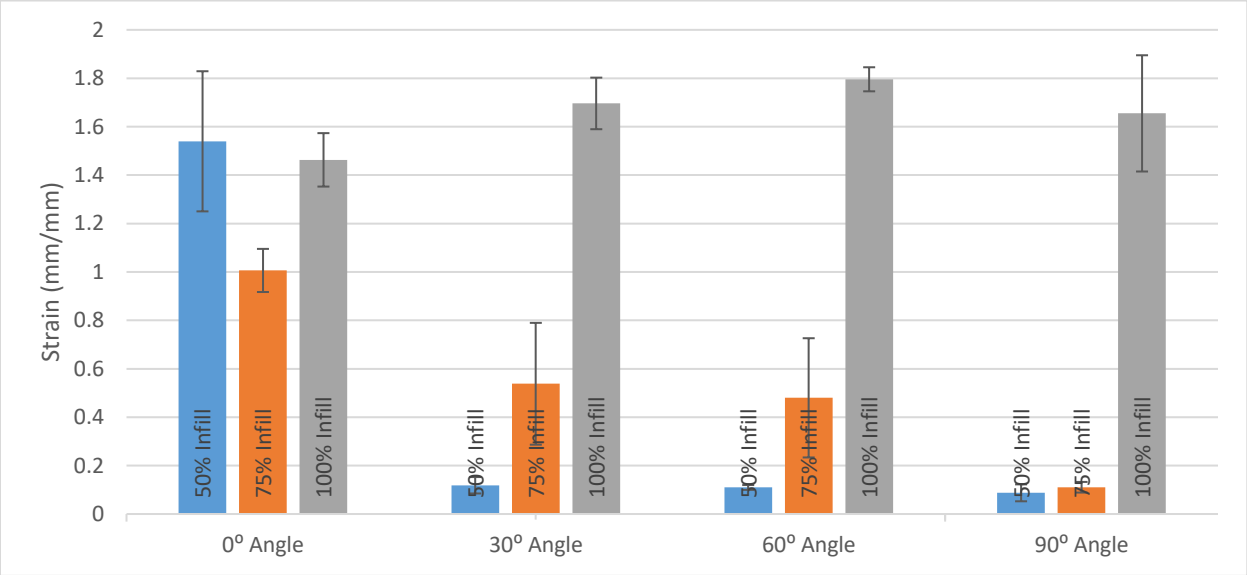

Figure 3-11 Maximum Strain Before Failure at Different at Infill Percentage Comparison

Table 3-13 Percentage comparison between extreme angle cases for Maximum Strain at failure

	Percentage difference between average Max Strain values of 0° and 90° print angle

50%	94.16%
75%	89.1%
100%	13.01%

Table 3-14 T-tests results for Strain Before Failure compared between different infill percentages grouped under different angles

Infill	50%	75%	100%	Angles
50%	-----			0
75%	0.11	-----		
100%	0.80	0.02	-----	
50%	-----			30
75%	0.14	-----		
100%	2.53E-05	4.25E-03	-----	
50%	-----			60
75%	0.17	-----		
100%	3.03E-03	3.23E-03	-----	
50%	-----			90
75%	0.22	-----		
100%	1.87E-03	1.76E-03	-----	

Moreover, results on the effects the variation of print angle has on maximum strain show that for 100% infill printed pieces there is not a statistically significant variation. However, for 75% and 50% infill printed samples, results show that printing at 0° angle does make a significant difference when compared to any other angle t-tests results that are shown on Table 3-15.

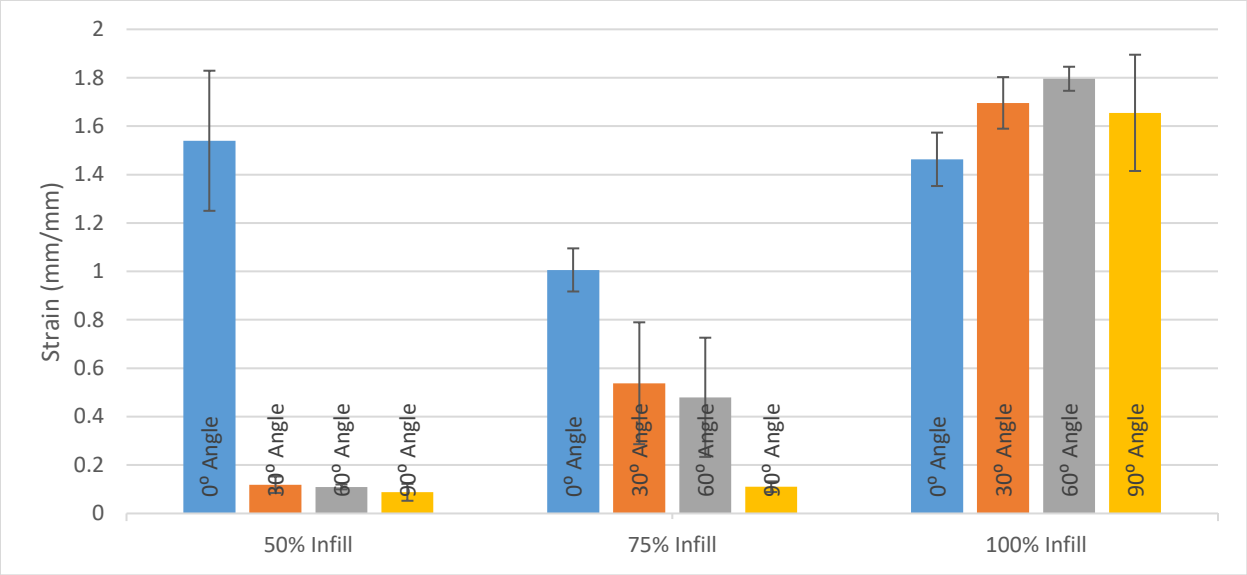

Figure 3-12 Maximum Strain Before Failure at Different Print Angles Comparison

Table 3-15 T-tests results for Strain Before Failure compared between different angles grouped under different infill percentages

Angles	0	30	60	90	Infill
0	-----				50%
30	0.01	-----			
60	1.06E-03	0.79	-----		
90	4.22E-03	0.20	0.20	----	
0	-----				75%
30	0.11	-----			
60	0.07	0.86	-----		
90	1.91E-04	0.13	0.17	----	
0	-----				100%
30	0.16	-----			
60	0.02	0.41	-----		
90	0.46	0.87	0.56	----	

The results shown in the previous charts present two different tendencies. The first trend applies for the elastic modulus and UTS and demonstrates that the higher the infill percentage the higher values both of these parameters reach. However, when taking into account the standard deviation for 75% infill and 100% infill printed pieces, they do not show a significant statistical difference

between each other. Thus, the 50% infill specimens are the only ones to make a statistical difference. The same trend is displayed when analyzing the effect of print angle in elastic modulus and UTS, in which the lower the print angle the higher the elastic modulus and UTS. Similarly, when looking at the 75% infill and 100% infill manufactures samples, this trend is generally not statistically different. For the 50% infill specimens, the print angle effect on both elastic modulus and UTS becomes statistically significant. Thus, the angle and infill effect becomes more noticeable and relative for lower infill percentages.

The second tendency appears in the maximum strain charts. Here, the chart reflects that for 30°, 60° and 90° angle printed specimens at 100% infill the strain is at least 3 times higher than for 75% or 50% printed samples. Therefore 100% infill is the only tested level to make a statistical difference. The 0° angle manufactured specimens, can be better examined when comparing the influence of this factor to 30°,60° and 90°. 0° print angle is statistically significant for all infill percentages except 100% (whose behavior is different because of the bonds its inner structure creates as it was previously explained). The strain capacity that 0° printed parts show may be occurring because the printing pattern is longitudinal to the strain direction, which permits the inner structure of the specimen to stretch instead of breaking.

3.4 Conclusions

The effects of print orientation and infill percentage on tensile properties of shape memory polymer samples processed by material extrusion additive manufacturing was studied. In order to obtain reliable results, a filament production process had to be implemented. External factors, such as humidity, proved to affect the mechanical properties of the tested specimens. Thus, preprocessing of the material was controlled in order to minimize and regulate this external factor. Specimens

were tested at 3 different infill percentage levels, 50% 75% and 100%, while print angles were tested at 0° 30° 60° and 90°.The tensile properties examined were elastic modulus, UTS and maximum strain. T-tests at 95% confidence level were implemented to compare all levels between each other producing the following results:

- The increase of infill percentage proved to increase the elastic modulus in a statistically significant manner.
- The decrease of print angle increased the elastic modulus. However, increasing the infill percentage decreased the impact of change of print angle on elastic modulus.
- The increase of infill percentage proved to increase the UTS in a statistically significant manner.
- The decrease of print angle increased the UTS. However, increasing the infill percentage decreased the significant impact of change of print angle on UTS.
- The results showed increase in maximum strain values as the infill percentage is increased except when the sample is printed at 0°. Among the maximum strain values of 30° 60° and 90° manufactured samples, only the ones printed with 100% infill showed to be statistically different.
- When analyzing the effect of print angle on maximum strain, only 0° angle printed samples showed a statistical difference, except for 100% infill. When printing at 0° print angle, 100% infill and 50% infill levels showed to be statistically higher that 75% but had no difference between each other.

3.5 References

[1] A. Lendlein and S. Kelch, "Shape Memory Polymer," in Shape Memory Effect, Teltow, Wiley, 2002, pp. 2034-2037.

[2] J. Guo, Z. Wang, L. Tong, H. Lv and W. Liang, "Shape memory and thermo-mechanical properties of shape memory," Composites, pp. 162-165, 2015.

[3] C.-S. Zhang and Q.-Q. Ni, "Bending behavior of shape memory polymer based laminates," composite structures, pp. 153-156, 2005.

[4] H. Tamagawa, "Thermo-responsive two-way shape changeable polymeric laminate," Materials Letters, pp. 749-751, 2010.

[5] M. Hager, S. Bode, C. Weber and U. S. Schubert, "Shape memory polymers: Past, present and future," Progress in Polymer Science, pp. 3-33, 2015.

[6] J. Raasch, M. Ivey, D. Aldrich, D. S. Nobes and C. Ayranci, "Characterization of polyurethane shape memory polymer processed," Additive Manufacturing, pp. 132-141, 2015.

[7] H. Meng and G. Li, "A review of stimuli-responsive shape memory polymer composites," Polymer, pp. 2199-2221, 2013.

[8] O. Mohamed, S. Masood and J. Bhowmik, "Optimization of fused deposition modeling process parameters:," Advanced Manufacture, pp. 42-53, 2015.

[9] B. Wendel, D. Rietzel, F. Kuhnlein and R. Feulner, "Additive Processing of Polymers," Macromolecular and Materials Engineering, p. 799–809, 2008.

[10] C. Bellehumeur, L. Li, Q. Sun and P. Gu, "Modeling of Bond Formation Between Polymer Filaments in the Fused Deposition Modeling Process," Journal of Manufacturing Processes, pp. 170-179, 2004.

[11] ASTM International, " ASTM D638-10 Standard Test Method for Tensile Properties of plastics," pp. 1-16, 2010.

4 SHAPE MEMORY RECOVERY ANALYSIS

(*) A version of this chapter will be submitted to Rapid Prototyping Journal as a journal paper with the authors: J. Villacres, D. Nobes, C. Ayranci.

4.1 Introduction

Shape memory materials (SMM) are characterized by having the ability to recover their original shape after being subject to a deformation. In order to recover their original shape, an external stimulus such as heat, electrical current or magnetic fields need to be applied to the material [1,2]. Shape memory polymers (SMP) and shape memory alloys (SMA) are the most common types of SMM. SMP that activate when heated over its glass transition temperature are called thermo-responsive [1,2,3,4]. The unstrained shape of the material can be set by conventional polymer manufacture techniques, such as extrusion or injection molding and this process can be repeated many times [1,5]. SMP possesses the advantages of being moldable, lightweight, economical and have a high shape recovery ratio compared to SMA [1,6]. Given all these characteristics, SMP are currently under extensive research for potential applications such as light modulator display devices or orthodontic arch wires [7].

Material Extrusion Additive Manufacturing (MEAM) is the process in which three dimensional objects are manufactured by successively adding and fusing together different layers of material [8]. Each layer is built by extruding material through a nozzle onto a platform in different paths defined by a computer aided design (CAD) data file [8,9]. Advantages of this manufacturing process include cost effectiveness, shorter build time and low cost. Many applications for the use

of this manufacturing process are currently being developed in the aerospace, automotive and biomedical fields [8]. The most common materials used for MEAM are thermoplastic polymers.

Three dimensional SMP components can be produced through MEAM. As a result, we can obtain different parts with the ability to regain their original shape after being deformed. There is great potential for the use of components with these characteristics in numerous applications. However, the shape recovery properties of the SMP MEAM parts needs to be characterized first. This chapter reports on the production process for creating printed SMP samples and studies the print parameters' effects on the shape memory recovery behavior of the printed samples by performing two different tests, a shape memory recovery force and a shape memory recovery ratio test.

4.2 Material Extrusion Additive Manufacturing

4.2.1 Sample Modeling and G-Code generation

After obtaining the SMP filaments, they were fed into a commercial MEAM machine (Ultimaker 2+). The nozzle from this machine possesses a 0.4 mm diameter opening through which the material is extruded onto a heated glass bed. Numerous parameters must be set for the MEAM process such as printing speed or nozzle temperature. Any alteration in these parameters may affect print quality and properties manufactured part [10].

Table 4-1 displays the parameters set for this process. Furthermore, the heat of the bed was shut down after the second layer of the material was constructed. This prevents variations between layers caused by the temperature gradient the heat bed produces.

Table 4-1 MEAM Parameters

Nozzle Temperature	220° C
Bed Temperature	40° C
Layer Height	0.1mm
Shell Thickness	0.4 mm

Outline Direction	Inside Out
Printing Speed	1200 mm/min
Outline Under speed	50%

In this project, our goal was to analyze the effects of the print angle and the infill percentage on the shape recovery properties of the specimens. To achieve this goal, a full factorial experiment design was used with 4 levels of print angle and 3 levels of infill percentage each repeated five times. This distribution was employed for the shape recovery ratio and the shape recovery force test. Table 4-2 displays the level distribution for the different SMP printed samples.

Table 4-2 Level distribution for test samples

Print angle	Infill Percentage	SMR force test number of samples	SMR ratio test number of samples
0°	50%	5	5
	75%	5	5
	100%	5	5
[30°/-30°]	50%	5	5
	75%	5	5
	100%	5	5
[60°/-60°]	50%	5	5
	75%	5	5
	100%	5	5
90°	50%	5	5
	75%	5	5
	100%	5	5
	Total # of samples tested	120	

The test specimens model was constructed through the commercial software Solidworks®. The test specimens were rectangular prisms of dimensions 50 mm × 10 mm × 4 mm. After generating the model, its CAD file was exported to the commercial software Simplify 3D. This software slices the specimen into different layers and correspondingly creates the nozzle extrusion path for every

layer and calculates the amount of extruded material used while manufacturing the sample. All this information was saved in a numerical control file to be used by the MEAM machine. *Figure 4-1* shows an example of the samples prepared by Simplify 3D at different angles (30° and 90° angles with respect to the longitudinal direction).

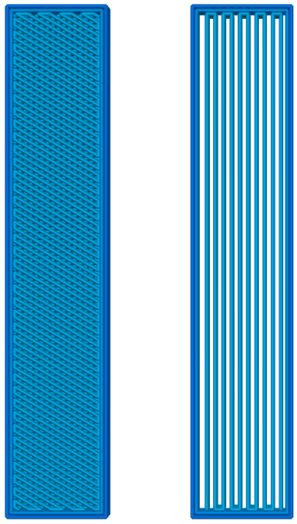

Figure 4-1 Test sample printed at 30° angle 75% infill (left) and 0° angle 50% infill (right)

In this study, the infill percentage of the specimens was changed as well to outline its effect on mechanical properties. At each different infill percentage level, the amount of material used in every specimen varied, thus the density of every sample varied too. The average weight and density of all the different pieces is displayed in

Table 4-3.

Table 4-3 Weight and density averages of the printed specimens

Infill Percentage	Weight Average (grams)	Density Average (gr/cm^3)	
50%	1.28	0.64	0°

75%	1.78	0.89	
100%	2.31	1.16	
50%	1.35	0.68	30°
75%	1.85	0.93	
100%	2.34	1.17	
50%	1.34	0.67	60°
75%	1.84	0.92	
100%	2.36	1.18	
50%	1.31	0.66	90°
75%	1.89	0.95	
100%	2.35	1.18	

Prior to testing all samples were placed in a vacuum oven at 40° C for 14 hours to be dried. Once the samples were dried they were kept in vacuum sealed packages to avoid the SMP to absorb humidity from the surrounding environment.

4.3 Shape Memory Recovery (SMR)Tests

4.3.1 Shape Memory Recovery Ratio Test

The SMR ratio tests were done using a universal tensile/compression test machine with machine with a 3-point test fixture (Electroforce3200, Bose). The system is enclosed in a controlled heat chamber and the upper actuator of the system is equipped with a load cell which can measure forces up to 450 N [11,5]. The distance between the two support points was set as 25mm. For a better explanation, the test procedure has been broken down into 4 different steps and can be observed in Figure 4-2.

1) The test specimen is placed on the three-point test bed and the temperature of the chamber is raised up to 45 °C.

2) After 10 minutes at 45°C the upper actuator lowers down, touches the specimen and then continues on lowering 5mm while bending the specimen.

3) The hot air is released, ventilation is turned on and the temperature is lowered down to 25°C. After 10 minutes at 25°C the upper actuator is raised up releasing the specimen. Given that the specimen has cooled to 25°C it maintains its deformed shape. This temperature is held for 5 more minutes after the upper actuator has returned to its initial position.

4) Subsequently, the temperature of the chamber is raised up to 75°C at a rate 0.2°C per second [11]. Thus, the recovery effect of the material is activated. As soon as the heated chamber is activated, a camera starts recording the recovery effect process until the specimen fully recovers its preprogrammed shape.

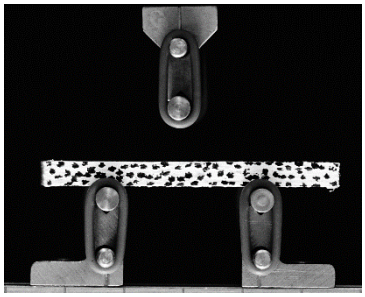

Step 1

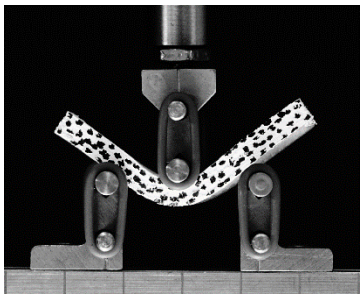

Step 2

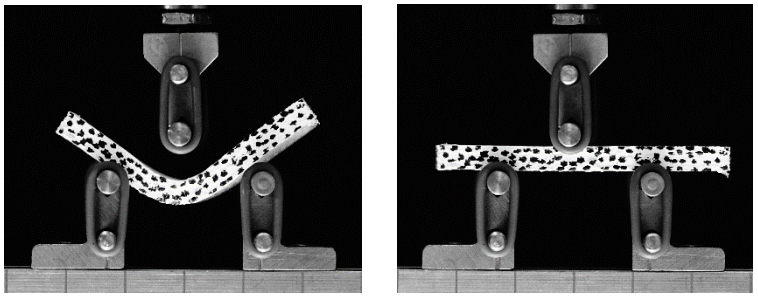

Step 3 Step 4

Figure 4-2 Shape Memory Recovery Ratio Test Procedure

The image measuring system was programmed in the ImageJ open software. Images were collected at a speed of four frames per second. The program converts each image into a binary picture format. Hence, the background of the image is removed and only the speckle pattern painted over the test specimen can be appreciated. A speckle pattern was painted over every tested sample, so future work can characterize the recovery movement of the sample at every point in the specimen. However, for this project only the position of the speckle at the center of the specimen is recorded for every image in a Cartesian format. This information is later compared between images and the shape recovery properties can be obtained. The shape recovery properties obtained from this test are the shape recovery speed and activation time.

The two parameters obtained from this test are shape recovery speed and activation time. Shape recovery speed was obtained by measuring the displaced distance from one frame to the next frame of the analyzed speckle and dividing it by 0.25 which is the time elapsed between frames (four frames per second). The activation time was obtained by locating the first frame where the speckle shows shape recovery movement and then detecting the elapsed time from the activation of the heated chamber until this frame is obtained. Given that the samples take several minutes to finish its recovery movement, sampling at 0.25 seconds is sufficient to characterize the recovery movement accurately.

4.3.2 Shape Memory Recovery Force Test

This test was performed using the same procedure and settings from the SMR ratio test. The only difference lies in the fourth step of the procedure and can be better appreciated in Figure 4-3. In contrast to the SMR ratio test, here the upper actuator lowers down once again until the load cell measures 0.1 [N]. As a result, the actuator touches the specimen but does not apply any additional pressure to it. As soon as this has been accomplished the temperature of the chamber is elevated up to 75°C, at a rate of 0.2°C per second, activating the recovery effect of the material [11]. As the specimen attempts to recover its pre-programmed shape it encounters the upper actuator and exerts pressure onto it. This pressure is measured by the load cell equipped in the actuator.

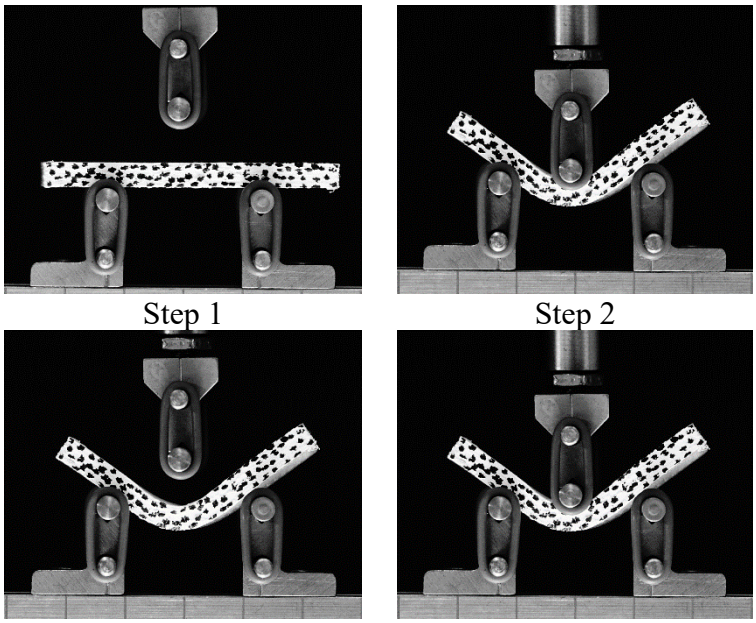

Figure 4-3 Shape Memory Recovery Force Test Procedure

4.4 Results and Discussion

4.4.1 Raw Material preprocessing

Moisture caught from the environment by the SMP pellets influenced the formation of air gaps in the filament, which created voids in the MEAM manufactured piece and cause inconsistent mechanical properties between the specimens. Therefore, the SMP pellets had to be dried before extruding. The pellets were heated in a vacuum oven at 80°C and were weighted every hour to define the sufficient drying time. The weight of the pellets steadied after being dried for 10 hours. Thus, for this work the pellets were dried for 12 hours before being extruded.

4.4.2 Shape Memory Recovery Ratio Test

Two parameters were examined with this test, the shape memory recovery speed and activation time. In order to define whether a change in angle or infill percentage makes a significant difference, t-tests with a 95% confidence were conducted between the results of the three levels of infill percentage (100%, 75% and 50%) and the four different levels of print angle (0°, 30°/-30°, 60°/-60° and 90°). If the resultant p-value of the t-test we can conclude that there is a statistically significant difference between the compared levels [12].

Figure 4-4 shows the representative SMR activation curve of the tested samples printed at a 0° angle using different infill percentages, and *Figure 4-5* shows the representative SMR activation curves of the tested samples printed at 50% infill but at different print angles. The graphs display on the Y axis the recovery percentage of the activated sample. Recovery percentage settled close to 100% every time. The lowest recovery percentage average recorded 98.38 and belongs to samples printed at 0° angle and 50% infill. However, the measured output parameters that did

show significant differences when the print angle or infill percentage were modified are the shape recovery speed and the elapsed time until the samples started their recovery movement.

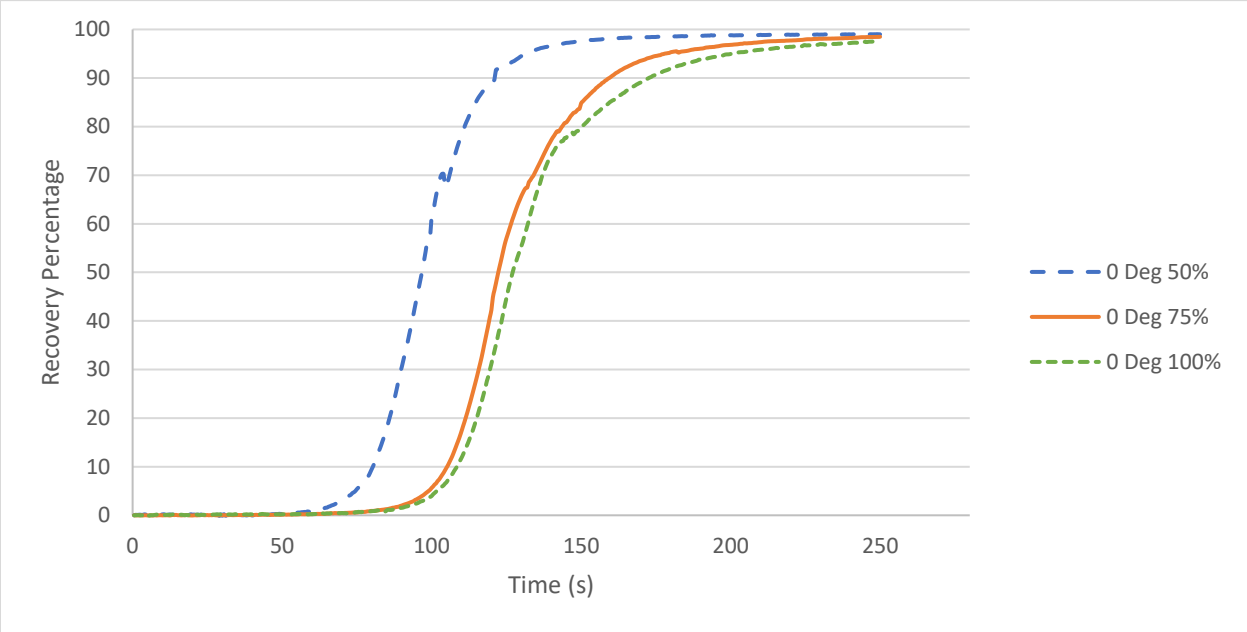

Figure 4-4 Representative recovery ratio curve for specimens printed at the same angle but different infill percentages

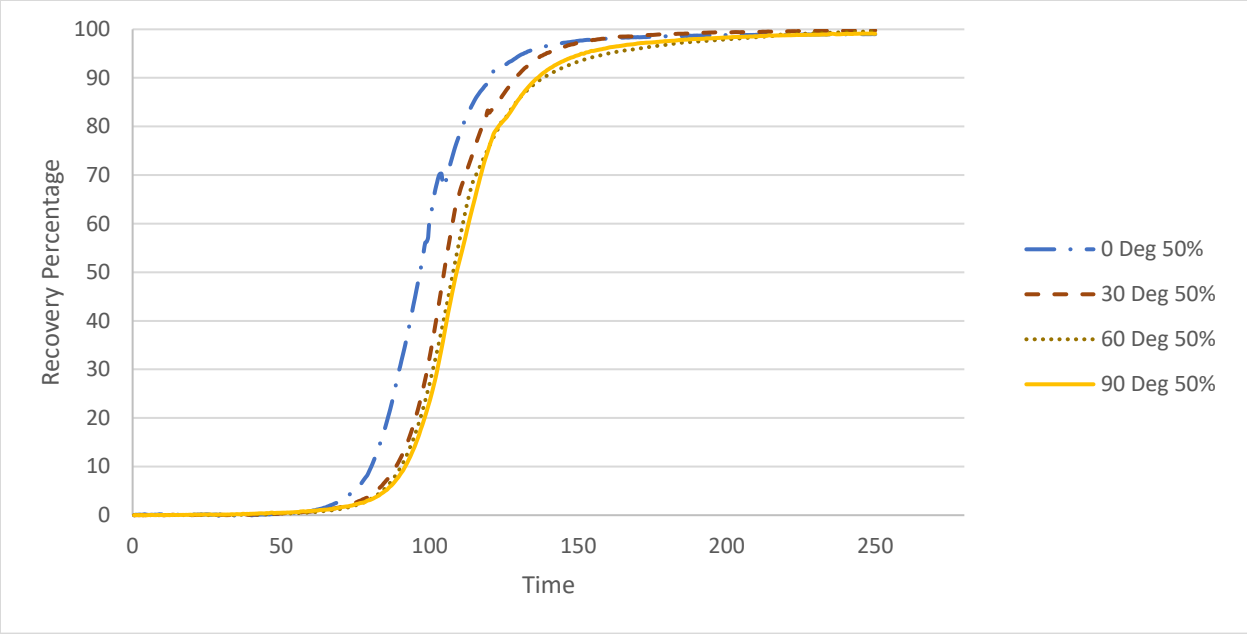

Figure 4-5 Representative recovery ratio curve for specimens printed at the same infill percentage but different angles

4.4.3 Shape Memory Recovery Speed

Figure 4-6 presents the values of the average recovery speed for each level and its corresponding standard deviations. This data has been grouped under different print angles for a better comparison and observation of trends between the displayed results. Figure 4-6 Shape Recovery Speed grouped under different print angles

Table 4-4 presents the values used to develop Figure 4-6 and a percentage difference between the infill extreme cases (50% and 100%) for every angle. Table 4-5 displays the resultant p-value of the different t-tests performed between every infill value grouped under each print angle.

An increasing trend in SMR speed can be perceived from Figure 4-6, this implies that the lower the infill percentage of the sample the faster the sample recovers its original shape. This can be highlighted when taking into account the percentage difference between 50% infill and a 100% infill presented in the same table. This differences are 28%, 58.62%, 12.31% and 34.69% for 0º, 30º, 60º and 90 º print angle respectively. Likewise, Table 4-5 proves that in most of the analyzed cases a statistical significant difference exists. These values emphasize the presented trend. This trend appears because when printing with lower infill percentage, less material is needed for building the sample. Therefore, the sample heats up at a faster rate and as a result, the sample recovers its shape faster as well.

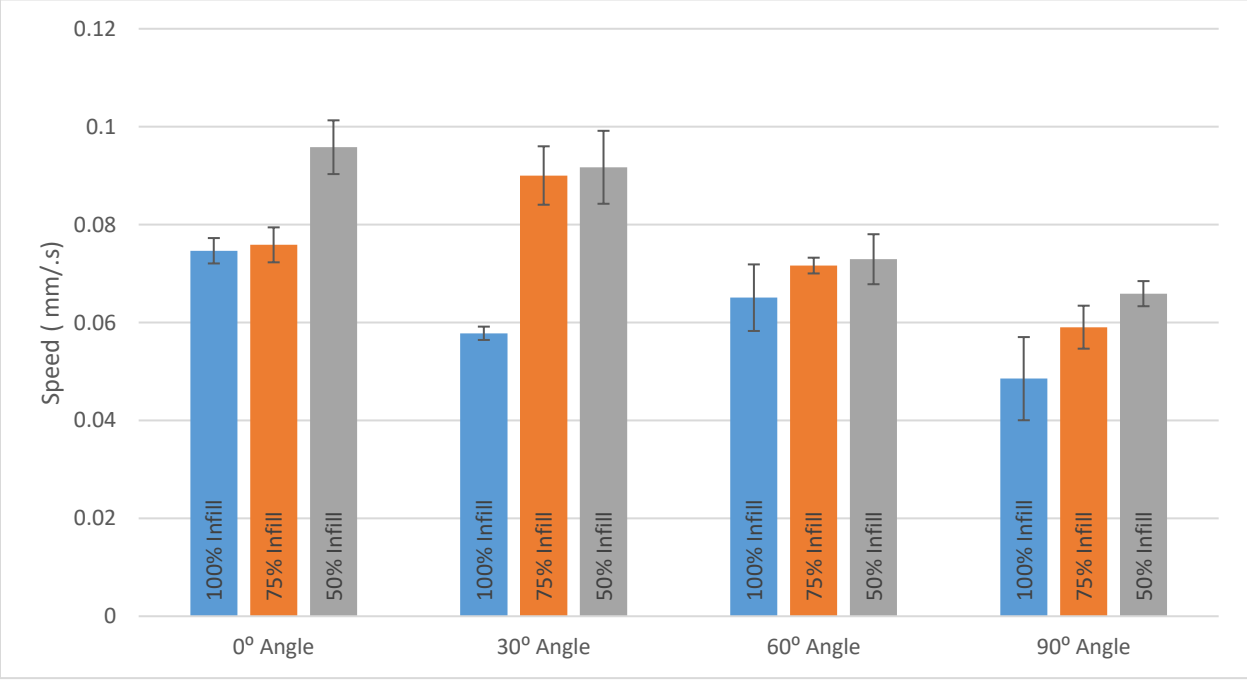

Figure 4-6 Shape Recovery Speed grouped under different print angles

Table 4-4 Average Shape Recovery Speed (+/- Standard Deviation) Results (mm/s)

	100% Infill	75% Infill	50% Infill	Percent difference between average 50% and 100 % infill values
0° Angle	0.075(+/-2.59E-03)	0.076(+/-3.57E-03)	0.096(+/-5.49E-03)	28
30° Angle	0.058(+/-1.36E-03)	0.09(+/-5.97E-03)	0.092(+/-7.45E-03)	58.62
60° Angle	0.065(+/-6.80E-03)	0.072(+/-1.61E-03)	0.073(+/-5.11E-03)	12.31
90° Angle	0.049(+/-8.50E-03)	0.059(+/-4.39E-03)	0.066(+/-2.56E-03)	34.69

Table 4-5 T-tests (95% confidence) results for Shape Recovery Speed compared between different infill percentages grouped under different angles

Infill	50%	75%	100%	
50%	----			0° Angle
75%	0.028	----		
100%	0.023	0.79	----	
50%	----			30° Angle
75%	0.87	----		
100%	0.018	0.01	----	
50%	----			60° Angle
75%	0.29	----		
100%	0.39	0.86	----	
50%	----			90° Angle
75%	0.24	----		
100%	0.03	0.3	----	

Figure 4-7 is plotted using the same values as Figure 4-6. Nonetheless, the values are grouped under infill percentage levels for an ease of observation of any trend regarding the change of printing angle. Table 4-6 displays a percentage comparison between the printing angle extreme

cases (0°-90°). Table 4-7 present the p-values of the different t-tests performed with a 95% confidence level between every print angle grouped under each infill percentage level.

In contrast to what was observed in Figure 4-6**,** for Figure 4-7 a trend is not clearly observable from the displayed results. However, by spotting only the extreme cases (0º and 90º) there can be seen that 0º print angle pieces present a higher recovery speed than 90º print angle pieces for every infill percentage level. Moreover, Table 4-6 presents a percentage difference between these two printing angles of 53.53%, 28.48% and 45.39% for 100%, 75% and 50% infill percentage level respectively. Additionally, in Table 4-7 the results of the t-tests show a statistically significant difference between these two printing angles. The results from these two tables highlight the influence the change of printing angle has on the shape recovery speed of the activated sample.

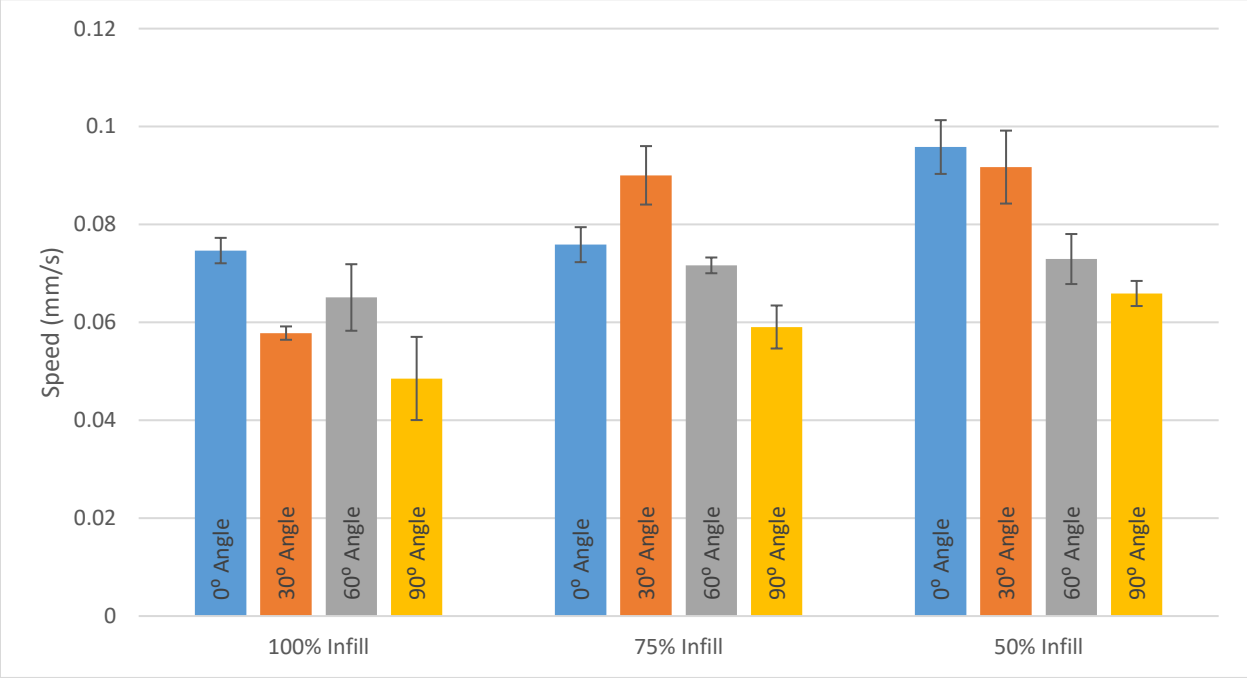

Figure 4-7 Shape Recovery Speed grouped under different infill percentages

Table 4-6 Percentage comparison between extreme angle cases for Shape Recovery Speed

	Percent difference between average 0° Angle and 90° Angle infill values
100% Infill	53.83
75% Infill	28.48
50% Infill	45.39

Table 4-7 T-tests results for Elastic Shape Recovery Speed compared between different angles grouped under different infill percentages

Angles	0	30	60	90	
0	-----				50%
30	0.67	-----			
60	0.003	0.029	-----		
90	0.007	0.03	0.89	----	
0	-----				75%
30	0.09	-----			
60	0.23	0.04	-----		
90	0.02	0.007	0.06	----	
0	-----				100%
30	0.003	-----			
60	0.80	0.11	-----		
90	0.05	0.36	0.07	----	

4.4.4 Shape recovery activation time

Figure 4-8 displays the values of the average shape recovery activation time for each level and its corresponding standard deviations. This data has been grouped under different print angles for an ease of observation. Table 4-8 presents the numerical values used to plot Figure 4-8 and the percentage difference between the infill of the extreme cases (50% and 100%) for every angle. Table 4-9 presents the p-value obtained from the t-tests performed between every infill value grouped under each print angle.

Considering the average results, we can observe a trend in the average values of the shape recovery activation time. This trend becomes more noticeable when taking into account the extreme cases. We can observe that 50% infill samples require less time to activate than 100% infill values for every analyzed print angle. The reason this happens is because 100% infill printed samples require more time for all the material to be heated evenly. The percentage difference between these two levels are 18.71%, 17.92%, 23.49% and 8.68% for 0º, 30º, 60º and 90º pint angles respectively.

Furthermore, the t-tests results in Table 4-9 confirm a statistically significant difference between the print angle extreme cases at every infill percentage value except for the 90º print angle. These results emphasize the tailorable capabilities of shape recovery activation time by altering the infill percentage of the sample.

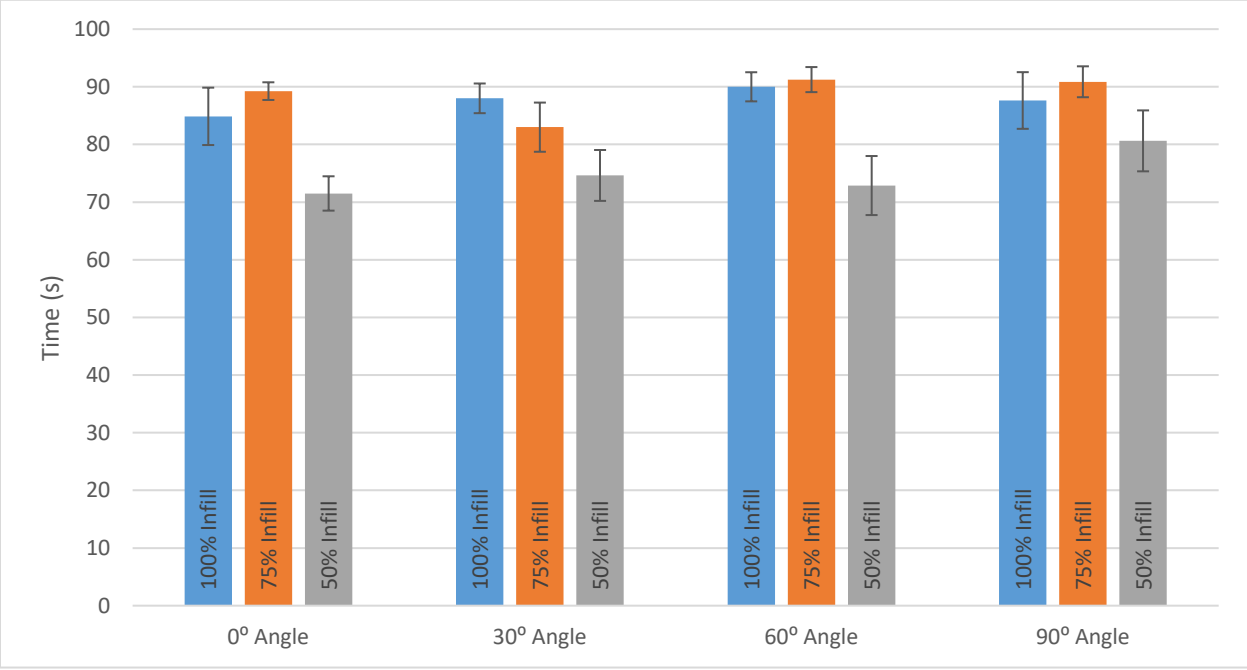

Figure 4-8 Shape Recovery Activation Time grouped under different print angles

Table 4-8 Average Shape Recovery Activation Time (+/- Standard Deviation) Results (s)

	100% Infill	75% Infill	50% Infill	Percent difference between average 50% and 100 % infill values
0° Angle	84.88(+/-4.98)	89.25(+/-1.53)	71.5(+/-2.98)	18.71
30° Angle	88(+/-2.57)	83(+/-4.26)	74.63(+/-4.41)	17.92
60° Angle	90(+/-2.52)	91.25(+/-2.17)	72.88(+/-5.12)	23.49
90° Angle	87.63(+/-4.91)	90.88(+/-2.68)	80.63(+/-5.29)	8.68

Table 4-9 T-tests (95% confidence) results for Shape Recovery Activation Time compared between different infill percentages grouped under different angles

Infill	50%	75%	100%	
50%	----			0°
75%	0.004	----		
100%	0.07	0.453476	----	
50%	----			30°
75%	0.27	----		
100%	0.054	0.43	----	
50%	----			60°
75%	0.31	----		
100%	0.04	0.03	----	
50%	----			90°
75%	0.15	----		
100%	0.36	0.58	----	

Figure 4-9 is plotted using the same values of Figure 4-8; nonetheless, these values were grouped under different infill percentages for ease of observation of the influence that the print angle has on shape recovery activation time. In Table 4-10 we can observe the percentage comparison between printing angle extreme cases, 0º and 90º. Additionally, the t-test results are presented in Table 4-11.

By simple observation of the shape recovery activation time grouped by infill percentages, a trend does not seem to appear when altering the print angle. The shape recovery activation time seems steady within every infill percentage group. Likewise, by analyzing the extreme angle cases for shape recovery activation time we find low percentage differences between each other which are 3.14%, 1.79% and 11.32% for 100%, 75% and 50% infill respectively. Furthermore, none of the t-test results show a statistical difference between any print angle level. These results demonstrate that the print angle has no significant influence in the shape recovery activation time.

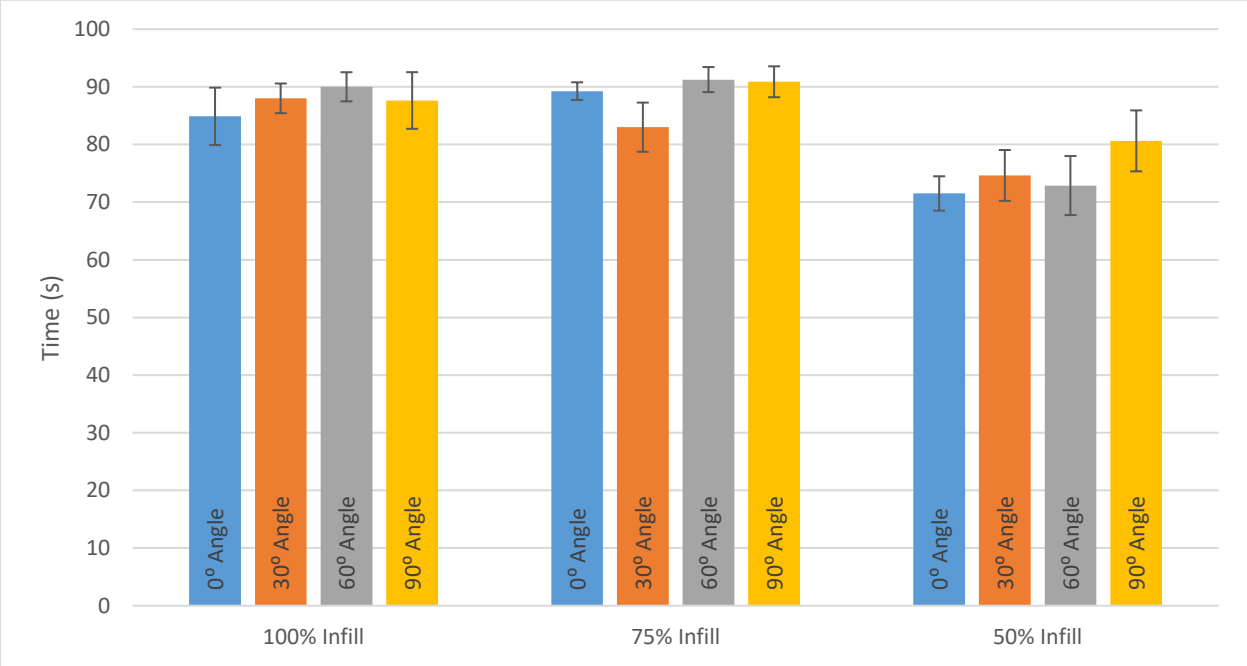

Figure 4-9 Shape Recovery Activation Time grouped under different infill percentages

Table 4-10 Percentage comparison between extreme angle cases for Shape Recovery Activation Time

	Percent difference between average 0° Angle and 90° Angle infill values
100% Infill	3.14%
75% Infill	1.79%
50% Infill	11.32%

Table 4-11 T-tests results for Shape Recovery Activation Time compared between different angles grouped under different infill percentages

Angles	0	30	60	90	
0	-----				50%
30	0.60	-----			
60	0.30	0.59	-----		
90	0.70	0.94	0.68	----	
0	-----				75%
30	0.33	-----			
60	0.45	0.22	-----		
90	0.62	0.25	0.91	----	
0	-----				100%
30	0.58	-----			
60	0.93	0.91	-----		
90	0.19	0.41	0.65	----	

4.4.5 Shape Memory Recovery Force

Figure 4-10 displays the change in shape memory recovery force and its standard deviation with respect to infill percentages grouped under different print angle.

Table 4-12 Table 4-12 outlines the values used for plotting Figure 4-10 and the comparison of the percent difference in the average results of the extreme cases of infill percentage for all printing angles. Table 4-13 shows the results for the t-test between every infill percentage for all the analyzed printing angles.

Figure 4-10 shows a similar trend to that of shape recovery activation time. The higher the infill percentage the higher the shape recovery force. However, the difference for the extreme cases is much higher. Moreover, the t-test results present a statistically significant difference between all the infill percentage extreme values except for 0º angle. Additionally, the t-test results show a

statistical difference between the extreme cases but between 50% and 75% infill as well for all angles except 0º angle, and between 75% and 100% for 60º and 90º angle. These results support the trend stating that the higher the infill percentage the more shape memory recovery force the sample exerts.

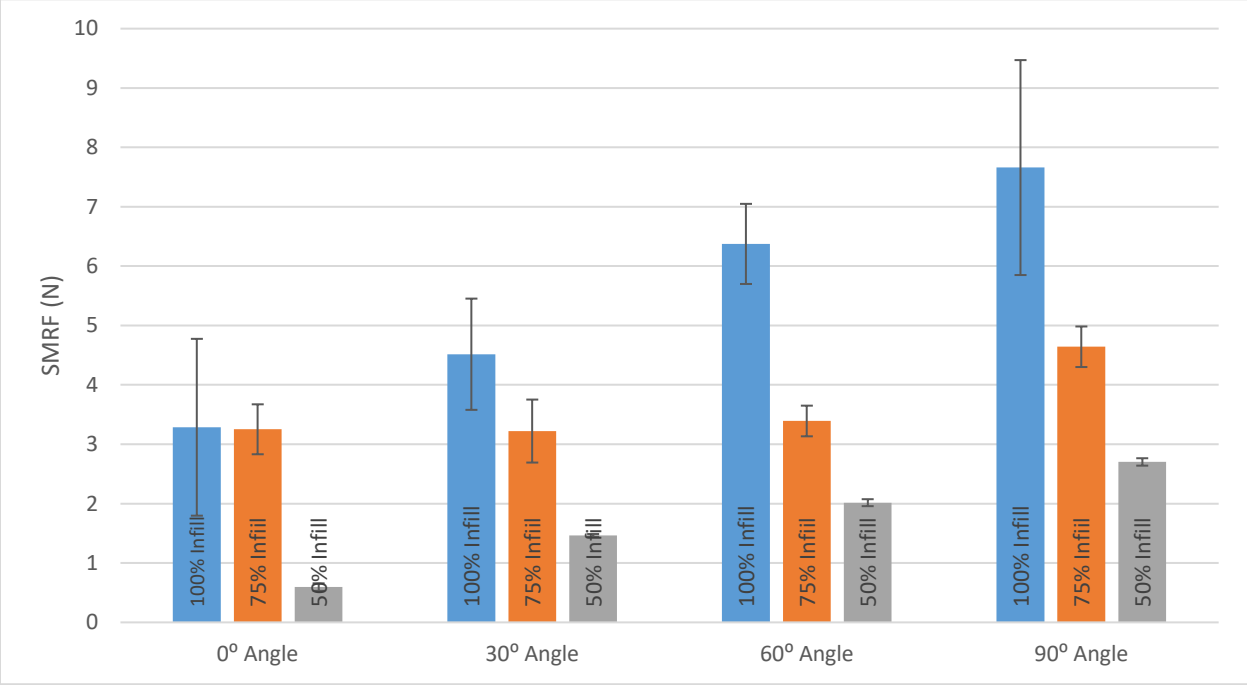

Figure 4-10 Shape Memory Recovery Force grouped under different print angles

Table 4-12 Average Shape Memory Recovery Force (+/- Standard Deviation) Results (N)

	100% Infill	75% Infill	50% Infill	Percent difference between average 50% and 100 % infill values
0° Angle	3.29(+/-1.49)	3.25(+/-0.42)	0.59(+/-0.06)	453.2%
30° Angle	4.52(+/-0.94)	3.22(+/-0.53)	1.47(+/-0.02)	208.26%
60° Angle	6.37(+/-0.67)	3.39(+/-0.26)	2.02(+/-0.06)	216.17%
90° Angle	7.66(+/-1.81)	4.64(+/-0.34)	2.7(+/-0.06)	183.49%

Table 4-13 T-tests (95% confidence) results for Shape Recovery Force compared between different infill percentages grouped under different angles

Infill	50%	75%	100%	
50%	----			0° Angle
75%	0.002	----		
100%	0.14	0.98	----	
50%	----			30° Angle
75%	0.03	----		
100%	0.03	0.27	----	
50%	----			60° Angle
75%	0.004	----		
100%	0.002	0.008	----	
50%	----			90° Angle
75%	0.004	----		
100%	0.007	0.03	----	

Figure 4-11 is plotted using the same values of Figure 4-10; however, the values were grouped under different infills for ease of observation in discussing the influence of the print angle on the shape memory recovery force. Table 4-14 displays the percent difference between extreme angle cases at every infill percentage level. Table 4-15 presents the results of the t-tests performed with a 95% confidence level.

Figure 4-11 shows an increasing tendency with the increase of printing angle for every infill percentage. Additionally, the analysis of the percent difference between the extreme cases in Table 4-14 corroborates this tendency. However, when analyzing the t tests results in Table 4-15, we can observe that for samples printed at 100% and 75% infill, we can only find statistically significant difference between the extreme values given the standard deviation of the results. On the other hand, for the 50% infill value, the standard deviation decreases drastically and the values present a significant statistical difference between each other. These values support the increasing tendency of shape memory recovery force and this tendency presents itself clearer when printing at low infill percentages.

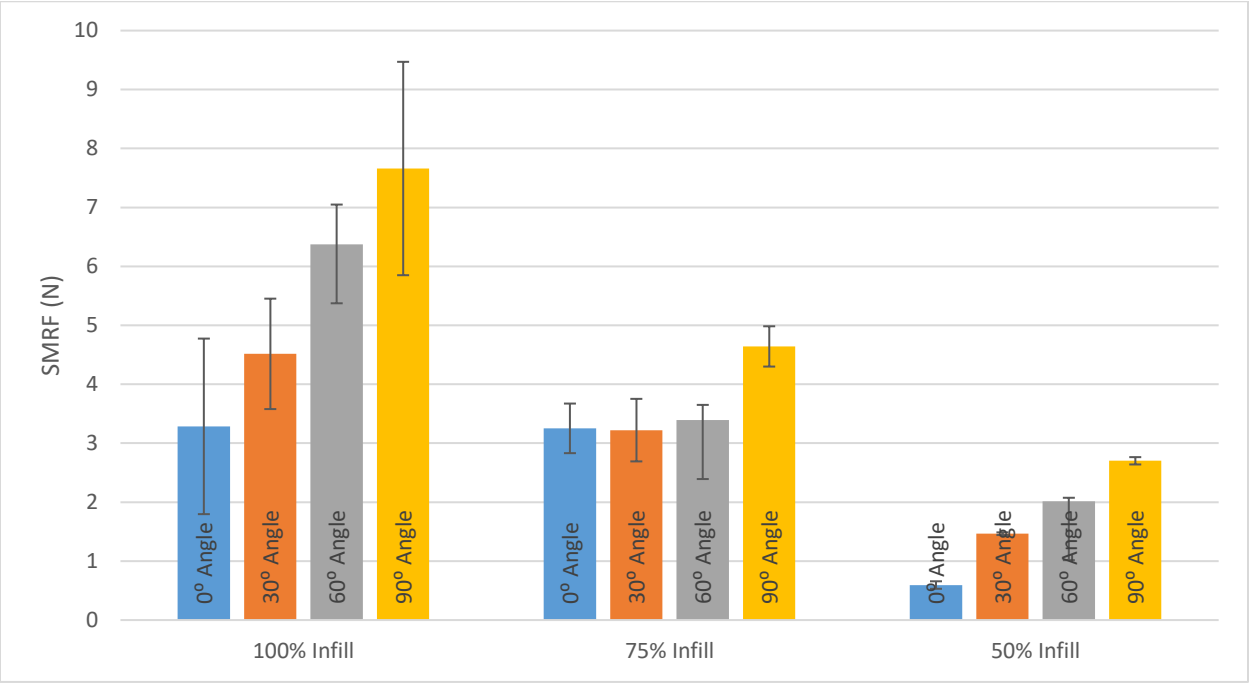

Figure 4-11 Shape Memory Recovery Force grouped under different infill percentages

Table 4-14 Percentage comparison between extreme angle cases for Shape Memory Recovery Force

	Percent difference between average 0° Angle and 90° Angle infill values
100% Infill	133.11%
75% Infill	42.74%
50% Infill	354.88%

Table 4-15 T-tests results for Shape Memory Recovery Force compared between different angles grouped under different infill percentages

Angles	0	30	60	90	
0	-----				50%
30	4.83E-05	-----			
60	2.03E-07	2.66E-05	-----		
90	1.08E-08	7.2E-06	4.38E-05	----	
0	-----				75%
30	0.96	-----			
60	0.78	0.78	-----		
90	0.03	0.06	0.02	----	
0	-----				100%
30	0.51				
60	0.11	0.15	-----		
90	0.04	0.04	0.27	----	

4.5 Conclusions

In this project, the effects of printing orientation and infill percentage on shape memory recovery properties of shape memory polymers specimens constructed by material extrusion additive manufacturing was analyzed. Samples were tested at 3 different infill percentage levels 50% 75% and 100%, and at 4 different print angles 0°, 30°, 60° and 90°. Each test was conducted 5 times. External factors such as humidity proved to disrupt the reliability of the results. In order to obtain consistent results, a preprocessing of the polymer needed to be implemented. Thus, specimens were dried for 12 hours before extrusion. The examined properties were shape memory recovery speed, recovery activation time and shape memory recovery force. In order to determine whether the change of infill percentage or printing angle has a significant influence on the shape memory recovery properties, t-tests at 95% confidence factor were implemented between all levels. This analysis produced the following results:

- The decrease in infill percentage demonstrated to increase in a statistically significant matter the shape memory recovery speed of the samples.
- The variation of printing angle proved to have a statistically significant impact on shape memory recovery speed only when comparing the extreme cases 0° and 90°. Pieces printed at 0° showed a significantly faster recovery speed than pieces printed at 90°.
- The increase in infill percentage proved to increase in a statistically significant matter the time elapsed until the specimen starts recovering its shape.
- A variation in printing angle proved to have no impact in the shape recovery activation time.
- The increase in infill percentage proved to produce a statistically significant rise in the shape memory recovery force.
- Shape memory recovery force showed an increasing trend when printing at a higher angle. However, for 100% infill printed parts, only the difference between 0° and 90° proved to be statistically different. Nonetheless, 50% infill printed parts showed a statistically significant difference between all of their printing angles. Therefore, we can conclude that the higher the printing angle the higher the shape recovery force as well and this difference becomes more significant when printing at lower infill percentages.

4.6 References

[1] A. Lendlein and S. Kelch, "Shape Memory Polymer," in Shape Memory Effect, Teltow, Wiley, 2002, pp. 2034-2037.

[2] J. Guo, Z. Wang, L. Tong, H. Lv and W. Liang, "Shape memory and thermo-mechanical properties of shape memory," Composites, pp. 162-165, 2015.

[3] H. Tamagawa, "Thermo-responsive two-way shape changeable polymeric laminate," Materials Letters, pp. 749-751, 2010.

[4] M. Hager, S. Bode, C. Weber and U. S. Schubert, "Shape memory polymers: Past, present and future," Progress in Polymer Science, pp. 3-33, 2015.

[5] J. Raasch, M. Ivey, D. Aldrich, D. S. Nobes and C. Ayranci, "Characterization of polyurethane shape memory polymer processed," Additive Manufacturing, pp. 132-141, 2015.

[6] C.-S. Zhang and Q.-Q. Ni, "Bending behavior of shape memory polymer based laminates," composite structures, pp. 153-156, 2005.

[7] H. Meng and G. Li, "A review of stimuli-responsive shape memory polymer composites," Polymer, pp. 2199-2221, 2013.

[8] O. Mohamed, S. Masood and J. Bhowmik, "Optimization of fused deposition modeling process parameters:," Advanced Manufacture, pp. 42-53, 2015.

[9] B. Wendel, D. Rietzel, F. Kuhnlein and R. Feulner, "Additive Processing of Polymers".

[10] C. Bellehumeur, L. Li, Q. Sun and P. Gu, "Modeling of Bond Formation Between Polymer Filaments in the Fused Deposition Modeling Process," Journal of Manufacturing Processes, pp. 170-179, 2004.

[11] H. Tobushi, D. Shimada, S. Hayashi and M. Endo, "Shape fixity and shape recovery of polyurethane shape-memory polymer foams," Materials: Design and Applications, vol. 217, pp. 135-143, 2003.

[12] P. Baldi and A. Long, "A Bayesian framework for the analysis of microarray expression data: regularized t-test and statistical inferences of gene changes," Bioinformatics, vol. 17, pp. 509-519, 2001.

5 CONCLUSIONS AND FUTURE WORK

The effects of print orientation and infill percentage on tensile properties of shape memory polymer samples processed by material extrusion additive manufacturing was studied. In order to obtain reliable results, a filament production process had to be implemented. External factors such as humidity proved to affect the mechanical properties of the tested specimens. Thus, preprocessing procedure of the material was established in order to minimize and regulate this external factor. Specimens were tested at three different infill percentage levels; 50% 75% and 100%, while print angle was tested at 0°, 30°, 60° and 90° and each test was conducted 5 times for repeatability purposes. The tensile properties examined were elastic modulus, UTS and maximum strain. T-tests at 95% confidence factor were implemented to compare all levels between each other producing the following results:

- The increase of infill percentage proved to increase the elastic modulus in a statistically significant manner.
- The decrease of print angle increased the elastic modulus. However, the more the infill percentage lowers the significant impact of change of print angle on elastic modulus.
- The increase of infill percentage proved to increase the UTS in a statistically significant manner.
- The decrease of print angle increased the UTS. However, the more the infill percentage lowers the more significant the impact of change of print angle on UTS becomes.
- Regarding maximum strain, the results showed that the higher the infill percentage the higher maximum strain becomes except when the sample is printed at 0°. Nevertheless, for 30°, 60° and 90° manufactured samples only the 100% infill level showed to be statistically different.

- When analyzing print angle, only 0° angle printed samples showed a statistical difference except for 100% infill level. When printing at 0°, 100% and 50% infill levels showed to be statistically higher that 75% but had no difference between each other.

Additionally, the effects of printing orientation and infill percentage on shape memory recovery properties of shape memory polymers specimens constructed by material extrusion additive manufacturing was analyzed as well. Similar to the mechanical properties analysis, samples were tested at three different infill percentage levels 50% 75% and 100%, and at four different print angles 0°, 30°, 60° and 90°. Each test was conducted five times. The examined properties were shape memory recovery speed, recovery activation time and shape memory recovery force. In order to determine whether the change of infill percentage or printing angle has a significant influence on the shape memory recovery properties, t-tests at 95% confidence factor were implemented between all levels. This analysis produced the following results:

- The decrease in infill percentage demonstrated to increase in a statistically significant matter the shape memory recovery speed of the samples.
- The variation of printing angle proved to have a statistically significant impact on shape memory recovery speed only when comparing the extreme cases 0° and 90°. Pieces printed at 0° showed a significantly faster recovery speed than pieces printed at 90°.
- The increase in infill percentage proved to increase in a statistically significant matter the time elapsed until the specimen starts recovering its shape.
- A variation in printing angle proved to have no impact in the shape recovery activation time.

- The increase in infill percentage proved to produce a statistically significant rise in the shape memory recovery force.
- Shape memory recovery force showed an increasing trend when printing at a higher angle. However, for 100% infill printed parts, only the difference between 0° and 90° proved to be statistically different. Nonetheless, 50% infill printed parts showed a statistically significant difference between all of their printing angles. Therefore, we can conclude that the higher the printing angle the higher the shape recovery force as well and this difference becomes more significant when printing at lower infill percentages.

This thesis offers an important foundation on which further research can be built on. To begin with, given that tensile and shape recovery properties of FDM parts are tailorable, a mathematical model can be obtained to anticipate the appropriate infill percentage and print angle levels needed to obtain the tensile and shape recovery values required of a specific design/application.

Additionally, the tailorability of more mechanical properties can be analyzed. For example, by performing an impact test with FDM samples manufactured with different levels of infill percentage and print angle, toughness of the material can be outlines. This would provide a more complete idea of the interaction between manufacture and mechanical properties of FDM parts.

Furthermore, additional components (reinforcements or functional additives) could be added to the SMP filament during the filament manufacture process. FDM manufactured samples produced with this new filament could be tested and determine whether additional components can improve the mechanical and shape recovery properties of the part.

For tensile properties, the results could be compared to the classical lamination theory of composite materials. If results are similar, additional research could be performed to define whether FDM

produced parts can be analyzed with the same procedures as advanced composite materials. If this were the case, additional analysis could be performed before manufacture such as failure analysis.

Finally, based on the results of this work, parts can be designed for different applications and the appropriate infill percentage and printing angle can be predetermined.

6 BIBLIOGRAPHY

ASTM, 2015. *Standard Test Method for Tensile Properties of Plastics,* s.l.: DESIGNATION: D638 - 14.

Chia, H. & Wu, B., 2015. Recent advances in 3D printing of biomaterials. *Journal of Biological Engineering,* pp. 2-14.

Gibson, I., 2017. The changing face of additive manufacturing. *Journal of Manufacturing Technology Management,* 28(1), pp. 10-17.

Gibson, I., Rosen, D. & Stucker, B., 2015. *Additive Manufacturing Technologies.* New York: Springer.

Guo, J. et al., 2015. Shape memory and thermo-mechanical properties of shape memory. *Composites,* pp. 162-165.

Hager, M., Bode, S., Weber, C. & Schubert, U. S., 2015. Shape memory polymers: Past, present and future. *Progress in Polymer Science,* pp. 3-33.

Khoo, Z. X. et al., 2015. 3D printing of smart materials: A review on recent progresses in 4D printing. *Virtual and Physical Prototyping,* 10(3), pp. 103-122.

Lendlein, A. & Kelch, S., 2002. Shape Memory Polymer. In: *Shape Memory Effect.* Teltow: Wiley, pp. 2034-2037.

Liu, C., Qin, H. & Mather, P., 2007. Review of progress in shape-memory polymers. *Journal of Materials Chemistry,* Volume 17, pp. 1543-1558.

Montgomery, D., 2013. *Design and Analysis of Experiments.* Tempe: Wiley.

Raasch, J. et al., 2015. Characterization of polyurethane shape memory polymer processed. *Additive Manufacturing,* pp. 132-141.

Rauwendaal, C., 2014. *Polymer Extrusion.* Munich: Hanser.

SMP Technologies, 2012. *Shape Memory Polymer.* [Online] Available at: http://www2.smptechno.com/en/smp/ [Accessed February 2016].

Tadmor, Z. & Gogos, C., 2006. *Principles of Polymer Processing.* Hoboken : Wiley.

Tamagawa, H., 2010. Thermo-responsive two-way shape changeable polymeric laminate. *Materials Letters,* pp. 749-751.

Tymrak, B., Kreiger, M. & J.M.Pearce, 2014. Mechanical Properties of Components fabricated with open source 3-D printes under realistic environmental conditions. *Materials and Design,* Volume 58, pp. 242-246.

Ultimaker, n.d. *Ultimaker 2+ Speceifications.* [Online] [Accessed 06 2016].

Wong, K. & Hernandez, A., 2012. A Review of Additive Manufacturing. *ISRN Mechanical Engineering,* Volume 2012, p. 10.

Wu, W. et al., 2015. Influence of Layer Thickness and Raster Angle on the Mechanical Properties of 3D-Printed PEEK and a Comparative Mechanical Study between PEEK and ABS. *Open Access Materials,* Volume 8, pp. 5835-5846.

Yang, Y., Chen, Y., Wei, Y. & Li, Y., 2015. 3D printing of shape memory polymer for functional part fabrication. *Advanced Manufacturing Technologies.*

Zhang, C.-S. & Ni, Q.-Q., 2005. Bending behavior of shape memory polymer based laminates. *composite structures,* pp. 153-156.

APPENDICES

Appendix A: A Load Cell Filtering Process

The recovery force applied by the SMP piece while trying to recover was obtained by an analog load cell. This load cell's signal was sampled by a data acquisition system (DAQ) made by the same company as the testing equipment (Wintest 7, BOSE). The load cell used in this test can measure forces up to 350 [N] and the DAQ has a 12-bit resolution. This means that we had steps of 0.085[N] per bit for the analog to digital conversion. Furthermore, the data was sampled at a frequency of 10Hz. Given that the recovery force signal changed very slowly every minute and we are sampling the signal 10 times per second, we can safely assume that our sampling rate is significantly higher than the Nyquist sampling rate and we will not have any aliasing problems. In figure A1, we can appreciate an example of the raw data. In this figure, we can observe that the signal has a high amount of noise in it that needs to be filtered out in order to obtain the highest quality signal possible.

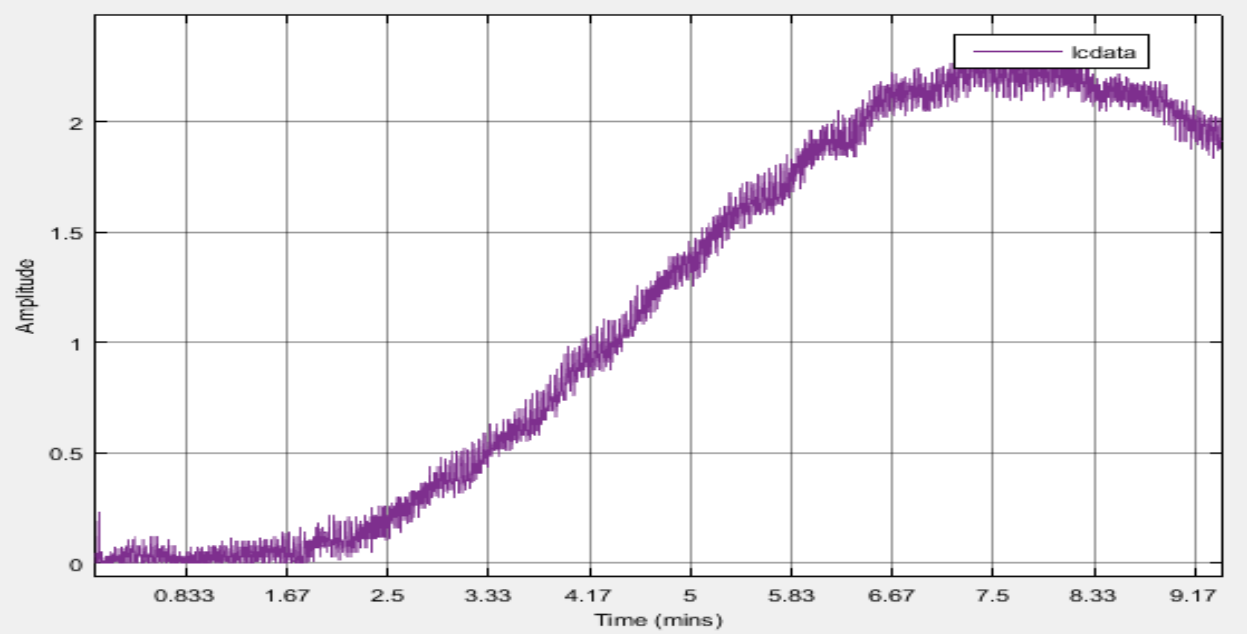

Figure A1 Load Cell Raw Data

In order to have a better appreciation of the parameters of the signal, this was processed by applying the Fourier Transformation and the magnitude and phase responses were obtained. As seen in figure A2. In this figure, we can appreciate that most if not all the signal is contained between 0 and 0.5 Hertz.

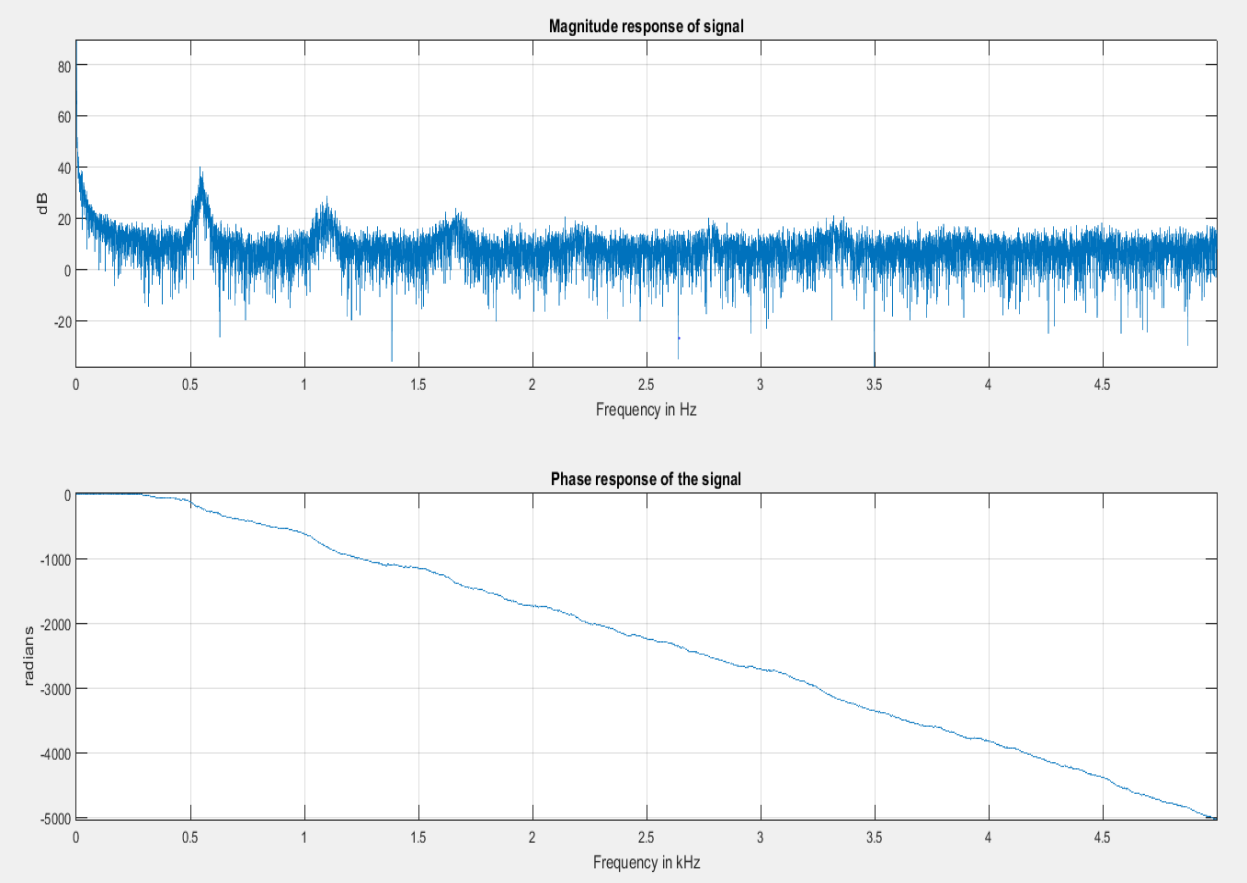

Figure A2 Magnitude and Phase Response

The main objective of the designed filter is to greatly reduce noise without increasing or diminishing the signal values. Time shift was not considered important for this application since the data will be analyzed after is obtained. Nonetheless, it was extremely important for the purposes of the investigation that the value of the signal was not increased or reduced. Taking this

into account, and remembering that the data of the signal was contained between 0 and 0.5 Hz, the following parameters were chosen in order to design our filter.

Lowpass filter

PB edge 0.15 Hz

SB edge 0.5 Hz

SB Attenuation=40dB

Sampling frequency=10Hz

Gain at 40 Db=0.01

In order to begin the filter design process, first we have to choose an appropriate filter window that will meet our requirements. For this application, a Hanning window was used. This will be beneficial for the implementation of the filter. Subsequently, the following steps were followed for the design of the filter.

1st Step: Find the edge frequency in Hz for the filter in the middle of the transition width

$$f1 = Desired\ pass\ band\ edge\ frequency + Transition\frac{width}{2} f1 = 0.15 + \frac{0.35}{2}$$

$$= 0.325\ [Hz]$$

2nd Step: Find the value of Ω1

$$\Omega 1 = \frac{2\pi f1}{fs} = \frac{2\pi 0.325}{10} = \frac{13 * \pi}{200}$$

$$f1 = frequency\ value\ obtained\ on\ step\ 1$$

$$fs = sampling\ frequency$$

Thus, we replace this value in h1 [n], which is the infinite impulse response for an ideal low-pass filter:

$$h1[n] = \frac{\sin(n * \Omega 1)}{n * \pi}$$

$$h1[n] = \frac{\sin\left(n * \frac{13\pi}{200}\right)}{n * \pi}$$

3rd Step: Calculate number of non-zero window terms. We use an odd number of terms to obtain an impulse response that is perfectly symmetrical. This will avoid phase distortion in final filter.

Number of terms for Hanning Window

$$Number\ of\ Terms = 3.32 * \frac{sampling\ frequency}{transition\ width} Number\ of\ Terms = 3.32 * \frac{10}{0.325}$$

$$= 102.1 \approx \mathbf{103}$$

4th Step: Evaluate window function

$$\omega[n]\ for\ |n| \leq \frac{N-1}{2}$$

Window function for Hanning window

$$\omega[n] = 0.5 + \frac{0.5\cos(2\pi * n)}{N-1} \omega[n] = 0.5 + \frac{0.5\cos(2\pi * n)}{102}$$

5th Step: Calculate finite impulse response

$$h[n] = h1[n] * \omega[n] \; for \; |n| \leq \frac{N-1}{2}$$

For steps 4 and 5, Matlab software was used to acquire the 103 terms. Furthermore, the impulse response has been shifted to the right by 51 terms and plotted in order to obtain the filters causal impulse response on figure A3.

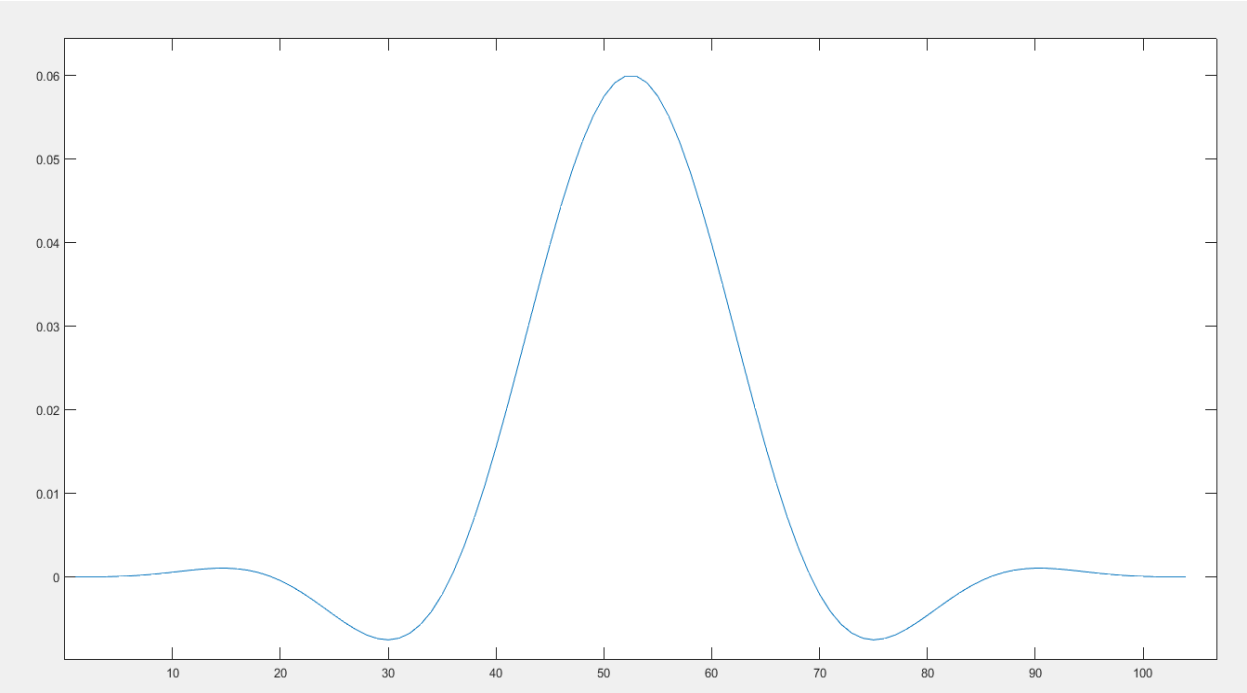

Figure A3 Low pass Filter Causal impulse response

Likewise, the pole zero map and the Magnitude response of the filter were found via Matlab. By looking at the Magnitude response on figure A4 we can observe that the passband edge is located at 0.159 Hz and the stopband edge is located at 0.487 Hz. Hence, we can conclude that the pre-established parameters for the filter were met.

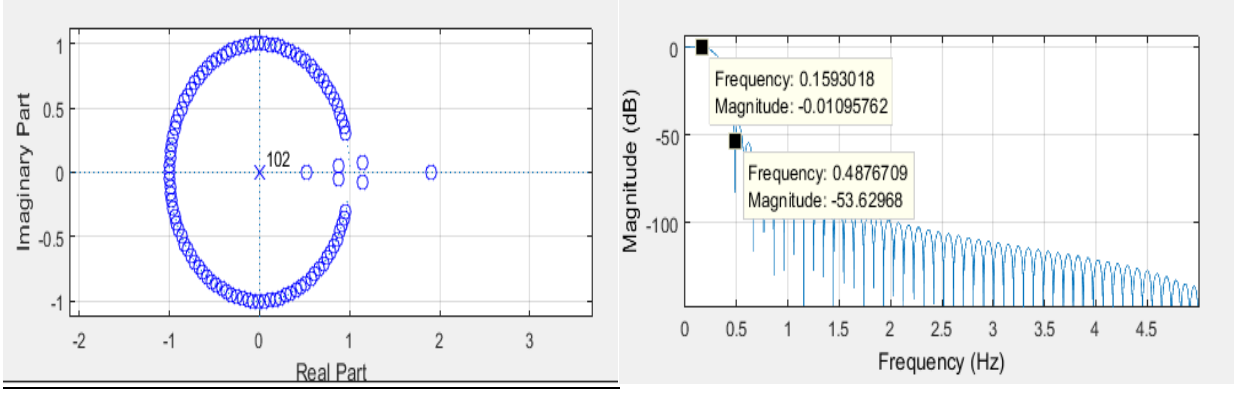

Figure A4 Pole Zero Map and Magnitude Response of Lowpass Filter

Now that we obtained our lowpass filter, we can acquire the filtered signal by convoluting the original signal with the designed filter. On figure A5 we can observe our filtered signal.

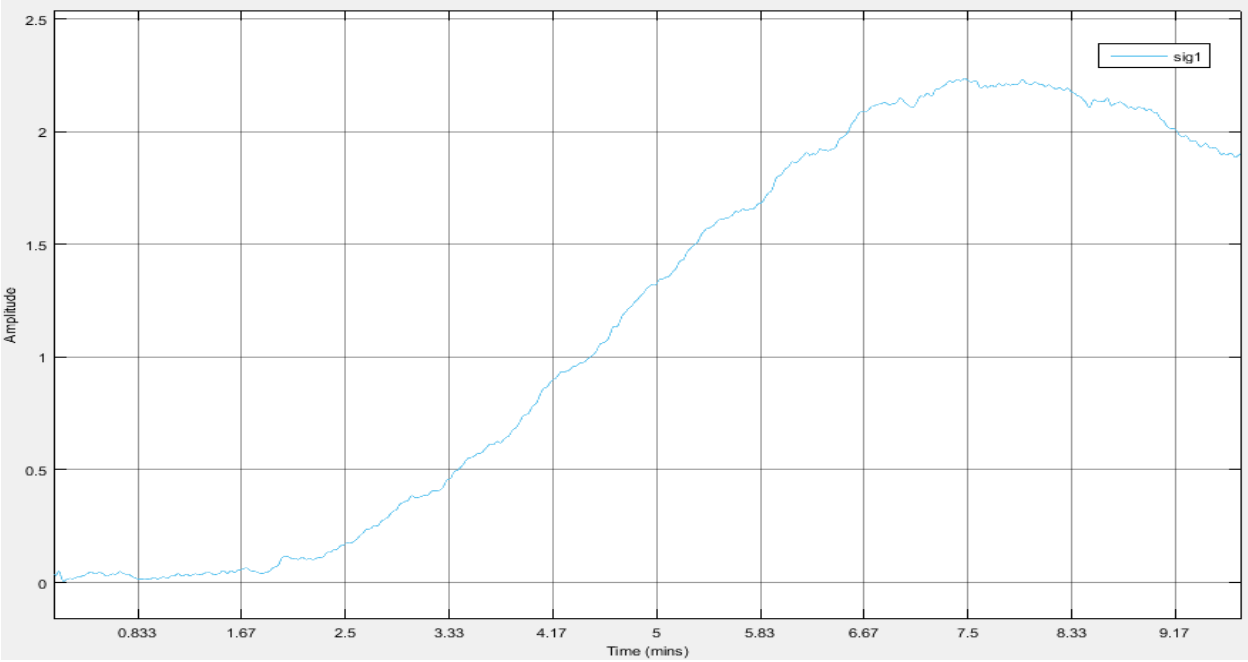

Figure A5 Filtered Signal

As we can appreciate the noise has been greatly filtered out and the values of our signal have not increased nor decreased their value.

Furtheremore, by analyzing the frequency response of the filtered signal on figure A6, we can clearly observe how the data containing frequencies over 0.5 Hz has completely dissapeared.

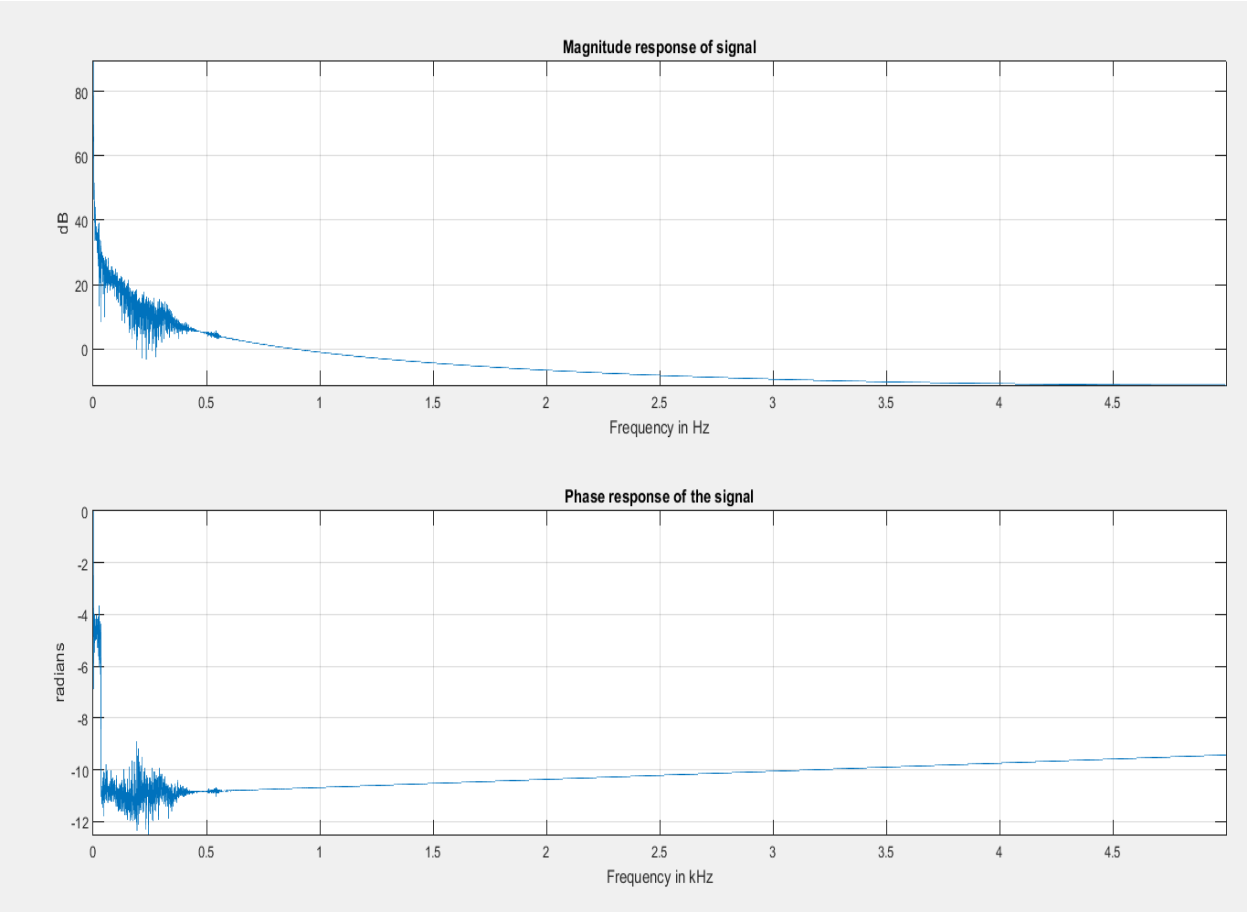

Figure 13 Frequency Response of filtered signal

Appendix B: Sensor Filtering Matlab Program

```
Fs = 10;
Nfft=length(datay);
F = ((0:1/NFFT:1-1/NFFT)*Fs).';
dataf=fft(datay,Nfft);
magnitudef = abs(dataf);        % Magnitude of the FFT
phasef = unwrap(angle(dataf));  % Phase of the FFT

helperFrequencyAnalysisPlot3(F,magnitudef,phasef,NFFT)
```

```
function helperFrequencyAnalysisPlot1(F,Ymag,Yangle,NFFT,ttlMag,ttlPhase)
% Plot helper function for the FrequencyAnalysisExample

% Copyright 2012 The MathWorks, Inc.

figure
subplot(2,1,1)
plot(F(1:NFFT/2)/1,20*log10(Ymag(1:NFFT/2)));
if nargin > 4 && ~isempty(ttlMag)
  tstr = {'Magnitude response of signal',ttlMag};
else
  tstr = {'Magnitude response of signal'};
end
title(tstr)
xlabel('Frequency in Hz')
ylabel('dB')
grid on;
axis tight
subplot(2,1,2)
plot(F(1:NFFT/2)/1,Yangle(1:NFFT/2));
if nargin > 5
  tstr = {'Phase response of the signal',ttlPhase};
else
  tstr = {'Phase response of the signal'};
end
title(tstr)
xlabel('Frequency in kHz')
ylabel('radians')
grid on;
axis tight
```

Appendix C: Fiji-Image J Speckle Tracking Program

```
i=0;

while(i<1500)

{

makeRectangle(1172, 232, 772, 2416)

run("Crop");

setOption("BlackBackground", false);

run("Make Binary");

run("Subtract Background...", "rolling=30 light create");

run("Make Binary");

doWand(340, 136);

run("Measure");

call("MTrack2_.setProperty","minSize","2");

call("MTrack2_.setProperty","maxSize","20");

call("MTrack2_.setProperty","minTrackLength","3");

call("MTrack2_.setProperty","maxVelocity","4");

call("MTrack2_.setProperty","saveResultsFile","false");
```

```
call("MTrack2_.setProperty","showPaths","true");

call("MTrack2_.setProperty","showPathLengths","true");

call("MTrack2_.setProperty","showLabels","false");

call("MTrack2_.setProperty","showPositions","true");

call("MTrack2_.setProperty","skipDialogue","true");

run("MTrack2 ");

i=i+1

}
```

Appendix D: Electroforce 3200 Tensile Test Program Code

Upper actuator Fixed at 0

Heating Chamber fixed at 25º C

Lower Actuator:

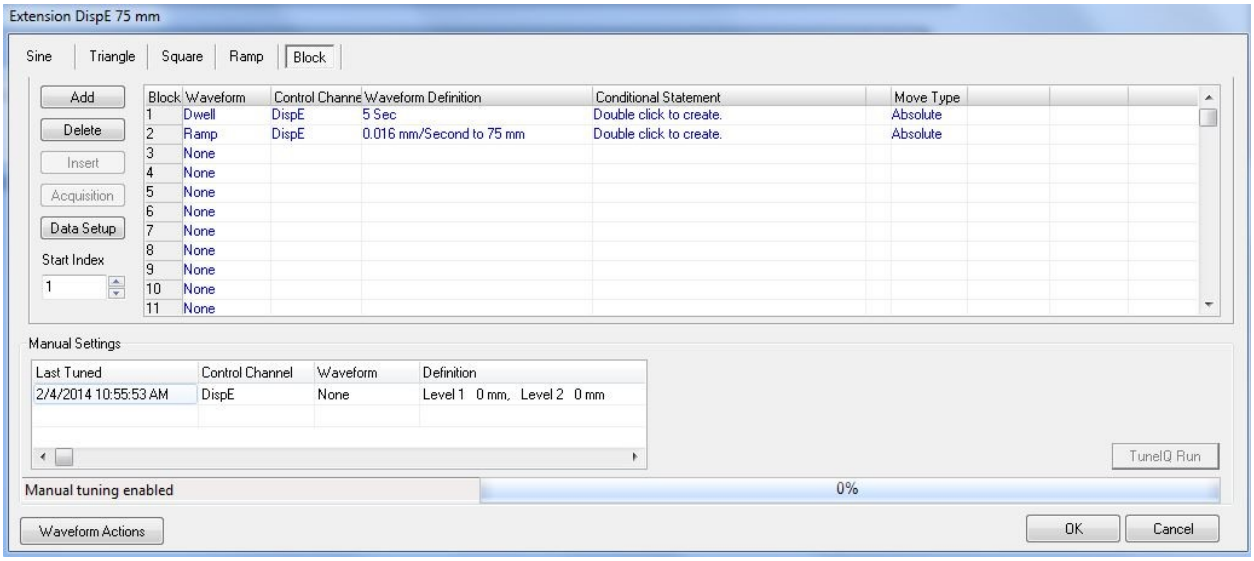

Appendix E: Electroforce 3200 3 Point Bending Test Program Code

Shape Memory Recovery Force Test:

Lower Actuator: Fixed at 0

Upper Actuator:

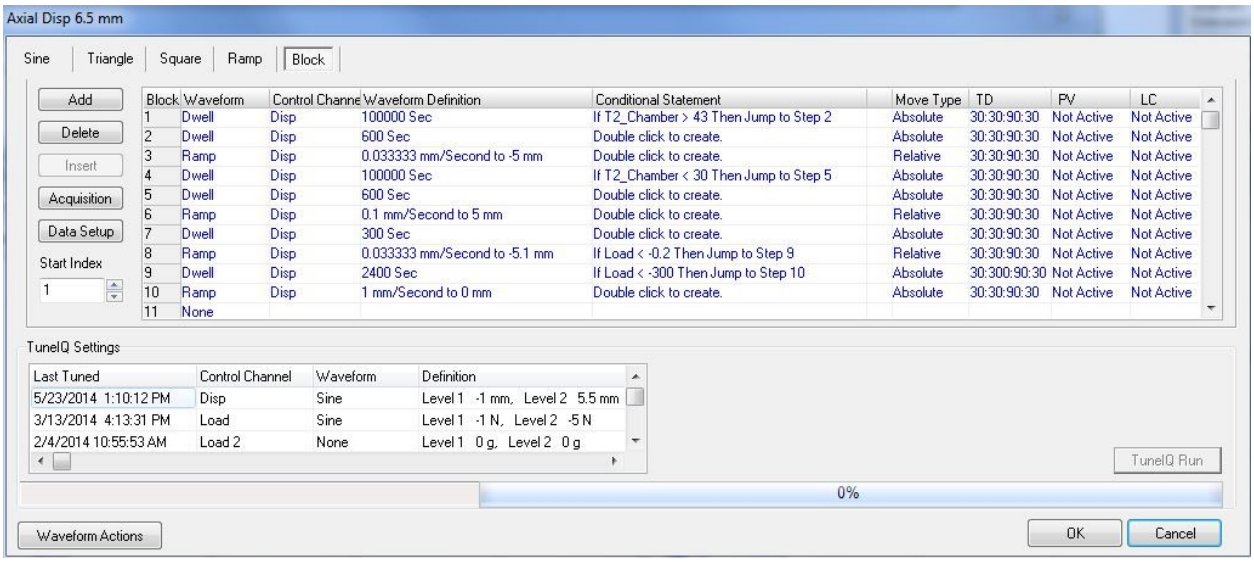

Heating Chamber:

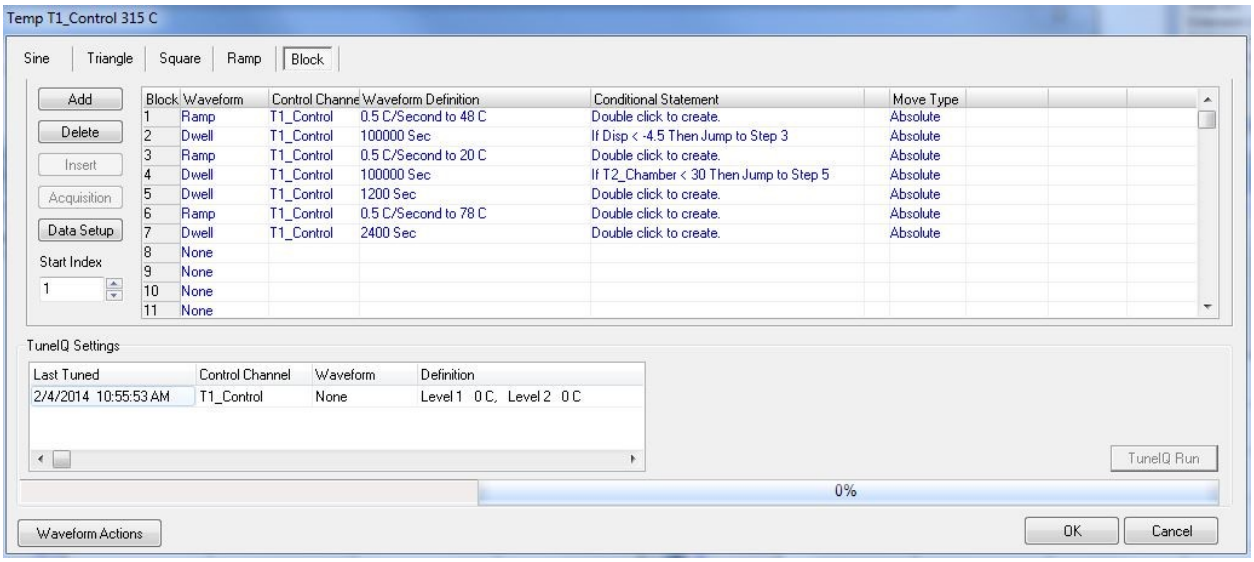

Shape Memory Recovery Ratio Test

Lower Actuator: Fixed at 0

Upper Actuator:

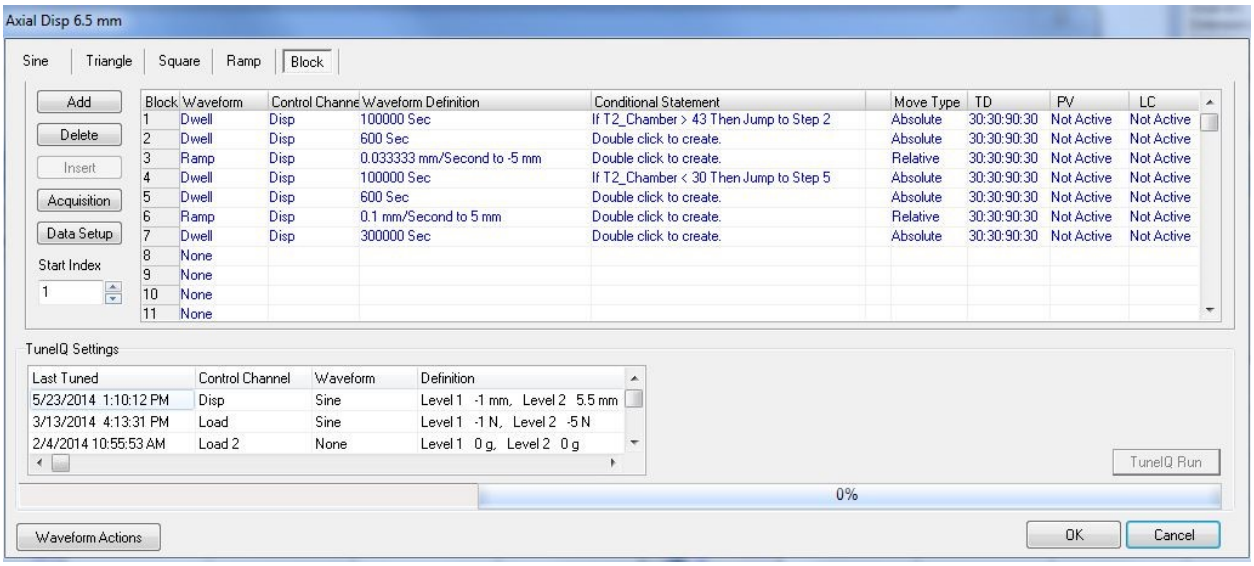

Heating Chamber:

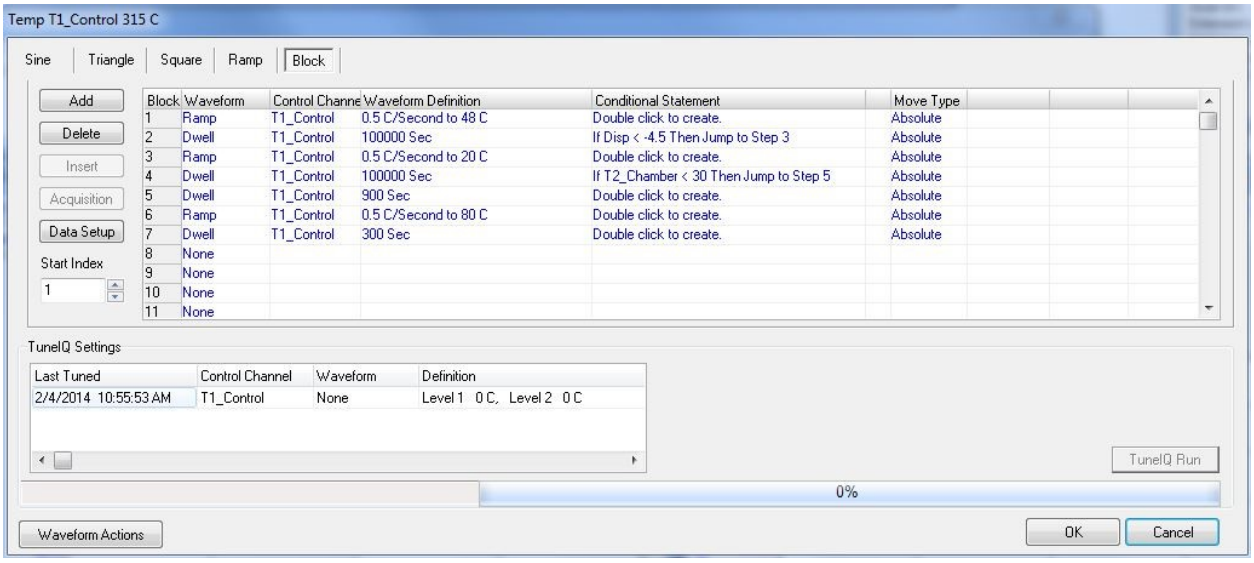

Appendix F: G-Code Example Type V Dogbone [30/-30] at 75% Infill

```
; G-Code generated by Simplify3D(R) Version 3.0.0
; March 23, 2016 at 9:34:27 PM
; Settings Summary
;   processName,Process1
;   applyToModels,type v short
;   profileName,New Printer(7) (modified)
;   profileVersion,2016-12-17 03:22:10
;   baseProfile,Default
;   printMaterial,PLA
;   printQuality,Medium
;   printExtruders,
;   extruderName,Extruder 1
;   extruderToolheadNumber,0
;   extruderDiameter,0.4
;   extruderAutoWidth,0
;   extruderWidth,0.4
;   extrusionMultiplier,0.9
;   extruderUseRetract,1
;   extruderRetractionDistance,1
;   extruderExtraRestartDistance,0
;   extruderRetractionZLift,0
;   extruderRetractionSpeed,1800
;   extruderUseCoasting,0
;   extruderCoastingDistance,0.2
;   extruderUseWipe,0
;   extruderWipeDistance,5
;   primaryExtruder,0
;   layerHeight,0.2
;   topSolidLayers,0
;   bottomSolidLayers,0
;   perimeterOutlines,1
;   printPerimetersInsideOut,1
;   startPointOption,2
;   startPointOriginX,0
;   startPointOriginY,0
;   startPointOriginZ,300
;   sequentialIslands,0
;   spiralVaseMode,0
;   firstLayerHeightPercentage,100
;   firstLayerWidthPercentage,100
;   firstLayerUnderspeed,1
;   useRaft,0
;   raftExtruder,0
;   raftLayers,3
;   raftOffset,3
;   raftSeparationDistance,0.14
;   raftInfill,85
;   disableRaftBaseLayers,0
;   useSkirt,0
;   skirtExtruder,0
;   skirtLayers,1
```

```
;   skirtOutlines,0
;   skirtOffset,4
;   usePrimePillar,0
;   primePillarExtruder,999
;   primePillarWidth,12
;   primePillarLocation,7
;   primePillarSpeedMultiplier,1
;   useOozeShield,0
;   oozeShieldExtruder,999
;   oozeShieldOffset,2
;   oozeShieldOutlines,1
;   oozeShieldSidewallShape,1
;   oozeShieldSidewallAngle,30
;   oozeShieldSpeedMultiplier,1
;   infillExtruder,0
;   internalInfillPattern,Rectilinear
;   externalInfillPattern,Rectilinear
;   infillPercentage,75
;   outlineOverlapPercentage,20
;   infillExtrusionWidthPercentage,100
;   minInfillLength,5
;   infillLayerInterval,1
;   infillAngles,30,150
;   overlapInfillAngles,0
;   generateSupport,0
;   supportExtruder,0
;   supportInfillPercentage,30
;   supportExtraInflation,0
;   denseSupportLayers,0
;   denseSupportInfillPercentage,70
;   supportLayerInterval,1
;   supportHorizontalPartOffset,0.3
;   supportUpperSeparationLayers,1
;   supportLowerSeparationLayers,1
;   supportType,0
;   supportGridSpacing,4
;   maxOverhangAngle,45
;   supportAngles,0
;   temperatureName,Extruder 1 Temperature,Bed
;   temperatureNumber,0,0
;   temperatureSetpointCount,1,1
;   temperatureSetpointLayers,1,1
;   temperatureSetpointTemperatures,220,40
;   temperatureStabilizeAtStartup,1,1
;   temperatureHeatedBed,0,1
;   temperatureRelayBetweenLayers,0,0
;   temperatureRelayBetweenLoops,0,0
;   fanLayers,1,2
;   fanSpeeds,0,100
;   blipFanToFullPower,0
;   adjustSpeedForCooling,1
;   minSpeedLayerTime,15
;   minCoolingSpeedSlowdown,20
;   increaseFanForCooling,0
```

```
;   minFanLayerTime,45
;   maxCoolingFanSpeed,100
;   increaseFanForBridging,0
;   bridgingFanSpeed,100
;   use5D,1
;   relativeEdistances,0
;   allowEaxisZeroing,1
;   independentExtruderAxes,0
;   includeM10123,0
;   stickySupport,1
;   applyToolheadOffsets,0
;   gcodeXoffset,0
;   gcodeYoffset,0
;   gcodeZoffset,0
;   overrideMachineDefinition,1
;   machineTypeOverride,0
;   strokeXoverride,100
;   strokeYoverride,100
;   strokeZoverride,100
;   originOffsetXoverride,0
;   originOffsetYoverride,0
;   originOffsetZoverride,0
;   homeXdirOverride,-1
;   homeYdirOverride,-1
;   homeZdirOverride,-1
;   flipXoverride,1
;   flipYoverride,-1
;   flipZoverride,1
;   toolheadOffsets,0,0|0,0|0,0|0,0|0,0|0,0
;   overrideFirmwareConfiguration,1
;   firmwareTypeOverride,RepRap (Marlin/Repetier/Sprinter)
;   GPXconfigOverride,r2
;   baudRateOverride,115200
;   overridePrinterModels,0
;   printerModelsOverride
;   startingGcode,G28 ; home all axes
;   layerChangeGcode,
;   retractionGcode,
;   toolChangeGcode,
;   endingGcode,M104 S0 ; turn off extruder,M140 S0 ; turn off bed,M84 ;
disable motors
;   createX3G,0
;   celebration,0
;   celebrationSong,Random Song
;   createMB5G,0
;   postProcessing,
;   defaultSpeed,600
;   outlineUnderspeed,0.5
;   solidInfillUnderspeed,0.8
;   supportUnderspeed,0.8
;   rapidXYspeed,4800
;   rapidZspeed,1000
;   minBridgingArea,50
;   bridgingExtraInflation,0
```

```
;   bridgingExtrusionMultiplier,1
;   bridgingSpeedMultiplier,1
;   filamentDiameter,1.75
;   filamentPricePerKg,46
;   filamentDensity,1.25
;   useMinPrintHeight,0
;   minPrintHeight,0
;   useMaxPrintHeight,0
;   maxPrintHeight,0
;   useDiaphragm,0
;   diaphragmLayerInterval,20
;   robustSlicing,1
;   mergeAllIntoSolid,0
;   onlyRetractWhenCrossingOutline,1
;   retractBetweenLayers,1
;   useRetractionMinTravel,0
;   retractionMinTravel,3
;   retractWhileWiping,0
;   onlyWipeOutlines,1
;   avoidCrossingOutline,0
;   maxMovementDetourFactor,3
;   toolChangeRetractionDistance,12
;   toolChangeExtraRestartDistance,-0.5
;   toolChangeRetractionSpeed,600
;   allowThinWallGapFill,1
;   thinWallAllowedOverlapPercentage,10
;   horizontalSizeCompensation,0
G90
M82
M106 S0
M140 S40
M190 S40
M104 S220 T0
M109 S220 T0
G28 ; home all axes
G92 E0
G1 E-1.0000 F1800
G1 Z0.200 F1000
; layer 1, Z = 0.2
T0
; tool H0.200 W0.400
; outer perimeter
G1 X40.435 Y29.965 F4800
G1 E0.0000 F540
G92 E0
G1 X49.565 Y29.965 E0.2733 F300
G1 X49.565 Y41.531 E0.6195
G1 X48.660 Y42.692 E0.6636
G1 X47.858 Y44.022 E0.7101
G1 X47.223 Y45.439 E0.7566
G1 X46.762 Y46.922 E0.8030
G1 X46.483 Y48.450 E0.8495
G1 X46.390 Y49.994 E0.8958
G1 X46.390 Y59.536 E1.1815
```

```
G1 X46.483 Y61.080 E1.2278
G1 X46.762 Y62.608 E1.2743
G1 X47.223 Y64.091 E1.3208
G1 X47.858 Y65.508 E1.3672
G1 X48.659 Y66.838 E1.4137
G1 X49.565 Y67.999 E1.4578
G1 X49.565 Y79.565 E1.8040
G1 X40.435 Y79.565 E2.0773
G1 X40.435 Y67.999 E2.4235
G1 X41.340 Y66.838 E2.4676
G1 X42.142 Y65.508 E2.5141
G1 X42.777 Y64.091 E2.5606
G1 X43.238 Y62.608 E2.6071
G1 X43.517 Y61.080 E2.6535
G1 X43.610 Y59.536 E2.6998
G1 X43.610 Y49.994 E2.9855
G1 X43.517 Y48.450 E3.0318
G1 X43.238 Y46.922 E3.0783
G1 X42.777 Y45.439 E3.1248
G1 X42.142 Y44.022 E3.1712
G1 X41.340 Y42.692 E3.2177
G1 X40.435 Y41.531 E3.2618
G1 X40.435 Y29.965 E3.6080
; infill
G1 X48.466 Y30.285 F4800
G92 E0
G1 X49.245 Y30.735 E0.0269 F600
G1 X49.245 Y31.351 E0.0454
G1 X47.399 Y30.285 E0.1092
G1 X46.333 Y30.285 E0.1411
G1 X49.245 Y31.966 E0.2417
G1 X49.245 Y32.582 E0.2602
G1 X45.266 Y30.285 E0.3977
G1 X44.199 Y30.285 E0.4296
G1 X49.245 Y33.198 E0.6040
G1 X49.245 Y33.814 E0.6225
G1 X43.133 Y30.285 E0.8338
G1 X42.066 Y30.285 E0.8657
G1 X49.245 Y34.430 E1.1138
G1 X49.245 Y35.046 E1.1323
G1 X40.999 Y30.285 E1.4173
G1 X40.755 Y30.285 E1.4246
G1 X40.755 Y30.760 E1.4388
G1 X49.245 Y35.661 E1.7322
G1 X49.245 Y36.277 E1.7507
G1 X40.755 Y31.376 E2.0441
G1 X40.755 Y31.991 E2.0626
G1 X49.245 Y36.893 E2.3560
G1 X49.245 Y37.509 E2.3745
G1 X40.755 Y32.607 E2.6679
G1 X40.755 Y33.223 E2.6864
G1 X49.245 Y38.125 E2.9798
G1 X49.245 Y38.741 E2.9982
G1 X40.755 Y33.839 E3.2917
```

```
G1 X40.755 Y34.455 E3.3101
G1 X49.245 Y39.356 E3.6036
G1 X49.245 Y39.972 E3.6220
G1 X40.755 Y35.071 E3.9155
G1 X40.755 Y35.686 E3.9339
G1 X49.245 Y40.588 E4.2274
G1 X49.245 Y41.204 E4.2458
G1 X40.755 Y36.302 E4.5393
G1 X40.755 Y36.918 E4.5577
G1 X49.030 Y41.696 E4.8437
G1 X48.699 Y42.121 E4.8599
G1 X40.755 Y37.534 E5.1345
G1 X40.755 Y38.150 E5.1529
G1 X48.373 Y42.548 E5.4162
G1 X48.097 Y43.005 E5.4322
G1 X40.755 Y38.766 E5.6859
G1 X40.755 Y39.382 E5.7044
G1 X47.822 Y43.462 E5.9487
G1 X47.574 Y43.873 E5.9630
G1 X47.553 Y43.922 E5.9646
G1 X40.755 Y39.997 E6.1996
G1 X40.755 Y40.613 E6.2180
G1 X47.333 Y44.411 E6.4454
G1 X47.114 Y44.900 E6.4614
G1 X40.755 Y41.229 E6.6812
G1 X40.755 Y41.421 E6.6870
G1 X41.357 Y42.192 E6.7163
G1 X46.902 Y45.394 E6.9079
G1 X46.740 Y45.916 E6.9243
G1 X42.012 Y43.186 E7.0877
G1 X42.426 Y43.873 E7.1117
G1 X42.527 Y44.100 E7.1191
G1 X46.577 Y46.438 E7.2591
G1 X46.451 Y46.846 E7.2719
G1 X46.429 Y46.968 E7.2756
G1 X42.900 Y44.931 E7.3976
G1 X43.077 Y45.326 E7.4105
G1 X43.199 Y45.719 E7.4229
G1 X46.327 Y47.525 E7.5310
G1 X46.225 Y48.082 E7.5479
G1 X43.432 Y46.470 E7.6445
G1 X43.549 Y46.846 E7.6562
G1 X43.612 Y47.189 E7.6667
G1 X46.150 Y48.655 E7.7544
G1 X46.114 Y49.250 E7.7723
G1 X43.738 Y47.878 E7.8544
G1 X43.835 Y48.411 E7.8707
G1 X43.844 Y48.555 E7.8750
G1 X46.078 Y49.845 E7.9522
G1 X46.070 Y49.984 E7.9564
G1 X46.070 Y50.456 E7.9705
G1 X43.882 Y49.193 E8.0461
G1 X43.921 Y49.831 E8.0653
G1 X46.070 Y51.072 E8.1396
```

```
G1 X46.070 Y51.688 E8.1580
G1 X43.930 Y50.452 E8.2320
G1 X43.930 Y51.068 E8.2504
G1 X46.070 Y52.304 E8.3244
G1 X46.070 Y52.919 E8.3428
G1 X43.930 Y51.684 E8.4168
G1 X43.930 Y52.300 E8.4352
G1 X46.070 Y53.535 E8.5092
G1 X46.070 Y54.151 E8.5276
G1 X43.930 Y52.916 E8.6016
G1 X43.930 Y53.531 E8.6200
G1 X46.070 Y54.767 E8.6940
G1 X46.070 Y55.383 E8.7124
G1 X43.930 Y54.147 E8.7864
G1 X43.930 Y54.763 E8.8048
G1 X46.070 Y55.999 E8.8788
G1 X46.070 Y56.614 E8.8972
G1 X43.930 Y55.379 E8.9712
G1 X43.930 Y55.995 E8.9896
G1 X46.070 Y57.230 E9.0636
G1 X46.070 Y57.846 E9.0820
G1 X43.930 Y56.611 E9.1560
G1 X43.930 Y57.226 E9.1744
G1 X46.070 Y58.462 E9.2484
G1 X46.070 Y59.078 E9.2668
G1 X43.930 Y57.842 E9.3408
G1 X43.930 Y58.458 E9.3592
G1 X46.079 Y59.699 E9.4335
G1 X46.118 Y60.337 E9.4527
G1 X43.930 Y59.074 E9.5283
G1 X43.930 Y59.546 E9.5424
G1 X43.922 Y59.685 E9.5466
G1 X46.156 Y60.975 E9.6238
G1 X46.165 Y61.119 E9.6281
G1 X46.262 Y61.652 E9.6444
G1 X43.886 Y60.280 E9.7265
G1 X43.850 Y60.875 E9.7443
G1 X46.388 Y62.341 E9.8321
G1 X46.451 Y62.684 E9.8425
G1 X46.568 Y63.060 E9.8543
G1 X43.775 Y61.448 E9.9508
G1 X43.673 Y62.005 E9.9678
G1 X46.801 Y63.811 E10.0759
G1 X46.923 Y64.204 E10.0882
G1 X47.100 Y64.599 E10.1012
G1 X43.571 Y62.562 E10.2232
G1 X43.549 Y62.684 E10.2269
G1 X43.423 Y63.092 E10.2397
G1 X47.473 Y65.430 E10.3797
G1 X47.574 Y65.657 E10.3871
G1 X47.988 Y66.344 E10.4111
G1 X43.260 Y63.614 E10.5745
G1 X43.098 Y64.136 E10.5909
G1 X48.643 Y67.338 E10.7825
```

```
G1 X49.245 Y68.109 E10.8118
G1 X49.245 Y68.301 E10.8176
G1 X42.886 Y64.630 E11.0373
G1 X42.667 Y65.119 E11.0534
G1 X49.245 Y68.917 E11.2808
G1 X49.245 Y69.533 E11.2992
G1 X42.447 Y65.608 E11.5342
G1 X42.426 Y65.657 E11.5357
G1 X42.178 Y66.068 E11.5501
G1 X49.245 Y70.149 E11.7944
G1 X49.245 Y70.764 E11.8128
G1 X41.903 Y66.525 E12.0666
G1 X41.627 Y66.982 E12.0826
G1 X49.245 Y71.380 E12.3459
G1 X49.245 Y71.996 E12.3643
G1 X41.301 Y67.409 E12.6389
G1 X40.970 Y67.834 E12.6550
G1 X49.245 Y72.612 E12.9411
G1 X49.245 Y73.228 E12.9595
G1 X40.755 Y68.326 E13.2530
G1 X40.755 Y68.942 E13.2714
G1 X49.245 Y73.844 E13.5649
G1 X49.245 Y74.459 E13.5833
G1 X40.755 Y69.558 E13.8768
G1 X40.755 Y70.174 E13.8952
G1 X49.245 Y75.075 E14.1887
G1 X49.245 Y75.691 E14.2071
G1 X40.755 Y70.789 E14.5005
G1 X40.755 Y71.405 E14.5190
G1 X49.245 Y76.307 E14.8124
G1 X49.245 Y76.923 E14.8309
G1 X40.755 Y72.021 E15.1243
G1 X40.755 Y72.637 E15.1428
G1 X49.245 Y77.539 E15.4362
G1 X49.245 Y78.154 E15.4547
G1 X40.755 Y73.253 E15.7481
G1 X40.755 Y73.869 E15.7665
G1 X49.245 Y78.770 E16.0600
G1 X49.245 Y79.245 E16.0742
G1 X49.001 Y79.245 E16.0815
G1 X40.755 Y74.484 E16.3665
G1 X40.755 Y75.100 E16.3850
G1 X47.934 Y79.245 E16.6331
G1 X46.867 Y79.245 E16.6650
G1 X40.755 Y75.716 E16.8763
G1 X40.755 Y76.332 E16.8947
G1 X45.801 Y79.245 E17.0691
G1 X44.734 Y79.245 E17.1011
G1 X40.755 Y76.948 E17.2386
G1 X40.755 Y77.564 E17.2570
G1 X43.667 Y79.245 E17.3577
G1 X42.601 Y79.245 E17.3896
G1 X40.755 Y78.179 E17.4534
G1 X40.755 Y78.795 E17.4719
```

```
G1 X41.534 Y79.245 E17.4988
G92 E0
G1 E-1.0000 F1800
; layer 2, Z = 0.4
M106 S255
; outer perimeter
G1 X40.435 Y79.565 F4800
G1 Z0.400 F1000
G1 E0.0000 F1800
G92 E0
G1 X40.435 Y67.999 E0.3462 F300
G1 X41.340 Y66.838 E0.3903
G1 X42.142 Y65.508 E0.4368
G1 X42.777 Y64.091 E0.4833
G1 X43.238 Y62.608 E0.5297
G1 X43.517 Y61.080 E0.5762
G1 X43.610 Y59.536 E0.6225
G1 X43.610 Y49.994 E0.9082
G1 X43.517 Y48.450 E0.9545
G1 X43.238 Y46.922 E1.0010
G1 X42.777 Y45.439 E1.0475
G1 X42.142 Y44.022 E1.0939
G1 X41.340 Y42.692 E1.1404
G1 X40.435 Y41.531 E1.1845
G1 X40.435 Y29.965 E1.5307
G1 X49.565 Y29.965 E1.8040
G1 X49.565 Y41.531 E2.1502
G1 X48.660 Y42.692 E2.1943
G1 X47.858 Y44.022 E2.2408
G1 X47.223 Y45.439 E2.2873
G1 X46.762 Y46.922 E2.3338
G1 X46.483 Y48.450 E2.3802
G1 X46.390 Y49.994 E2.4265
G1 X46.390 Y59.536 E2.7122
G1 X46.483 Y61.080 E2.7585
G1 X46.762 Y62.608 E2.8050
G1 X47.223 Y64.091 E2.8515
G1 X47.858 Y65.508 E2.8979
G1 X48.659 Y66.838 E2.9444
G1 X49.565 Y67.999 E2.9885
G1 X49.565 Y79.565 E3.3347
G1 X40.435 Y79.565 E3.6080
; infill
G1 X49.245 Y78.795 F4800
G92 E0
G1 X48.466 Y79.245 E0.0269 F600
G1 X47.399 Y79.245 E0.0589
G1 X49.245 Y78.179 E0.1226
G1 X49.245 Y77.564 E0.1411
G1 X46.333 Y79.245 E0.2417
G1 X45.266 Y79.245 E0.2737
G1 X49.245 Y76.948 E0.4112
G1 X49.245 Y76.332 E0.4296
G1 X44.199 Y79.245 E0.6040
```

```
G1 X43.133 Y79.245 E0.6360
G1 X49.245 Y75.716 E0.8472
G1 X49.245 Y75.100 E0.8657
G1 X42.066 Y79.245 E1.1138
G1 X40.999 Y79.245 E1.1457
G1 X49.245 Y74.484 E1.4307
G1 X49.245 Y73.869 E1.4492
G1 X40.755 Y78.770 E1.7426
G1 X40.755 Y78.154 E1.7611
G1 X49.245 Y73.253 E2.0545
G1 X49.245 Y72.637 E2.0730
G1 X40.755 Y77.539 E2.3664
G1 X40.755 Y76.923 E2.3848
G1 X49.245 Y72.021 E2.6783
G1 X49.245 Y71.405 E2.6967
G1 X40.755 Y76.307 E2.9902
G1 X40.755 Y75.691 E3.0086
G1 X49.245 Y70.789 E3.3021
G1 X49.245 Y70.174 E3.3205
G1 X40.755 Y75.075 E3.6140
G1 X40.755 Y74.459 E3.6324
G1 X49.245 Y69.558 E3.9259
G1 X49.245 Y68.942 E3.9443
G1 X40.755 Y73.844 E4.2378
G1 X40.755 Y73.228 E4.2562
G1 X49.245 Y68.326 E4.5496
G1 X49.245 Y68.109 E4.5561
G1 X49.030 Y67.834 E4.5666
G1 X40.755 Y72.612 E4.8526
G1 X40.755 Y71.996 E4.8711
G1 X48.699 Y67.409 E5.1457
G1 X48.395 Y67.020 E5.1604
G1 X48.373 Y66.982 E5.1618
G1 X40.755 Y71.380 E5.4251
G1 X40.755 Y70.764 E5.4435
G1 X48.097 Y66.525 E5.6973
G1 X47.822 Y66.068 E5.7133
G1 X40.755 Y70.149 E5.9575
G1 X40.755 Y69.533 E5.9760
G1 X47.553 Y65.608 E6.2109
G1 X47.333 Y65.119 E6.2270
G1 X40.755 Y68.917 E6.4543
G1 X40.755 Y68.301 E6.4728
G1 X47.114 Y64.630 E6.6926
G1 X46.923 Y64.204 E6.7065
G1 X46.902 Y64.136 E6.7087
G1 X41.357 Y67.338 E6.9003
G1 X41.605 Y67.020 E6.9124
G1 X42.012 Y66.344 E6.9360
G1 X46.740 Y63.614 E7.0994
G1 X46.577 Y63.092 E7.1158
G1 X42.527 Y65.430 E7.2558
G1 X42.900 Y64.599 E7.2831
G1 X46.429 Y62.562 E7.4050
```

```
G1 X46.327 Y62.005 E7.4220
G1 X43.199 Y63.811 E7.5301
G1 X43.432 Y63.060 E7.5536
G1 X46.225 Y61.448 E7.6501
G1 X46.165 Y61.119 E7.6601
G1 X46.150 Y60.875 E7.6674
G1 X43.612 Y62.341 E7.7552
G1 X43.738 Y61.652 E7.7761
G1 X46.114 Y60.280 E7.8583
G1 X46.078 Y59.685 E7.8761
G1 X43.844 Y60.975 E7.9534
G1 X43.882 Y60.337 E7.9725
G1 X46.070 Y59.074 E8.0481
G1 X46.070 Y58.458 E8.0665
G1 X43.921 Y59.699 E8.1408
G1 X43.930 Y59.546 E8.1454
G1 X43.930 Y59.078 E8.1594
G1 X46.070 Y57.842 E8.2334
G1 X46.070 Y57.226 E8.2518
G1 X43.930 Y58.462 E8.3258
G1 X43.930 Y57.846 E8.3442
G1 X46.070 Y56.611 E8.4182
G1 X46.070 Y55.995 E8.4367
G1 X43.930 Y57.230 E8.5106
G1 X43.930 Y56.614 E8.5291
G1 X46.070 Y55.379 E8.6030
G1 X46.070 Y54.763 E8.6215
G1 X43.930 Y55.999 E8.6954
G1 X43.930 Y55.383 E8.7139
G1 X46.070 Y54.147 E8.7878
G1 X46.070 Y53.531 E8.8063
G1 X43.930 Y54.767 E8.8802
G1 X43.930 Y54.151 E8.8987
G1 X46.070 Y52.916 E8.9726
G1 X46.070 Y52.300 E8.9911
G1 X43.930 Y53.535 E9.0650
G1 X43.930 Y52.919 E9.0835
G1 X46.070 Y51.684 E9.1574
G1 X46.070 Y51.068 E9.1759
G1 X43.930 Y52.304 E9.2499
G1 X43.930 Y51.688 E9.2683
G1 X46.070 Y50.452 E9.3423
G1 X46.070 Y49.984 E9.3563
G1 X46.079 Y49.831 E9.3609
G1 X43.930 Y51.072 E9.4351
G1 X43.930 Y50.456 E9.4536
G1 X46.118 Y49.193 E9.5292
G1 X46.156 Y48.555 E9.5483
G1 X43.922 Y49.845 E9.6256
G1 X43.886 Y49.250 E9.6434
G1 X46.262 Y47.878 E9.7256
G1 X46.388 Y47.189 E9.7465
G1 X43.850 Y48.655 E9.8343
G1 X43.835 Y48.411 E9.8416
```

```
G1 X43.775 Y48.082 E9.8516
G1 X46.568 Y46.470 E9.9481
G1 X46.801 Y45.720 E9.9716
G1 X43.673 Y47.525 E10.0797
G1 X43.571 Y46.968 E10.0967
G1 X47.100 Y44.931 E10.2186
G1 X47.473 Y44.100 E10.2459
G1 X43.423 Y46.438 E10.3859
G1 X43.260 Y45.916 E10.4023
G1 X47.988 Y43.186 E10.5657
G1 X48.395 Y42.510 E10.5893
G1 X48.643 Y42.192 E10.6014
G1 X43.098 Y45.394 E10.7930
G1 X43.077 Y45.326 E10.7952
G1 X42.886 Y44.900 E10.8091
G1 X49.245 Y41.229 E11.0289
G1 X49.245 Y40.613 E11.0473
G1 X42.667 Y44.411 E11.2747
G1 X42.447 Y43.922 E11.2908
G1 X49.245 Y39.997 E11.5257
G1 X49.245 Y39.382 E11.5441
G1 X42.178 Y43.462 E11.7884
G1 X41.903 Y43.005 E11.8044
G1 X49.245 Y38.766 E12.0582
G1 X49.245 Y38.150 E12.0766
G1 X41.627 Y42.548 E12.3399
G1 X41.605 Y42.510 E12.3412
G1 X41.301 Y42.121 E12.3560
G1 X49.245 Y37.534 E12.6306
G1 X49.245 Y36.918 E12.6490
G1 X40.970 Y41.696 E12.9351
G1 X40.755 Y41.421 E12.9455
G1 X40.755 Y41.204 E12.9520
G1 X49.245 Y36.302 E13.2455
G1 X49.245 Y35.686 E13.2639
G1 X40.755 Y40.588 E13.5574
G1 X40.755 Y39.972 E13.5758
G1 X49.245 Y35.071 E13.8693
G1 X49.245 Y34.455 E13.8877
G1 X40.755 Y39.357 E14.1812
G1 X40.755 Y38.741 E14.1996
G1 X49.245 Y33.839 E14.4930
G1 X49.245 Y33.223 E14.5115
G1 X40.755 Y38.125 E14.8049
G1 X40.755 Y37.509 E14.8234
G1 X49.245 Y32.607 E15.1168
G1 X49.245 Y31.991 E15.1353
G1 X40.755 Y36.893 E15.4287
G1 X40.755 Y36.277 E15.4472
G1 X49.245 Y31.376 E15.7406
G1 X49.245 Y30.760 E15.7590
G1 X40.755 Y35.661 E16.0525
G1 X40.755 Y35.046 E16.0709
G1 X49.001 Y30.285 E16.3559
```

```
G1 X47.934 Y30.285 E16.3879
G1 X40.755 Y34.430 E16.6360
G1 X40.755 Y33.814 E16.6545
G1 X46.867 Y30.285 E16.8657
G1 X45.801 Y30.285 E16.8977
G1 X40.755 Y33.198 E17.0721
G1 X40.755 Y32.582 E17.0905
G1 X44.734 Y30.285 E17.2280
G1 X43.667 Y30.285 E17.2600
G1 X40.755 Y31.966 E17.3606
G1 X40.755 Y31.351 E17.3791
G1 X42.601 Y30.285 E17.4429
G1 X41.534 Y30.285 E17.4748
G1 X40.755 Y30.735 E17.5017
G92 E0
G1 E-1.0000 F1800
; layer 3, Z = 0.6
; outer perimeter
G1 X40.435 Y29.965 F4800
G1 Z0.600 F1000
G1 E0.0000 F1800
G92 E0
G1 X49.565 Y29.965 E0.2733 F300
G1 X49.565 Y41.531 E0.6195
G1 X48.660 Y42.692 E0.6636
G1 X47.858 Y44.022 E0.7101
G1 X47.223 Y45.439 E0.7566
G1 X46.762 Y46.922 E0.8030
G1 X46.483 Y48.450 E0.8495
G1 X46.390 Y49.994 E0.8958
G1 X46.390 Y59.536 E1.1815
G1 X46.483 Y61.080 E1.2278
G1 X46.762 Y62.608 E1.2743
G1 X47.223 Y64.091 E1.3208
G1 X47.858 Y65.508 E1.3672
G1 X48.659 Y66.838 E1.4137
G1 X49.565 Y67.999 E1.4578
G1 X49.565 Y79.565 E1.8040
G1 X40.435 Y79.565 E2.0773
G1 X40.435 Y67.999 E2.4235
G1 X41.340 Y66.838 E2.4676
G1 X42.142 Y65.508 E2.5141
G1 X42.777 Y64.091 E2.5606
G1 X43.238 Y62.608 E2.6071
G1 X43.517 Y61.080 E2.6535
G1 X43.610 Y59.536 E2.6998
G1 X43.610 Y49.994 E2.9855
G1 X43.517 Y48.450 E3.0318
G1 X43.238 Y46.922 E3.0783
G1 X42.777 Y45.439 E3.1248
G1 X42.142 Y44.022 E3.1712
G1 X41.340 Y42.692 E3.2177
G1 X40.435 Y41.531 E3.2618
G1 X40.435 Y29.965 E3.6080
```

```
; infill
G1 X48.466 Y30.285 F4800
G92 E0
G1 X49.245 Y30.735 E0.0269 F600
G1 X49.245 Y31.351 E0.0454
G1 X47.399 Y30.285 E0.1092
G1 X46.333 Y30.285 E0.1411
G1 X49.245 Y31.966 E0.2417
G1 X49.245 Y32.582 E0.2602
G1 X45.266 Y30.285 E0.3977
G1 X44.199 Y30.285 E0.4296
G1 X49.245 Y33.198 E0.6040
G1 X49.245 Y33.814 E0.6225
G1 X43.133 Y30.285 E0.8338
G1 X42.066 Y30.285 E0.8657
G1 X49.245 Y34.430 E1.1138
G1 X49.245 Y35.046 E1.1323
G1 X40.999 Y30.285 E1.4173
G1 X40.755 Y30.285 E1.4246
G1 X40.755 Y30.760 E1.4388
G1 X49.245 Y35.661 E1.7322
G1 X49.245 Y36.277 E1.7507
G1 X40.755 Y31.376 E2.0441
G1 X40.755 Y31.991 E2.0626
G1 X49.245 Y36.893 E2.3560
G1 X49.245 Y37.509 E2.3745
G1 X40.755 Y32.607 E2.6679
G1 X40.755 Y33.223 E2.6864
G1 X49.245 Y38.125 E2.9798
G1 X49.245 Y38.741 E2.9982
G1 X40.755 Y33.839 E3.2917
G1 X40.755 Y34.455 E3.3101
G1 X49.245 Y39.356 E3.6036
G1 X49.245 Y39.972 E3.6220
G1 X40.755 Y35.071 E3.9155
G1 X40.755 Y35.686 E3.9339
G1 X49.245 Y40.588 E4.2274
G1 X49.245 Y41.204 E4.2458
G1 X40.755 Y36.302 E4.5393
G1 X40.755 Y36.918 E4.5577
G1 X49.030 Y41.696 E4.8437
G1 X48.699 Y42.121 E4.8599
G1 X40.755 Y37.534 E5.1345
G1 X40.755 Y38.150 E5.1529
G1 X48.373 Y42.548 E5.4162
G1 X48.097 Y43.005 E5.4322
G1 X40.755 Y38.766 E5.6859
G1 X40.755 Y39.382 E5.7044
G1 X47.822 Y43.462 E5.9487
G1 X47.574 Y43.873 E5.9630
G1 X47.553 Y43.922 E5.9646
G1 X40.755 Y39.997 E6.1996
G1 X40.755 Y40.613 E6.2180
G1 X47.333 Y44.411 E6.4454
```

```
G1 X47.114 Y44.900 E6.4614
G1 X40.755 Y41.229 E6.6812
G1 X40.755 Y41.421 E6.6870
G1 X41.357 Y42.192 E6.7163
G1 X46.902 Y45.394 E6.9079
G1 X46.740 Y45.916 E6.9243
G1 X42.012 Y43.186 E7.0877
G1 X42.426 Y43.873 E7.1117
G1 X42.527 Y44.100 E7.1191
G1 X46.577 Y46.438 E7.2591
G1 X46.451 Y46.846 E7.2719
G1 X46.429 Y46.968 E7.2756
G1 X42.900 Y44.931 E7.3976
G1 X43.077 Y45.326 E7.4105
G1 X43.199 Y45.719 E7.4229
G1 X46.327 Y47.525 E7.5310
G1 X46.225 Y48.082 E7.5479
G1 X43.432 Y46.470 E7.6445
G1 X43.549 Y46.846 E7.6562
G1 X43.612 Y47.189 E7.6667
G1 X46.150 Y48.655 E7.7544
G1 X46.114 Y49.250 E7.7723
G1 X43.738 Y47.878 E7.8544
G1 X43.835 Y48.411 E7.8707
G1 X43.844 Y48.555 E7.8750
G1 X46.078 Y49.845 E7.9522
G1 X46.070 Y49.984 E7.9564
G1 X46.070 Y50.456 E7.9705
G1 X43.882 Y49.193 E8.0461
G1 X43.921 Y49.831 E8.0653
G1 X46.070 Y51.072 E8.1396
G1 X46.070 Y51.688 E8.1580
G1 X43.930 Y50.452 E8.2320
G1 X43.930 Y51.068 E8.2504
G1 X46.070 Y52.304 E8.3244
G1 X46.070 Y52.919 E8.3428
G1 X43.930 Y51.684 E8.4168
G1 X43.930 Y52.300 E8.4352
G1 X46.070 Y53.535 E8.5092
G1 X46.070 Y54.151 E8.5276
G1 X43.930 Y52.916 E8.6016
G1 X43.930 Y53.531 E8.6200
G1 X46.070 Y54.767 E8.6940
G1 X46.070 Y55.383 E8.7124
G1 X43.930 Y54.147 E8.7864
G1 X43.930 Y54.763 E8.8048
G1 X46.070 Y55.999 E8.8788
G1 X46.070 Y56.614 E8.8972
G1 X43.930 Y55.379 E8.9712
G1 X43.930 Y55.995 E8.9896
G1 X46.070 Y57.230 E9.0636
G1 X46.070 Y57.846 E9.0820
G1 X43.930 Y56.611 E9.1560
G1 X43.930 Y57.226 E9.1744
```

```
G1 X46.070 Y58.462 E9.2484
G1 X46.070 Y59.078 E9.2668
G1 X43.930 Y57.842 E9.3408
G1 X43.930 Y58.458 E9.3592
G1 X46.079 Y59.699 E9.4335
G1 X46.118 Y60.337 E9.4527
G1 X43.930 Y59.074 E9.5283
G1 X43.930 Y59.546 E9.5424
G1 X43.922 Y59.685 E9.5466
G1 X46.156 Y60.975 E9.6238
G1 X46.165 Y61.119 E9.6281
G1 X46.262 Y61.652 E9.6444
G1 X43.886 Y60.280 E9.7265
G1 X43.850 Y60.875 E9.7443
G1 X46.388 Y62.341 E9.8321
G1 X46.451 Y62.684 E9.8425
G1 X46.568 Y63.060 E9.8543
G1 X43.775 Y61.448 E9.9508
G1 X43.673 Y62.005 E9.9678
G1 X46.801 Y63.811 E10.0759
G1 X46.923 Y64.204 E10.0882
G1 X47.100 Y64.599 E10.1012
G1 X43.571 Y62.562 E10.2232
G1 X43.549 Y62.684 E10.2269
G1 X43.423 Y63.092 E10.2397
G1 X47.473 Y65.430 E10.3797
G1 X47.574 Y65.657 E10.3871
G1 X47.988 Y66.344 E10.4111
G1 X43.260 Y63.614 E10.5745
G1 X43.098 Y64.136 E10.5909
G1 X48.643 Y67.338 E10.7825
G1 X49.245 Y68.109 E10.8118
G1 X49.245 Y68.301 E10.8176
G1 X42.886 Y64.630 E11.0373
G1 X42.667 Y65.119 E11.0534
G1 X49.245 Y68.917 E11.2808
G1 X49.245 Y69.533 E11.2992
G1 X42.447 Y65.608 E11.5342
G1 X42.426 Y65.657 E11.5357
G1 X42.178 Y66.068 E11.5501
G1 X49.245 Y70.149 E11.7944
G1 X49.245 Y70.764 E11.8128
G1 X41.903 Y66.525 E12.0666
G1 X41.627 Y66.982 E12.0826
G1 X49.245 Y71.380 E12.3459
G1 X49.245 Y71.996 E12.3643
G1 X41.301 Y67.409 E12.6389
G1 X40.970 Y67.834 E12.6550
G1 X49.245 Y72.612 E12.9411
G1 X49.245 Y73.228 E12.9595
G1 X40.755 Y68.326 E13.2530
G1 X40.755 Y68.942 E13.2714
G1 X49.245 Y73.844 E13.5649
G1 X49.245 Y74.459 E13.5833
```

```
G1 X40.755 Y69.558 E13.8768
G1 X40.755 Y70.174 E13.8952
G1 X49.245 Y75.075 E14.1887
G1 X49.245 Y75.691 E14.2071
G1 X40.755 Y70.789 E14.5005
G1 X40.755 Y71.405 E14.5190
G1 X49.245 Y76.307 E14.8124
G1 X49.245 Y76.923 E14.8309
G1 X40.755 Y72.021 E15.1243
G1 X40.755 Y72.637 E15.1428
G1 X49.245 Y77.539 E15.4362
G1 X49.245 Y78.154 E15.4547
G1 X40.755 Y73.253 E15.7481
G1 X40.755 Y73.869 E15.7665
G1 X49.245 Y78.770 E16.0600
G1 X49.245 Y79.245 E16.0742
G1 X49.001 Y79.245 E16.0815
G1 X40.755 Y74.484 E16.3665
G1 X40.755 Y75.100 E16.3850
G1 X47.934 Y79.245 E16.6331
G1 X46.867 Y79.245 E16.6650
G1 X40.755 Y75.716 E16.8763
G1 X40.755 Y76.332 E16.8947
G1 X45.801 Y79.245 E17.0691
G1 X44.734 Y79.245 E17.1011
G1 X40.755 Y76.948 E17.2386
G1 X40.755 Y77.564 E17.2570
G1 X43.667 Y79.245 E17.3577
G1 X42.601 Y79.245 E17.3896
G1 X40.755 Y78.179 E17.4534
G1 X40.755 Y78.795 E17.4719
G1 X41.534 Y79.245 E17.4988
G92 E0
G1 E-1.0000 F1800
; layer 4, Z = 0.8
; outer perimeter
G1 X40.435 Y79.565 F4800
G1 Z0.800 F1000
G1 E0.0000 F1800
G92 E0
G1 X40.435 Y67.999 E0.3462 F300
G1 X41.340 Y66.838 E0.3903
G1 X42.142 Y65.508 E0.4368
G1 X42.777 Y64.091 E0.4833
G1 X43.238 Y62.608 E0.5297
G1 X43.517 Y61.080 E0.5762
G1 X43.610 Y59.536 E0.6225
G1 X43.610 Y49.994 E0.9082
G1 X43.517 Y48.450 E0.9545
G1 X43.238 Y46.922 E1.0010
G1 X42.777 Y45.439 E1.0475
G1 X42.142 Y44.022 E1.0939
G1 X41.340 Y42.692 E1.1404
G1 X40.435 Y41.531 E1.1845
```

```
G1 X40.435 Y29.965 E1.5307
G1 X49.565 Y29.965 E1.8040
G1 X49.565 Y41.531 E2.1502
G1 X48.660 Y42.692 E2.1943
G1 X47.858 Y44.022 E2.2408
G1 X47.223 Y45.439 E2.2873
G1 X46.762 Y46.922 E2.3338
G1 X46.483 Y48.450 E2.3802
G1 X46.390 Y49.994 E2.4265
G1 X46.390 Y59.536 E2.7122
G1 X46.483 Y61.080 E2.7585
G1 X46.762 Y62.608 E2.8050
G1 X47.223 Y64.091 E2.8515
G1 X47.858 Y65.508 E2.8979
G1 X48.659 Y66.838 E2.9444
G1 X49.565 Y67.999 E2.9885
G1 X49.565 Y79.565 E3.3347
G1 X40.435 Y79.565 E3.6080
; infill
G1 X49.245 Y78.795 F4800
G92 E0
G1 X48.466 Y79.245 E0.0269 F600
G1 X47.399 Y79.245 E0.0589
G1 X49.245 Y78.179 E0.1226
G1 X49.245 Y77.564 E0.1411
G1 X46.333 Y79.245 E0.2417
G1 X45.266 Y79.245 E0.2737
G1 X49.245 Y76.948 E0.4112
G1 X49.245 Y76.332 E0.4296
G1 X44.199 Y79.245 E0.6040
G1 X43.133 Y79.245 E0.6360
G1 X49.245 Y75.716 E0.8472
G1 X49.245 Y75.100 E0.8657
G1 X42.066 Y79.245 E1.1138
G1 X40.999 Y79.245 E1.1457
G1 X49.245 Y74.484 E1.4307
G1 X49.245 Y73.869 E1.4492
G1 X40.755 Y78.770 E1.7426
G1 X40.755 Y78.154 E1.7611
G1 X49.245 Y73.253 E2.0545
G1 X49.245 Y72.637 E2.0730
G1 X40.755 Y77.539 E2.3664
G1 X40.755 Y76.923 E2.3848
G1 X49.245 Y72.021 E2.6783
G1 X49.245 Y71.405 E2.6967
G1 X40.755 Y76.307 E2.9902
G1 X40.755 Y75.691 E3.0086
G1 X49.245 Y70.789 E3.3021
G1 X49.245 Y70.174 E3.3205
G1 X40.755 Y75.075 E3.6140
G1 X40.755 Y74.459 E3.6324
G1 X49.245 Y69.558 E3.9259
G1 X49.245 Y68.942 E3.9443
G1 X40.755 Y73.844 E4.2378
```

```
G1 X40.755 Y73.228 E4.2562
G1 X49.245 Y68.326 E4.5496
G1 X49.245 Y68.109 E4.5561
G1 X49.030 Y67.834 E4.5666
G1 X40.755 Y72.612 E4.8526
G1 X40.755 Y71.996 E4.8711
G1 X48.699 Y67.409 E5.1457
G1 X48.395 Y67.020 E5.1604
G1 X48.373 Y66.982 E5.1618
G1 X40.755 Y71.380 E5.4251
G1 X40.755 Y70.764 E5.4435
G1 X48.097 Y66.525 E5.6973
G1 X47.822 Y66.068 E5.7133
G1 X40.755 Y70.149 E5.9575
G1 X40.755 Y69.533 E5.9760
G1 X47.553 Y65.608 E6.2109
G1 X47.333 Y65.119 E6.2270
G1 X40.755 Y68.917 E6.4543
G1 X40.755 Y68.301 E6.4728
G1 X47.114 Y64.630 E6.6926
G1 X46.923 Y64.204 E6.7065
G1 X46.902 Y64.136 E6.7087
G1 X41.357 Y67.338 E6.9003
G1 X41.605 Y67.020 E6.9124
G1 X42.012 Y66.344 E6.9360
G1 X46.740 Y63.614 E7.0994
G1 X46.577 Y63.092 E7.1158
G1 X42.527 Y65.430 E7.2558
G1 X42.900 Y64.599 E7.2831
G1 X46.429 Y62.562 E7.4050
G1 X46.327 Y62.005 E7.4220
G1 X43.199 Y63.811 E7.5301
G1 X43.432 Y63.060 E7.5536
G1 X46.225 Y61.448 E7.6501
G1 X46.165 Y61.119 E7.6601
G1 X46.150 Y60.875 E7.6674
G1 X43.612 Y62.341 E7.7552
G1 X43.738 Y61.652 E7.7761
G1 X46.114 Y60.280 E7.8583
G1 X46.078 Y59.685 E7.8761
G1 X43.844 Y60.975 E7.9534
G1 X43.882 Y60.337 E7.9725
G1 X46.070 Y59.074 E8.0481
G1 X46.070 Y58.458 E8.0665
G1 X43.921 Y59.699 E8.1408
G1 X43.930 Y59.546 E8.1454
G1 X43.930 Y59.078 E8.1594
G1 X46.070 Y57.842 E8.2334
G1 X46.070 Y57.226 E8.2518
G1 X43.930 Y58.462 E8.3258
G1 X43.930 Y57.846 E8.3442
G1 X46.070 Y56.611 E8.4182
G1 X46.070 Y55.995 E8.4367
G1 X43.930 Y57.230 E8.5106
```

```
G1 X43.930 Y56.614 E8.5291
G1 X46.070 Y55.379 E8.6030
G1 X46.070 Y54.763 E8.6215
G1 X43.930 Y55.999 E8.6954
G1 X43.930 Y55.383 E8.7139
G1 X46.070 Y54.147 E8.7878
G1 X46.070 Y53.531 E8.8063
G1 X43.930 Y54.767 E8.8802
G1 X43.930 Y54.151 E8.8987
G1 X46.070 Y52.916 E8.9726
G1 X46.070 Y52.300 E8.9911
G1 X43.930 Y53.535 E9.0650
G1 X43.930 Y52.919 E9.0835
G1 X46.070 Y51.684 E9.1574
G1 X46.070 Y51.068 E9.1759
G1 X43.930 Y52.304 E9.2499
G1 X43.930 Y51.688 E9.2683
G1 X46.070 Y50.452 E9.3423
G1 X46.070 Y49.984 E9.3563
G1 X46.079 Y49.831 E9.3609
G1 X43.930 Y51.072 E9.4351
G1 X43.930 Y50.456 E9.4536
G1 X46.118 Y49.193 E9.5292
G1 X46.156 Y48.555 E9.5483
G1 X43.922 Y49.845 E9.6256
G1 X43.886 Y49.250 E9.6434
G1 X46.262 Y47.878 E9.7256
G1 X46.388 Y47.189 E9.7465
G1 X43.850 Y48.655 E9.8343
G1 X43.835 Y48.411 E9.8416
G1 X43.775 Y48.082 E9.8516
G1 X46.568 Y46.470 E9.9481
G1 X46.801 Y45.720 E9.9716
G1 X43.673 Y47.525 E10.0797
G1 X43.571 Y46.968 E10.0967
G1 X47.100 Y44.931 E10.2186
G1 X47.473 Y44.100 E10.2459
G1 X43.423 Y46.438 E10.3859
G1 X43.260 Y45.916 E10.4023
G1 X47.988 Y43.186 E10.5657
G1 X48.395 Y42.510 E10.5893
G1 X48.643 Y42.192 E10.6014
G1 X43.098 Y45.394 E10.7930
G1 X43.077 Y45.326 E10.7952
G1 X42.886 Y44.900 E10.8091
G1 X49.245 Y41.229 E11.0289
G1 X49.245 Y40.613 E11.0473
G1 X42.667 Y44.411 E11.2747
G1 X42.447 Y43.922 E11.2908
G1 X49.245 Y39.997 E11.5257
G1 X49.245 Y39.382 E11.5441
G1 X42.178 Y43.462 E11.7884
G1 X41.903 Y43.005 E11.8044
G1 X49.245 Y38.766 E12.0582
```

```
G1 X49.245 Y38.150 E12.0766
G1 X41.627 Y42.548 E12.3399
G1 X41.605 Y42.510 E12.3412
G1 X41.301 Y42.121 E12.3560
G1 X49.245 Y37.534 E12.6306
G1 X49.245 Y36.918 E12.6490
G1 X40.970 Y41.696 E12.9351
G1 X40.755 Y41.421 E12.9455
G1 X40.755 Y41.204 E12.9520
G1 X49.245 Y36.302 E13.2455
G1 X49.245 Y35.686 E13.2639
G1 X40.755 Y40.588 E13.5574
G1 X40.755 Y39.972 E13.5758
G1 X49.245 Y35.071 E13.8693
G1 X49.245 Y34.455 E13.8877
G1 X40.755 Y39.357 E14.1812
G1 X40.755 Y38.741 E14.1996
G1 X49.245 Y33.839 E14.4930
G1 X49.245 Y33.223 E14.5115
G1 X40.755 Y38.125 E14.8049
G1 X40.755 Y37.509 E14.8234
G1 X49.245 Y32.607 E15.1168
G1 X49.245 Y31.991 E15.1353
G1 X40.755 Y36.893 E15.4287
G1 X40.755 Y36.277 E15.4472
G1 X49.245 Y31.376 E15.7406
G1 X49.245 Y30.760 E15.7590
G1 X40.755 Y35.661 E16.0525
G1 X40.755 Y35.046 E16.0709
G1 X49.001 Y30.285 E16.3559
G1 X47.934 Y30.285 E16.3879
G1 X40.755 Y34.430 E16.6360
G1 X40.755 Y33.814 E16.6545
G1 X46.867 Y30.285 E16.8657
G1 X45.801 Y30.285 E16.8977
G1 X40.755 Y33.198 E17.0721
G1 X40.755 Y32.582 E17.0905
G1 X44.734 Y30.285 E17.2280
G1 X43.667 Y30.285 E17.2600
G1 X40.755 Y31.966 E17.3606
G1 X40.755 Y31.351 E17.3791
G1 X42.601 Y30.285 E17.4429
G1 X41.534 Y30.285 E17.4748
G1 X40.755 Y30.735 E17.5017
G92 E0
G1 E-1.0000 F1800
; layer 5, Z = 1
; outer perimeter
G1 X40.435 Y29.965 F4800
G1 Z1.000 F1000
G1 E0.0000 F1800
G92 E0
G1 X49.565 Y29.965 E0.2733 F300
G1 X49.565 Y41.531 E0.6195
```

```
G1 X48.660 Y42.692 E0.6636
G1 X47.858 Y44.022 E0.7101
G1 X47.223 Y45.439 E0.7566
G1 X46.762 Y46.922 E0.8030
G1 X46.483 Y48.450 E0.8495
G1 X46.390 Y49.994 E0.8958
G1 X46.390 Y59.536 E1.1815
G1 X46.483 Y61.080 E1.2278
G1 X46.762 Y62.608 E1.2743
G1 X47.223 Y64.091 E1.3208
G1 X47.858 Y65.508 E1.3672
G1 X48.659 Y66.838 E1.4137
G1 X49.565 Y67.999 E1.4578
G1 X49.565 Y79.565 E1.8040
G1 X40.435 Y79.565 E2.0773
G1 X40.435 Y67.999 E2.4235
G1 X41.340 Y66.838 E2.4676
G1 X42.142 Y65.508 E2.5141
G1 X42.777 Y64.091 E2.5606
G1 X43.238 Y62.608 E2.6071
G1 X43.517 Y61.080 E2.6535
G1 X43.610 Y59.536 E2.6998
G1 X43.610 Y49.994 E2.9855
G1 X43.517 Y48.450 E3.0318
G1 X43.238 Y46.922 E3.0783
G1 X42.777 Y45.439 E3.1248
G1 X42.142 Y44.022 E3.1712
G1 X41.340 Y42.692 E3.2177
G1 X40.435 Y41.531 E3.2618
G1 X40.435 Y29.965 E3.6080
; infill
G1 X48.466 Y30.285 F4800
G92 E0
G1 X49.245 Y30.735 E0.0269 F600
G1 X49.245 Y31.351 E0.0454
G1 X47.399 Y30.285 E0.1092
G1 X46.333 Y30.285 E0.1411
G1 X49.245 Y31.966 E0.2417
G1 X49.245 Y32.582 E0.2602
G1 X45.266 Y30.285 E0.3977
G1 X44.199 Y30.285 E0.4296
G1 X49.245 Y33.198 E0.6040
G1 X49.245 Y33.814 E0.6225
G1 X43.133 Y30.285 E0.8338
G1 X42.066 Y30.285 E0.8657
G1 X49.245 Y34.430 E1.1138
G1 X49.245 Y35.046 E1.1323
G1 X40.999 Y30.285 E1.4173
G1 X40.755 Y30.285 E1.4246
G1 X40.755 Y30.760 E1.4388
G1 X49.245 Y35.661 E1.7322
G1 X49.245 Y36.277 E1.7507
G1 X40.755 Y31.376 E2.0441
G1 X40.755 Y31.991 E2.0626
```

```
G1 X49.245 Y36.893 E2.3560
G1 X49.245 Y37.509 E2.3745
G1 X40.755 Y32.607 E2.6679
G1 X40.755 Y33.223 E2.6864
G1 X49.245 Y38.125 E2.9798
G1 X49.245 Y38.741 E2.9982
G1 X40.755 Y33.839 E3.2917
G1 X40.755 Y34.455 E3.3101
G1 X49.245 Y39.356 E3.6036
G1 X49.245 Y39.972 E3.6220
G1 X40.755 Y35.071 E3.9155
G1 X40.755 Y35.686 E3.9339
G1 X49.245 Y40.588 E4.2274
G1 X49.245 Y41.204 E4.2458
G1 X40.755 Y36.302 E4.5393
G1 X40.755 Y36.918 E4.5577
G1 X49.030 Y41.696 E4.8437
G1 X48.699 Y42.121 E4.8599
G1 X40.755 Y37.534 E5.1345
G1 X40.755 Y38.150 E5.1529
G1 X48.373 Y42.548 E5.4162
G1 X48.097 Y43.005 E5.4322
G1 X40.755 Y38.766 E5.6859
G1 X40.755 Y39.382 E5.7044
G1 X47.822 Y43.462 E5.9487
G1 X47.574 Y43.873 E5.9630
G1 X47.553 Y43.922 E5.9646
G1 X40.755 Y39.997 E6.1996
G1 X40.755 Y40.613 E6.2180
G1 X47.333 Y44.411 E6.4454
G1 X47.114 Y44.900 E6.4614
G1 X40.755 Y41.229 E6.6812
G1 X40.755 Y41.421 E6.6870
G1 X41.357 Y42.192 E6.7163
G1 X46.902 Y45.394 E6.9079
G1 X46.740 Y45.916 E6.9243
G1 X42.012 Y43.186 E7.0877
G1 X42.426 Y43.873 E7.1117
G1 X42.527 Y44.100 E7.1191
G1 X46.577 Y46.438 E7.2591
G1 X46.451 Y46.846 E7.2719
G1 X46.429 Y46.968 E7.2756
G1 X42.900 Y44.931 E7.3976
G1 X43.077 Y45.326 E7.4105
G1 X43.199 Y45.719 E7.4229
G1 X46.327 Y47.525 E7.5310
G1 X46.225 Y48.082 E7.5479
G1 X43.432 Y46.470 E7.6445
G1 X43.549 Y46.846 E7.6562
G1 X43.612 Y47.189 E7.6667
G1 X46.150 Y48.655 E7.7544
G1 X46.114 Y49.250 E7.7723
G1 X43.738 Y47.878 E7.8544
G1 X43.835 Y48.411 E7.8707
```

```
G1 X43.844 Y48.555 E7.8750
G1 X46.078 Y49.845 E7.9522
G1 X46.070 Y49.984 E7.9564
G1 X46.070 Y50.456 E7.9705
G1 X43.882 Y49.193 E8.0461
G1 X43.921 Y49.831 E8.0653
G1 X46.070 Y51.072 E8.1396
G1 X46.070 Y51.688 E8.1580
G1 X43.930 Y50.452 E8.2320
G1 X43.930 Y51.068 E8.2504
G1 X46.070 Y52.304 E8.3244
G1 X46.070 Y52.919 E8.3428
G1 X43.930 Y51.684 E8.4168
G1 X43.930 Y52.300 E8.4352
G1 X46.070 Y53.535 E8.5092
G1 X46.070 Y54.151 E8.5276
G1 X43.930 Y52.916 E8.6016
G1 X43.930 Y53.531 E8.6200
G1 X46.070 Y54.767 E8.6940
G1 X46.070 Y55.383 E8.7124
G1 X43.930 Y54.147 E8.7864
G1 X43.930 Y54.763 E8.8048
G1 X46.070 Y55.999 E8.8788
G1 X46.070 Y56.614 E8.8972
G1 X43.930 Y55.379 E8.9712
G1 X43.930 Y55.995 E8.9896
G1 X46.070 Y57.230 E9.0636
G1 X46.070 Y57.846 E9.0820
G1 X43.930 Y56.611 E9.1560
G1 X43.930 Y57.226 E9.1744
G1 X46.070 Y58.462 E9.2484
G1 X46.070 Y59.078 E9.2668
G1 X43.930 Y57.842 E9.3408
G1 X43.930 Y58.458 E9.3592
G1 X46.079 Y59.699 E9.4335
G1 X46.118 Y60.337 E9.4527
G1 X43.930 Y59.074 E9.5283
G1 X43.930 Y59.546 E9.5424
G1 X43.922 Y59.685 E9.5466
G1 X46.156 Y60.975 E9.6238
G1 X46.165 Y61.119 E9.6281
G1 X46.262 Y61.652 E9.6444
G1 X43.886 Y60.280 E9.7265
G1 X43.850 Y60.875 E9.7443
G1 X46.388 Y62.341 E9.8321
G1 X46.451 Y62.684 E9.8425
G1 X46.568 Y63.060 E9.8543
G1 X43.775 Y61.448 E9.9508
G1 X43.673 Y62.005 E9.9678
G1 X46.801 Y63.811 E10.0759
G1 X46.923 Y64.204 E10.0882
G1 X47.100 Y64.599 E10.1012
G1 X43.571 Y62.562 E10.2232
G1 X43.549 Y62.684 E10.2269
```

```
G1 X43.423 Y63.092 E10.2397
G1 X47.473 Y65.430 E10.3797
G1 X47.574 Y65.657 E10.3871
G1 X47.988 Y66.344 E10.4111
G1 X43.260 Y63.614 E10.5745
G1 X43.098 Y64.136 E10.5909
G1 X48.643 Y67.338 E10.7825
G1 X49.245 Y68.109 E10.8118
G1 X49.245 Y68.301 E10.8176
G1 X42.886 Y64.630 E11.0373
G1 X42.667 Y65.119 E11.0534
G1 X49.245 Y68.917 E11.2808
G1 X49.245 Y69.533 E11.2992
G1 X42.447 Y65.608 E11.5342
G1 X42.426 Y65.657 E11.5357
G1 X42.178 Y66.068 E11.5501
G1 X49.245 Y70.149 E11.7944
G1 X49.245 Y70.764 E11.8128
G1 X41.903 Y66.525 E12.0666
G1 X41.627 Y66.982 E12.0826
G1 X49.245 Y71.380 E12.3459
G1 X49.245 Y71.996 E12.3643
G1 X41.301 Y67.409 E12.6389
G1 X40.970 Y67.834 E12.6550
G1 X49.245 Y72.612 E12.9411
G1 X49.245 Y73.228 E12.9595
G1 X40.755 Y68.326 E13.2530
G1 X40.755 Y68.942 E13.2714
G1 X49.245 Y73.844 E13.5649
G1 X49.245 Y74.459 E13.5833
G1 X40.755 Y69.558 E13.8768
G1 X40.755 Y70.174 E13.8952
G1 X49.245 Y75.075 E14.1887
G1 X49.245 Y75.691 E14.2071
G1 X40.755 Y70.789 E14.5005
G1 X40.755 Y71.405 E14.5190
G1 X49.245 Y76.307 E14.8124
G1 X49.245 Y76.923 E14.8309
G1 X40.755 Y72.021 E15.1243
G1 X40.755 Y72.637 E15.1428
G1 X49.245 Y77.539 E15.4362
G1 X49.245 Y78.154 E15.4547
G1 X40.755 Y73.253 E15.7481
G1 X40.755 Y73.869 E15.7665
G1 X49.245 Y78.770 E16.0600
G1 X49.245 Y79.245 E16.0742
G1 X49.001 Y79.245 E16.0815
G1 X40.755 Y74.484 E16.3665
G1 X40.755 Y75.100 E16.3850
G1 X47.934 Y79.245 E16.6331
G1 X46.867 Y79.245 E16.6650
G1 X40.755 Y75.716 E16.8763
G1 X40.755 Y76.332 E16.8947
G1 X45.801 Y79.245 E17.0691
```

```
G1 X44.734 Y79.245 E17.1011
G1 X40.755 Y76.948 E17.2386
G1 X40.755 Y77.564 E17.2570
G1 X43.667 Y79.245 E17.3577
G1 X42.601 Y79.245 E17.3896
G1 X40.755 Y78.179 E17.4534
G1 X40.755 Y78.795 E17.4719
G1 X41.534 Y79.245 E17.4988
G92 E0
G1 E-1.0000 F1800
; layer 6, Z = 1.2
; outer perimeter
G1 X40.435 Y79.565 F4800
G1 Z1.200 F1000
G1 E0.0000 F1800
G92 E0
G1 X40.435 Y67.999 E0.3462 F300
G1 X41.340 Y66.838 E0.3903
G1 X42.142 Y65.508 E0.4368
G1 X42.777 Y64.091 E0.4833
G1 X43.238 Y62.608 E0.5297
G1 X43.517 Y61.080 E0.5762
G1 X43.610 Y59.536 E0.6225
G1 X43.610 Y49.994 E0.9082
G1 X43.517 Y48.450 E0.9545
G1 X43.238 Y46.922 E1.0010
G1 X42.777 Y45.439 E1.0475
G1 X42.142 Y44.022 E1.0939
G1 X41.340 Y42.692 E1.1404
G1 X40.435 Y41.531 E1.1845
G1 X40.435 Y29.965 E1.5307
G1 X49.565 Y29.965 E1.8040
G1 X49.565 Y41.531 E2.1502
G1 X48.660 Y42.692 E2.1943
G1 X47.858 Y44.022 E2.2408
G1 X47.223 Y45.439 E2.2873
G1 X46.762 Y46.922 E2.3338
G1 X46.483 Y48.450 E2.3802
G1 X46.390 Y49.994 E2.4265
G1 X46.390 Y59.536 E2.7122
G1 X46.483 Y61.080 E2.7585
G1 X46.762 Y62.608 E2.8050
G1 X47.223 Y64.091 E2.8515
G1 X47.858 Y65.508 E2.8979
G1 X48.659 Y66.838 E2.9444
G1 X49.565 Y67.999 E2.9885
G1 X49.565 Y79.565 E3.3347
G1 X40.435 Y79.565 E3.6080
; infill
G1 X49.245 Y78.795 F4800
G92 E0
G1 X48.466 Y79.245 E0.0269 F600
G1 X47.399 Y79.245 E0.0589
G1 X49.245 Y78.179 E0.1226
```

```
G1 X49.245 Y77.564 E0.1411
G1 X46.333 Y79.245 E0.2417
G1 X45.266 Y79.245 E0.2737
G1 X49.245 Y76.948 E0.4112
G1 X49.245 Y76.332 E0.4296
G1 X44.199 Y79.245 E0.6040
G1 X43.133 Y79.245 E0.6360
G1 X49.245 Y75.716 E0.8472
G1 X49.245 Y75.100 E0.8657
G1 X42.066 Y79.245 E1.1138
G1 X40.999 Y79.245 E1.1457
G1 X49.245 Y74.484 E1.4307
G1 X49.245 Y73.869 E1.4492
G1 X40.755 Y78.770 E1.7426
G1 X40.755 Y78.154 E1.7611
G1 X49.245 Y73.253 E2.0545
G1 X49.245 Y72.637 E2.0730
G1 X40.755 Y77.539 E2.3664
G1 X40.755 Y76.923 E2.3848
G1 X49.245 Y72.021 E2.6783
G1 X49.245 Y71.405 E2.6967
G1 X40.755 Y76.307 E2.9902
G1 X40.755 Y75.691 E3.0086
G1 X49.245 Y70.789 E3.3021
G1 X49.245 Y70.174 E3.3205
G1 X40.755 Y75.075 E3.6140
G1 X40.755 Y74.459 E3.6324
G1 X49.245 Y69.558 E3.9259
G1 X49.245 Y68.942 E3.9443
G1 X40.755 Y73.844 E4.2378
G1 X40.755 Y73.228 E4.2562
G1 X49.245 Y68.326 E4.5496
G1 X49.245 Y68.109 E4.5561
G1 X49.030 Y67.834 E4.5666
G1 X40.755 Y72.612 E4.8526
G1 X40.755 Y71.996 E4.8711
G1 X48.699 Y67.409 E5.1457
G1 X48.395 Y67.020 E5.1604
G1 X48.373 Y66.982 E5.1618
G1 X40.755 Y71.380 E5.4251
G1 X40.755 Y70.764 E5.4435
G1 X48.097 Y66.525 E5.6973
G1 X47.822 Y66.068 E5.7133
G1 X40.755 Y70.149 E5.9575
G1 X40.755 Y69.533 E5.9760
G1 X47.553 Y65.608 E6.2109
G1 X47.333 Y65.119 E6.2270
G1 X40.755 Y68.917 E6.4543
G1 X40.755 Y68.301 E6.4728
G1 X47.114 Y64.630 E6.6926
G1 X46.923 Y64.204 E6.7065
G1 X46.902 Y64.136 E6.7087
G1 X41.357 Y67.338 E6.9003
G1 X41.605 Y67.020 E6.9124
```

```
G1 X42.012 Y66.344 E6.9360
G1 X46.740 Y63.614 E7.0994
G1 X46.577 Y63.092 E7.1158
G1 X42.527 Y65.430 E7.2558
G1 X42.900 Y64.599 E7.2831
G1 X46.429 Y62.562 E7.4050
G1 X46.327 Y62.005 E7.4220
G1 X43.199 Y63.811 E7.5301
G1 X43.432 Y63.060 E7.5536
G1 X46.225 Y61.448 E7.6501
G1 X46.165 Y61.119 E7.6601
G1 X46.150 Y60.875 E7.6674
G1 X43.612 Y62.341 E7.7552
G1 X43.738 Y61.652 E7.7761
G1 X46.114 Y60.280 E7.8583
G1 X46.078 Y59.685 E7.8761
G1 X43.844 Y60.975 E7.9534
G1 X43.882 Y60.337 E7.9725
G1 X46.070 Y59.074 E8.0481
G1 X46.070 Y58.458 E8.0665
G1 X43.921 Y59.699 E8.1408
G1 X43.930 Y59.546 E8.1454
G1 X43.930 Y59.078 E8.1594
G1 X46.070 Y57.842 E8.2334
G1 X46.070 Y57.226 E8.2518
G1 X43.930 Y58.462 E8.3258
G1 X43.930 Y57.846 E8.3442
G1 X46.070 Y56.611 E8.4182
G1 X46.070 Y55.995 E8.4367
G1 X43.930 Y57.230 E8.5106
G1 X43.930 Y56.614 E8.5291
G1 X46.070 Y55.379 E8.6030
G1 X46.070 Y54.763 E8.6215
G1 X43.930 Y55.999 E8.6954
G1 X43.930 Y55.383 E8.7139
G1 X46.070 Y54.147 E8.7878
G1 X46.070 Y53.531 E8.8063
G1 X43.930 Y54.767 E8.8802
G1 X43.930 Y54.151 E8.8987
G1 X46.070 Y52.916 E8.9726
G1 X46.070 Y52.300 E8.9911
G1 X43.930 Y53.535 E9.0650
G1 X43.930 Y52.919 E9.0835
G1 X46.070 Y51.684 E9.1574
G1 X46.070 Y51.068 E9.1759
G1 X43.930 Y52.304 E9.2499
G1 X43.930 Y51.688 E9.2683
G1 X46.070 Y50.452 E9.3423
G1 X46.070 Y49.984 E9.3563
G1 X46.079 Y49.831 E9.3609
G1 X43.930 Y51.072 E9.4351
G1 X43.930 Y50.456 E9.4536
G1 X46.118 Y49.193 E9.5292
G1 X46.156 Y48.555 E9.5483
```

```
G1 X43.922 Y49.845 E9.6256
G1 X43.886 Y49.250 E9.6434
G1 X46.262 Y47.878 E9.7256
G1 X46.388 Y47.189 E9.7465
G1 X43.850 Y48.655 E9.8343
G1 X43.835 Y48.411 E9.8416
G1 X43.775 Y48.082 E9.8516
G1 X46.568 Y46.470 E9.9481
G1 X46.801 Y45.720 E9.9716
G1 X43.673 Y47.525 E10.0797
G1 X43.571 Y46.968 E10.0967
G1 X47.100 Y44.931 E10.2186
G1 X47.473 Y44.100 E10.2459
G1 X43.423 Y46.438 E10.3859
G1 X43.260 Y45.916 E10.4023
G1 X47.988 Y43.186 E10.5657
G1 X48.395 Y42.510 E10.5893
G1 X48.643 Y42.192 E10.6014
G1 X43.098 Y45.394 E10.7930
G1 X43.077 Y45.326 E10.7952
G1 X42.886 Y44.900 E10.8091
G1 X49.245 Y41.229 E11.0289
G1 X49.245 Y40.613 E11.0473
G1 X42.667 Y44.411 E11.2747
G1 X42.447 Y43.922 E11.2908
G1 X49.245 Y39.997 E11.5257
G1 X49.245 Y39.382 E11.5441
G1 X42.178 Y43.462 E11.7884
G1 X41.903 Y43.005 E11.8044
G1 X49.245 Y38.766 E12.0582
G1 X49.245 Y38.150 E12.0766
G1 X41.627 Y42.548 E12.3399
G1 X41.605 Y42.510 E12.3412
G1 X41.301 Y42.121 E12.3560
G1 X49.245 Y37.534 E12.6306
G1 X49.245 Y36.918 E12.6490
G1 X40.970 Y41.696 E12.9351
G1 X40.755 Y41.421 E12.9455
G1 X40.755 Y41.204 E12.9520
G1 X49.245 Y36.302 E13.2455
G1 X49.245 Y35.686 E13.2639
G1 X40.755 Y40.588 E13.5574
G1 X40.755 Y39.972 E13.5758
G1 X49.245 Y35.071 E13.8693
G1 X49.245 Y34.455 E13.8877
G1 X40.755 Y39.357 E14.1812
G1 X40.755 Y38.741 E14.1996
G1 X49.245 Y33.839 E14.4930
G1 X49.245 Y33.223 E14.5115
G1 X40.755 Y38.125 E14.8049
G1 X40.755 Y37.509 E14.8234
G1 X49.245 Y32.607 E15.1168
G1 X49.245 Y31.991 E15.1353
G1 X40.755 Y36.893 E15.4287
```

```
G1 X40.755 Y36.277 E15.4472
G1 X49.245 Y31.376 E15.7406
G1 X49.245 Y30.760 E15.7590
G1 X40.755 Y35.661 E16.0525
G1 X40.755 Y35.046 E16.0709
G1 X49.001 Y30.285 E16.3559
G1 X47.934 Y30.285 E16.3879
G1 X40.755 Y34.430 E16.6360
G1 X40.755 Y33.814 E16.6545
G1 X46.867 Y30.285 E16.8657
G1 X45.801 Y30.285 E16.8977
G1 X40.755 Y33.198 E17.0721
G1 X40.755 Y32.582 E17.0905
G1 X44.734 Y30.285 E17.2280
G1 X43.667 Y30.285 E17.2600
G1 X40.755 Y31.966 E17.3606
G1 X40.755 Y31.351 E17.3791
G1 X42.601 Y30.285 E17.4429
G1 X41.534 Y30.285 E17.4748
G1 X40.755 Y30.735 E17.5017
G92 E0
G1 E-1.0000 F1800
; layer 7, Z = 1.4
; outer perimeter
G1 X40.435 Y29.965 F4800
G1 Z1.400 F1000
G1 E0.0000 F1800
G92 E0
G1 X49.565 Y29.965 E0.2733 F300
G1 X49.565 Y41.531 E0.6195
G1 X48.660 Y42.692 E0.6636
G1 X47.858 Y44.022 E0.7101
G1 X47.223 Y45.439 E0.7566
G1 X46.762 Y46.922 E0.8030
G1 X46.483 Y48.450 E0.8495
G1 X46.390 Y49.994 E0.8958
G1 X46.390 Y59.536 E1.1815
G1 X46.483 Y61.080 E1.2278
G1 X46.762 Y62.608 E1.2743
G1 X47.223 Y64.091 E1.3208
G1 X47.858 Y65.508 E1.3672
G1 X48.659 Y66.838 E1.4137
G1 X49.565 Y67.999 E1.4578
G1 X49.565 Y79.565 E1.8040
G1 X40.435 Y79.565 E2.0773
G1 X40.435 Y67.999 E2.4235
G1 X41.340 Y66.838 E2.4676
G1 X42.142 Y65.508 E2.5141
G1 X42.777 Y64.091 E2.5606
G1 X43.238 Y62.608 E2.6071
G1 X43.517 Y61.080 E2.6535
G1 X43.610 Y59.536 E2.6998
G1 X43.610 Y49.994 E2.9855
G1 X43.517 Y48.450 E3.0318
```

```
G1 X43.238 Y46.922 E3.0783
G1 X42.777 Y45.439 E3.1248
G1 X42.142 Y44.022 E3.1712
G1 X41.340 Y42.692 E3.2177
G1 X40.435 Y41.531 E3.2618
G1 X40.435 Y29.965 E3.6080
; infill
G1 X48.466 Y30.285 F4800
G92 E0
G1 X49.245 Y30.735 E0.0269 F600
G1 X49.245 Y31.351 E0.0454
G1 X47.399 Y30.285 E0.1092
G1 X46.333 Y30.285 E0.1411
G1 X49.245 Y31.966 E0.2417
G1 X49.245 Y32.582 E0.2602
G1 X45.266 Y30.285 E0.3977
G1 X44.199 Y30.285 E0.4296
G1 X49.245 Y33.198 E0.6040
G1 X49.245 Y33.814 E0.6225
G1 X43.133 Y30.285 E0.8338
G1 X42.066 Y30.285 E0.8657
G1 X49.245 Y34.430 E1.1138
G1 X49.245 Y35.046 E1.1323
G1 X40.999 Y30.285 E1.4173
G1 X40.755 Y30.285 E1.4246
G1 X40.755 Y30.760 E1.4388
G1 X49.245 Y35.661 E1.7322
G1 X49.245 Y36.277 E1.7507
G1 X40.755 Y31.376 E2.0441
G1 X40.755 Y31.991 E2.0626
G1 X49.245 Y36.893 E2.3560
G1 X49.245 Y37.509 E2.3745
G1 X40.755 Y32.607 E2.6679
G1 X40.755 Y33.223 E2.6864
G1 X49.245 Y38.125 E2.9798
G1 X49.245 Y38.741 E2.9982
G1 X40.755 Y33.839 E3.2917
G1 X40.755 Y34.455 E3.3101
G1 X49.245 Y39.356 E3.6036
G1 X49.245 Y39.972 E3.6220
G1 X40.755 Y35.071 E3.9155
G1 X40.755 Y35.686 E3.9339
G1 X49.245 Y40.588 E4.2274
G1 X49.245 Y41.204 E4.2458
G1 X40.755 Y36.302 E4.5393
G1 X40.755 Y36.918 E4.5577
G1 X49.030 Y41.696 E4.8437
G1 X48.699 Y42.121 E4.8599
G1 X40.755 Y37.534 E5.1345
G1 X40.755 Y38.150 E5.1529
G1 X48.373 Y42.548 E5.4162
G1 X48.097 Y43.005 E5.4322
G1 X40.755 Y38.766 E5.6859
G1 X40.755 Y39.382 E5.7044
```

```
G1 X47.822 Y43.462 E5.9487
G1 X47.574 Y43.873 E5.9630
G1 X47.553 Y43.922 E5.9646
G1 X40.755 Y39.997 E6.1996
G1 X40.755 Y40.613 E6.2180
G1 X47.333 Y44.411 E6.4454
G1 X47.114 Y44.900 E6.4614
G1 X40.755 Y41.229 E6.6812
G1 X40.755 Y41.421 E6.6870
G1 X41.357 Y42.192 E6.7163
G1 X46.902 Y45.394 E6.9079
G1 X46.740 Y45.916 E6.9243
G1 X42.012 Y43.186 E7.0877
G1 X42.426 Y43.873 E7.1117
G1 X42.527 Y44.100 E7.1191
G1 X46.577 Y46.438 E7.2591
G1 X46.451 Y46.846 E7.2719
G1 X46.429 Y46.968 E7.2756
G1 X42.900 Y44.931 E7.3976
G1 X43.077 Y45.326 E7.4105
G1 X43.199 Y45.719 E7.4229
G1 X46.327 Y47.525 E7.5310
G1 X46.225 Y48.082 E7.5479
G1 X43.432 Y46.470 E7.6445
G1 X43.549 Y46.846 E7.6562
G1 X43.612 Y47.189 E7.6667
G1 X46.150 Y48.655 E7.7544
G1 X46.114 Y49.250 E7.7723
G1 X43.738 Y47.878 E7.8544
G1 X43.835 Y48.411 E7.8707
G1 X43.844 Y48.555 E7.8750
G1 X46.078 Y49.845 E7.9522
G1 X46.070 Y49.984 E7.9564
G1 X46.070 Y50.456 E7.9705
G1 X43.882 Y49.193 E8.0461
G1 X43.921 Y49.831 E8.0653
G1 X46.070 Y51.072 E8.1396
G1 X46.070 Y51.688 E8.1580
G1 X43.930 Y50.452 E8.2320
G1 X43.930 Y51.068 E8.2504
G1 X46.070 Y52.304 E8.3244
G1 X46.070 Y52.919 E8.3428
G1 X43.930 Y51.684 E8.4168
G1 X43.930 Y52.300 E8.4352
G1 X46.070 Y53.535 E8.5092
G1 X46.070 Y54.151 E8.5276
G1 X43.930 Y52.916 E8.6016
G1 X43.930 Y53.531 E8.6200
G1 X46.070 Y54.767 E8.6940
G1 X46.070 Y55.383 E8.7124
G1 X43.930 Y54.147 E8.7864
G1 X43.930 Y54.763 E8.8048
G1 X46.070 Y55.999 E8.8788
G1 X46.070 Y56.614 E8.8972
```

```
G1 X43.930 Y55.379 E8.9712
G1 X43.930 Y55.995 E8.9896
G1 X46.070 Y57.230 E9.0636
G1 X46.070 Y57.846 E9.0820
G1 X43.930 Y56.611 E9.1560
G1 X43.930 Y57.226 E9.1744
G1 X46.070 Y58.462 E9.2484
G1 X46.070 Y59.078 E9.2668
G1 X43.930 Y57.842 E9.3408
G1 X43.930 Y58.458 E9.3592
G1 X46.079 Y59.699 E9.4335
G1 X46.118 Y60.337 E9.4527
G1 X43.930 Y59.074 E9.5283
G1 X43.930 Y59.546 E9.5424
G1 X43.922 Y59.685 E9.5466
G1 X46.156 Y60.975 E9.6238
G1 X46.165 Y61.119 E9.6281
G1 X46.262 Y61.652 E9.6444
G1 X43.886 Y60.280 E9.7265
G1 X43.850 Y60.875 E9.7443
G1 X46.388 Y62.341 E9.8321
G1 X46.451 Y62.684 E9.8425
G1 X46.568 Y63.060 E9.8543
G1 X43.775 Y61.448 E9.9508
G1 X43.673 Y62.005 E9.9678
G1 X46.801 Y63.811 E10.0759
G1 X46.923 Y64.204 E10.0882
G1 X47.100 Y64.599 E10.1012
G1 X43.571 Y62.562 E10.2232
G1 X43.549 Y62.684 E10.2269
G1 X43.423 Y63.092 E10.2397
G1 X47.473 Y65.430 E10.3797
G1 X47.574 Y65.657 E10.3871
G1 X47.988 Y66.344 E10.4111
G1 X43.260 Y63.614 E10.5745
G1 X43.098 Y64.136 E10.5909
G1 X48.643 Y67.338 E10.7825
G1 X49.245 Y68.109 E10.8118
G1 X49.245 Y68.301 E10.8176
G1 X42.886 Y64.630 E11.0373
G1 X42.667 Y65.119 E11.0534
G1 X49.245 Y68.917 E11.2808
G1 X49.245 Y69.533 E11.2992
G1 X42.447 Y65.608 E11.5342
G1 X42.426 Y65.657 E11.5357
G1 X42.178 Y66.068 E11.5501
G1 X49.245 Y70.149 E11.7944
G1 X49.245 Y70.764 E11.8128
G1 X41.903 Y66.525 E12.0666
G1 X41.627 Y66.982 E12.0826
G1 X49.245 Y71.380 E12.3459
G1 X49.245 Y71.996 E12.3643
G1 X41.301 Y67.409 E12.6389
G1 X40.970 Y67.834 E12.6550
```

```
G1 X49.245 Y72.612 E12.9411
G1 X49.245 Y73.228 E12.9595
G1 X40.755 Y68.326 E13.2530
G1 X40.755 Y68.942 E13.2714
G1 X49.245 Y73.844 E13.5649
G1 X49.245 Y74.459 E13.5833
G1 X40.755 Y69.558 E13.8768
G1 X40.755 Y70.174 E13.8952
G1 X49.245 Y75.075 E14.1887
G1 X49.245 Y75.691 E14.2071
G1 X40.755 Y70.789 E14.5005
G1 X40.755 Y71.405 E14.5190
G1 X49.245 Y76.307 E14.8124
G1 X49.245 Y76.923 E14.8309
G1 X40.755 Y72.021 E15.1243
G1 X40.755 Y72.637 E15.1428
G1 X49.245 Y77.539 E15.4362
G1 X49.245 Y78.154 E15.4547
G1 X40.755 Y73.253 E15.7481
G1 X40.755 Y73.869 E15.7665
G1 X49.245 Y78.770 E16.0600
G1 X49.245 Y79.245 E16.0742
G1 X49.001 Y79.245 E16.0815
G1 X40.755 Y74.484 E16.3665
G1 X40.755 Y75.100 E16.3850
G1 X47.934 Y79.245 E16.6331
G1 X46.867 Y79.245 E16.6650
G1 X40.755 Y75.716 E16.8763
G1 X40.755 Y76.332 E16.8947
G1 X45.801 Y79.245 E17.0691
G1 X44.734 Y79.245 E17.1011
G1 X40.755 Y76.948 E17.2386
G1 X40.755 Y77.564 E17.2570
G1 X43.667 Y79.245 E17.3577
G1 X42.601 Y79.245 E17.3896
G1 X40.755 Y78.179 E17.4534
G1 X40.755 Y78.795 E17.4719
G1 X41.534 Y79.245 E17.4988
G92 E0
G1 E-1.0000 F1800
; layer 8, Z = 1.6
; outer perimeter
G1 X40.435 Y79.565 F4800
G1 Z1.600 F1000
G1 E0.0000 F1800
G92 E0
G1 X40.435 Y67.999 E0.3462 F300
G1 X41.340 Y66.838 E0.3903
G1 X42.142 Y65.508 E0.4368
G1 X42.777 Y64.091 E0.4833
G1 X43.238 Y62.608 E0.5297
G1 X43.517 Y61.080 E0.5762
G1 X43.610 Y59.536 E0.6225
G1 X43.610 Y49.994 E0.9082
```

```
G1 X43.517 Y48.450 E0.9545
G1 X43.238 Y46.922 E1.0010
G1 X42.777 Y45.439 E1.0475
G1 X42.142 Y44.022 E1.0939
G1 X41.340 Y42.692 E1.1404
G1 X40.435 Y41.531 E1.1845
G1 X40.435 Y29.965 E1.5307
G1 X49.565 Y29.965 E1.8040
G1 X49.565 Y41.531 E2.1502
G1 X48.660 Y42.692 E2.1943
G1 X47.858 Y44.022 E2.2408
G1 X47.223 Y45.439 E2.2873
G1 X46.762 Y46.922 E2.3338
G1 X46.483 Y48.450 E2.3802
G1 X46.390 Y49.994 E2.4265
G1 X46.390 Y59.536 E2.7122
G1 X46.483 Y61.080 E2.7585
G1 X46.762 Y62.608 E2.8050
G1 X47.223 Y64.091 E2.8515
G1 X47.858 Y65.508 E2.8979
G1 X48.659 Y66.838 E2.9444
G1 X49.565 Y67.999 E2.9885
G1 X49.565 Y79.565 E3.3347
G1 X40.435 Y79.565 E3.6080
; infill
G1 X49.245 Y78.795 F4800
G92 E0
G1 X48.466 Y79.245 E0.0269 F600
G1 X47.399 Y79.245 E0.0589
G1 X49.245 Y78.179 E0.1226
G1 X49.245 Y77.564 E0.1411
G1 X46.333 Y79.245 E0.2417
G1 X45.266 Y79.245 E0.2737
G1 X49.245 Y76.948 E0.4112
G1 X49.245 Y76.332 E0.4296
G1 X44.199 Y79.245 E0.6040
G1 X43.133 Y79.245 E0.6360
G1 X49.245 Y75.716 E0.8472
G1 X49.245 Y75.100 E0.8657
G1 X42.066 Y79.245 E1.1138
G1 X40.999 Y79.245 E1.1457
G1 X49.245 Y74.484 E1.4307
G1 X49.245 Y73.869 E1.4492
G1 X40.755 Y78.770 E1.7426
G1 X40.755 Y78.154 E1.7611
G1 X49.245 Y73.253 E2.0545
G1 X49.245 Y72.637 E2.0730
G1 X40.755 Y77.539 E2.3664
G1 X40.755 Y76.923 E2.3848
G1 X49.245 Y72.021 E2.6783
G1 X49.245 Y71.405 E2.6967
G1 X40.755 Y76.307 E2.9902
G1 X40.755 Y75.691 E3.0086
G1 X49.245 Y70.789 E3.3021
```

```
G1 X49.245 Y70.174 E3.3205
G1 X40.755 Y75.075 E3.6140
G1 X40.755 Y74.459 E3.6324
G1 X49.245 Y69.558 E3.9259
G1 X49.245 Y68.942 E3.9443
G1 X40.755 Y73.844 E4.2378
G1 X40.755 Y73.228 E4.2562
G1 X49.245 Y68.326 E4.5496
G1 X49.245 Y68.109 E4.5561
G1 X49.030 Y67.834 E4.5666
G1 X40.755 Y72.612 E4.8526
G1 X40.755 Y71.996 E4.8711
G1 X48.699 Y67.409 E5.1457
G1 X48.395 Y67.020 E5.1604
G1 X48.373 Y66.982 E5.1618
G1 X40.755 Y71.380 E5.4251
G1 X40.755 Y70.764 E5.4435
G1 X48.097 Y66.525 E5.6973
G1 X47.822 Y66.068 E5.7133
G1 X40.755 Y70.149 E5.9575
G1 X40.755 Y69.533 E5.9760
G1 X47.553 Y65.608 E6.2109
G1 X47.333 Y65.119 E6.2270
G1 X40.755 Y68.917 E6.4543
G1 X40.755 Y68.301 E6.4728
G1 X47.114 Y64.630 E6.6926
G1 X46.923 Y64.204 E6.7065
G1 X46.902 Y64.136 E6.7087
G1 X41.357 Y67.338 E6.9003
G1 X41.605 Y67.020 E6.9124
G1 X42.012 Y66.344 E6.9360
G1 X46.740 Y63.614 E7.0994
G1 X46.577 Y63.092 E7.1158
G1 X42.527 Y65.430 E7.2558
G1 X42.900 Y64.599 E7.2831
G1 X46.429 Y62.562 E7.4050
G1 X46.327 Y62.005 E7.4220
G1 X43.199 Y63.811 E7.5301
G1 X43.432 Y63.060 E7.5536
G1 X46.225 Y61.448 E7.6501
G1 X46.165 Y61.119 E7.6601
G1 X46.150 Y60.875 E7.6674
G1 X43.612 Y62.341 E7.7552
G1 X43.738 Y61.652 E7.7761
G1 X46.114 Y60.280 E7.8583
G1 X46.078 Y59.685 E7.8761
G1 X43.844 Y60.975 E7.9534
G1 X43.882 Y60.337 E7.9725
G1 X46.070 Y59.074 E8.0481
G1 X46.070 Y58.458 E8.0665
G1 X43.921 Y59.699 E8.1408
G1 X43.930 Y59.546 E8.1454
G1 X43.930 Y59.078 E8.1594
G1 X46.070 Y57.842 E8.2334
```

```
G1 X46.070 Y57.226 E8.2518
G1 X43.930 Y58.462 E8.3258
G1 X43.930 Y57.846 E8.3442
G1 X46.070 Y56.611 E8.4182
G1 X46.070 Y55.995 E8.4367
G1 X43.930 Y57.230 E8.5106
G1 X43.930 Y56.614 E8.5291
G1 X46.070 Y55.379 E8.6030
G1 X46.070 Y54.763 E8.6215
G1 X43.930 Y55.999 E8.6954
G1 X43.930 Y55.383 E8.7139
G1 X46.070 Y54.147 E8.7878
G1 X46.070 Y53.531 E8.8063
G1 X43.930 Y54.767 E8.8802
G1 X43.930 Y54.151 E8.8987
G1 X46.070 Y52.916 E8.9726
G1 X46.070 Y52.300 E8.9911
G1 X43.930 Y53.535 E9.0650
G1 X43.930 Y52.919 E9.0835
G1 X46.070 Y51.684 E9.1574
G1 X46.070 Y51.068 E9.1759
G1 X43.930 Y52.304 E9.2499
G1 X43.930 Y51.688 E9.2683
G1 X46.070 Y50.452 E9.3423
G1 X46.070 Y49.984 E9.3563
G1 X46.079 Y49.831 E9.3609
G1 X43.930 Y51.072 E9.4351
G1 X43.930 Y50.456 E9.4536
G1 X46.118 Y49.193 E9.5292
G1 X46.156 Y48.555 E9.5483
G1 X43.922 Y49.845 E9.6256
G1 X43.886 Y49.250 E9.6434
G1 X46.262 Y47.878 E9.7256
G1 X46.388 Y47.189 E9.7465
G1 X43.850 Y48.655 E9.8343
G1 X43.835 Y48.411 E9.8416
G1 X43.775 Y48.082 E9.8516
G1 X46.568 Y46.470 E9.9481
G1 X46.801 Y45.720 E9.9716
G1 X43.673 Y47.525 E10.0797
G1 X43.571 Y46.968 E10.0967
G1 X47.100 Y44.931 E10.2186
G1 X47.473 Y44.100 E10.2459
G1 X43.423 Y46.438 E10.3859
G1 X43.260 Y45.916 E10.4023
G1 X47.988 Y43.186 E10.5657
G1 X48.395 Y42.510 E10.5893
G1 X48.643 Y42.192 E10.6014
G1 X43.098 Y45.394 E10.7930
G1 X43.077 Y45.326 E10.7952
G1 X42.886 Y44.900 E10.8091
G1 X49.245 Y41.229 E11.0289
G1 X49.245 Y40.613 E11.0473
G1 X42.667 Y44.411 E11.2747
```

```
G1 X42.447 Y43.922 E11.2908
G1 X49.245 Y39.997 E11.5257
G1 X49.245 Y39.382 E11.5441
G1 X42.178 Y43.462 E11.7884
G1 X41.903 Y43.005 E11.8044
G1 X49.245 Y38.766 E12.0582
G1 X49.245 Y38.150 E12.0766
G1 X41.627 Y42.548 E12.3399
G1 X41.605 Y42.510 E12.3412
G1 X41.301 Y42.121 E12.3560
G1 X49.245 Y37.534 E12.6306
G1 X49.245 Y36.918 E12.6490
G1 X40.970 Y41.696 E12.9351
G1 X40.755 Y41.421 E12.9455
G1 X40.755 Y41.204 E12.9520
G1 X49.245 Y36.302 E13.2455
G1 X49.245 Y35.686 E13.2639
G1 X40.755 Y40.588 E13.5574
G1 X40.755 Y39.972 E13.5758
G1 X49.245 Y35.071 E13.8693
G1 X49.245 Y34.455 E13.8877
G1 X40.755 Y39.357 E14.1812
G1 X40.755 Y38.741 E14.1996
G1 X49.245 Y33.839 E14.4930
G1 X49.245 Y33.223 E14.5115
G1 X40.755 Y38.125 E14.8049
G1 X40.755 Y37.509 E14.8234
G1 X49.245 Y32.607 E15.1168
G1 X49.245 Y31.991 E15.1353
G1 X40.755 Y36.893 E15.4287
G1 X40.755 Y36.277 E15.4472
G1 X49.245 Y31.376 E15.7406
G1 X49.245 Y30.760 E15.7590
G1 X40.755 Y35.661 E16.0525
G1 X40.755 Y35.046 E16.0709
G1 X49.001 Y30.285 E16.3559
G1 X47.934 Y30.285 E16.3879
G1 X40.755 Y34.430 E16.6360
G1 X40.755 Y33.814 E16.6545
G1 X46.867 Y30.285 E16.8657
G1 X45.801 Y30.285 E16.8977
G1 X40.755 Y33.198 E17.0721
G1 X40.755 Y32.582 E17.0905
G1 X44.734 Y30.285 E17.2280
G1 X43.667 Y30.285 E17.2600
G1 X40.755 Y31.966 E17.3606
G1 X40.755 Y31.351 E17.3791
G1 X42.601 Y30.285 E17.4429
G1 X41.534 Y30.285 E17.4748
G1 X40.755 Y30.735 E17.5017
G92 E0
G1 E-1.0000 F1800
; layer 9, Z = 1.8
; outer perimeter
```

```
G1 X40.435 Y29.965 F4800
G1 Z1.800 F1000
G1 E0.0000 F1800
G92 E0
G1 X49.565 Y29.965 E0.2733 F300
G1 X49.565 Y41.531 E0.6195
G1 X48.660 Y42.692 E0.6636
G1 X47.858 Y44.022 E0.7101
G1 X47.223 Y45.439 E0.7566
G1 X46.762 Y46.922 E0.8030
G1 X46.483 Y48.450 E0.8495
G1 X46.390 Y49.994 E0.8958
G1 X46.390 Y59.536 E1.1815
G1 X46.483 Y61.080 E1.2278
G1 X46.762 Y62.608 E1.2743
G1 X47.223 Y64.091 E1.3208
G1 X47.858 Y65.508 E1.3672
G1 X48.659 Y66.838 E1.4137
G1 X49.565 Y67.999 E1.4578
G1 X49.565 Y79.565 E1.8040
G1 X40.435 Y79.565 E2.0773
G1 X40.435 Y67.999 E2.4235
G1 X41.340 Y66.838 E2.4676
G1 X42.142 Y65.508 E2.5141
G1 X42.777 Y64.091 E2.5606
G1 X43.238 Y62.608 E2.6071
G1 X43.517 Y61.080 E2.6535
G1 X43.610 Y59.536 E2.6998
G1 X43.610 Y49.994 E2.9855
G1 X43.517 Y48.450 E3.0318
G1 X43.238 Y46.922 E3.0783
G1 X42.777 Y45.439 E3.1248
G1 X42.142 Y44.022 E3.1712
G1 X41.340 Y42.692 E3.2177
G1 X40.435 Y41.531 E3.2618
G1 X40.435 Y29.965 E3.6080
; infill
G1 X48.466 Y30.285 F4800
G92 E0
G1 X49.245 Y30.735 E0.0269 F600
G1 X49.245 Y31.351 E0.0454
G1 X47.399 Y30.285 E0.1092
G1 X46.333 Y30.285 E0.1411
G1 X49.245 Y31.966 E0.2417
G1 X49.245 Y32.582 E0.2602
G1 X45.266 Y30.285 E0.3977
G1 X44.199 Y30.285 E0.4296
G1 X49.245 Y33.198 E0.6040
G1 X49.245 Y33.814 E0.6225
G1 X43.133 Y30.285 E0.8338
G1 X42.066 Y30.285 E0.8657
G1 X49.245 Y34.430 E1.1138
G1 X49.245 Y35.046 E1.1323
G1 X40.999 Y30.285 E1.4173
```

```
G1 X40.755 Y30.285 E1.4246
G1 X40.755 Y30.760 E1.4388
G1 X49.245 Y35.661 E1.7322
G1 X49.245 Y36.277 E1.7507
G1 X40.755 Y31.376 E2.0441
G1 X40.755 Y31.991 E2.0626
G1 X49.245 Y36.893 E2.3560
G1 X49.245 Y37.509 E2.3745
G1 X40.755 Y32.607 E2.6679
G1 X40.755 Y33.223 E2.6864
G1 X49.245 Y38.125 E2.9798
G1 X49.245 Y38.741 E2.9982
G1 X40.755 Y33.839 E3.2917
G1 X40.755 Y34.455 E3.3101
G1 X49.245 Y39.356 E3.6036
G1 X49.245 Y39.972 E3.6220
G1 X40.755 Y35.071 E3.9155
G1 X40.755 Y35.686 E3.9339
G1 X49.245 Y40.588 E4.2274
G1 X49.245 Y41.204 E4.2458
G1 X40.755 Y36.302 E4.5393
G1 X40.755 Y36.918 E4.5577
G1 X49.030 Y41.696 E4.8437
G1 X48.699 Y42.121 E4.8599
G1 X40.755 Y37.534 E5.1345
G1 X40.755 Y38.150 E5.1529
G1 X48.373 Y42.548 E5.4162
G1 X48.097 Y43.005 E5.4322
G1 X40.755 Y38.766 E5.6859
G1 X40.755 Y39.382 E5.7044
G1 X47.822 Y43.462 E5.9487
G1 X47.574 Y43.873 E5.9630
G1 X47.553 Y43.922 E5.9646
G1 X40.755 Y39.997 E6.1996
G1 X40.755 Y40.613 E6.2180
G1 X47.333 Y44.411 E6.4454
G1 X47.114 Y44.900 E6.4614
G1 X40.755 Y41.229 E6.6812
G1 X40.755 Y41.421 E6.6870
G1 X41.357 Y42.192 E6.7163
G1 X46.902 Y45.394 E6.9079
G1 X46.740 Y45.916 E6.9243
G1 X42.012 Y43.186 E7.0877
G1 X42.426 Y43.873 E7.1117
G1 X42.527 Y44.100 E7.1191
G1 X46.577 Y46.438 E7.2591
G1 X46.451 Y46.846 E7.2719
G1 X46.429 Y46.968 E7.2756
G1 X42.900 Y44.931 E7.3976
G1 X43.077 Y45.326 E7.4105
G1 X43.199 Y45.719 E7.4229
G1 X46.327 Y47.525 E7.5310
G1 X46.225 Y48.082 E7.5479
G1 X43.432 Y46.470 E7.6445
```

```
G1 X43.549 Y46.846 E7.6562
G1 X43.612 Y47.189 E7.6667
G1 X46.150 Y48.655 E7.7544
G1 X46.114 Y49.250 E7.7723
G1 X43.738 Y47.878 E7.8544
G1 X43.835 Y48.411 E7.8707
G1 X43.844 Y48.555 E7.8750
G1 X46.078 Y49.845 E7.9522
G1 X46.070 Y49.984 E7.9564
G1 X46.070 Y50.456 E7.9705
G1 X43.882 Y49.193 E8.0461
G1 X43.921 Y49.831 E8.0653
G1 X46.070 Y51.072 E8.1396
G1 X46.070 Y51.688 E8.1580
G1 X43.930 Y50.452 E8.2320
G1 X43.930 Y51.068 E8.2504
G1 X46.070 Y52.304 E8.3244
G1 X46.070 Y52.919 E8.3428
G1 X43.930 Y51.684 E8.4168
G1 X43.930 Y52.300 E8.4352
G1 X46.070 Y53.535 E8.5092
G1 X46.070 Y54.151 E8.5276
G1 X43.930 Y52.916 E8.6016
G1 X43.930 Y53.531 E8.6200
G1 X46.070 Y54.767 E8.6940
G1 X46.070 Y55.383 E8.7124
G1 X43.930 Y54.147 E8.7864
G1 X43.930 Y54.763 E8.8048
G1 X46.070 Y55.999 E8.8788
G1 X46.070 Y56.614 E8.8972
G1 X43.930 Y55.379 E8.9712
G1 X43.930 Y55.995 E8.9896
G1 X46.070 Y57.230 E9.0636
G1 X46.070 Y57.846 E9.0820
G1 X43.930 Y56.611 E9.1560
G1 X43.930 Y57.226 E9.1744
G1 X46.070 Y58.462 E9.2484
G1 X46.070 Y59.078 E9.2668
G1 X43.930 Y57.842 E9.3408
G1 X43.930 Y58.458 E9.3592
G1 X46.079 Y59.699 E9.4335
G1 X46.118 Y60.337 E9.4527
G1 X43.930 Y59.074 E9.5283
G1 X43.930 Y59.546 E9.5424
G1 X43.922 Y59.685 E9.5466
G1 X46.156 Y60.975 E9.6238
G1 X46.165 Y61.119 E9.6281
G1 X46.262 Y61.652 E9.6444
G1 X43.886 Y60.280 E9.7265
G1 X43.850 Y60.875 E9.7443
G1 X46.388 Y62.341 E9.8321
G1 X46.451 Y62.684 E9.8425
G1 X46.568 Y63.060 E9.8543
G1 X43.775 Y61.448 E9.9508
```

```
G1 X43.673 Y62.005 E9.9678
G1 X46.801 Y63.811 E10.0759
G1 X46.923 Y64.204 E10.0882
G1 X47.100 Y64.599 E10.1012
G1 X43.571 Y62.562 E10.2232
G1 X43.549 Y62.684 E10.2269
G1 X43.423 Y63.092 E10.2397
G1 X47.473 Y65.430 E10.3797
G1 X47.574 Y65.657 E10.3871
G1 X47.988 Y66.344 E10.4111
G1 X43.260 Y63.614 E10.5745
G1 X43.098 Y64.136 E10.5909
G1 X48.643 Y67.338 E10.7825
G1 X49.245 Y68.109 E10.8118
G1 X49.245 Y68.301 E10.8176
G1 X42.886 Y64.630 E11.0373
G1 X42.667 Y65.119 E11.0534
G1 X49.245 Y68.917 E11.2808
G1 X49.245 Y69.533 E11.2992
G1 X42.447 Y65.608 E11.5342
G1 X42.426 Y65.657 E11.5357
G1 X42.178 Y66.068 E11.5501
G1 X49.245 Y70.149 E11.7944
G1 X49.245 Y70.764 E11.8128
G1 X41.903 Y66.525 E12.0666
G1 X41.627 Y66.982 E12.0826
G1 X49.245 Y71.380 E12.3459
G1 X49.245 Y71.996 E12.3643
G1 X41.301 Y67.409 E12.6389
G1 X40.970 Y67.834 E12.6550
G1 X49.245 Y72.612 E12.9411
G1 X49.245 Y73.228 E12.9595
G1 X40.755 Y68.326 E13.2530
G1 X40.755 Y68.942 E13.2714
G1 X49.245 Y73.844 E13.5649
G1 X49.245 Y74.459 E13.5833
G1 X40.755 Y69.558 E13.8768
G1 X40.755 Y70.174 E13.8952
G1 X49.245 Y75.075 E14.1887
G1 X49.245 Y75.691 E14.2071
G1 X40.755 Y70.789 E14.5005
G1 X40.755 Y71.405 E14.5190
G1 X49.245 Y76.307 E14.8124
G1 X49.245 Y76.923 E14.8309
G1 X40.755 Y72.021 E15.1243
G1 X40.755 Y72.637 E15.1428
G1 X49.245 Y77.539 E15.4362
G1 X49.245 Y78.154 E15.4547
G1 X40.755 Y73.253 E15.7481
G1 X40.755 Y73.869 E15.7665
G1 X49.245 Y78.770 E16.0600
G1 X49.245 Y79.245 E16.0742
G1 X49.001 Y79.245 E16.0815
G1 X40.755 Y74.484 E16.3665
```

```
G1 X40.755 Y75.100 E16.3850
G1 X47.934 Y79.245 E16.6331
G1 X46.867 Y79.245 E16.6650
G1 X40.755 Y75.716 E16.8763
G1 X40.755 Y76.332 E16.8947
G1 X45.801 Y79.245 E17.0691
G1 X44.734 Y79.245 E17.1011
G1 X40.755 Y76.948 E17.2386
G1 X40.755 Y77.564 E17.2570
G1 X43.667 Y79.245 E17.3577
G1 X42.601 Y79.245 E17.3896
G1 X40.755 Y78.179 E17.4534
G1 X40.755 Y78.795 E17.4719
G1 X41.534 Y79.245 E17.4988
G92 E0
G1 E-1.0000 F1800
; layer 10, Z = 2
; outer perimeter
G1 X40.435 Y79.565 F4800
G1 Z2.000 F1000
G1 E0.0000 F1800
G92 E0
G1 X40.435 Y67.999 E0.3462 F300
G1 X41.340 Y66.838 E0.3903
G1 X42.142 Y65.508 E0.4368
G1 X42.777 Y64.091 E0.4833
G1 X43.238 Y62.608 E0.5297
G1 X43.517 Y61.080 E0.5762
G1 X43.610 Y59.536 E0.6225
G1 X43.610 Y49.994 E0.9082
G1 X43.517 Y48.450 E0.9545
G1 X43.238 Y46.922 E1.0010
G1 X42.777 Y45.439 E1.0475
G1 X42.142 Y44.022 E1.0939
G1 X41.340 Y42.692 E1.1404
G1 X40.435 Y41.531 E1.1845
G1 X40.435 Y29.965 E1.5307
G1 X49.565 Y29.965 E1.8040
G1 X49.565 Y41.531 E2.1502
G1 X48.660 Y42.692 E2.1943
G1 X47.858 Y44.022 E2.2408
G1 X47.223 Y45.439 E2.2873
G1 X46.762 Y46.922 E2.3338
G1 X46.483 Y48.450 E2.3802
G1 X46.390 Y49.994 E2.4265
G1 X46.390 Y59.536 E2.7122
G1 X46.483 Y61.080 E2.7585
G1 X46.762 Y62.608 E2.8050
G1 X47.223 Y64.091 E2.8515
G1 X47.858 Y65.508 E2.8979
G1 X48.659 Y66.838 E2.9444
G1 X49.565 Y67.999 E2.9885
G1 X49.565 Y79.565 E3.3347
G1 X40.435 Y79.565 E3.6080
```

```
; infill
G1 X49.245 Y78.795 F4800
G92 E0
G1 X48.466 Y79.245 E0.0269 F600
G1 X47.399 Y79.245 E0.0589
G1 X49.245 Y78.179 E0.1226
G1 X49.245 Y77.564 E0.1411
G1 X46.333 Y79.245 E0.2417
G1 X45.266 Y79.245 E0.2737
G1 X49.245 Y76.948 E0.4112
G1 X49.245 Y76.332 E0.4296
G1 X44.199 Y79.245 E0.6040
G1 X43.133 Y79.245 E0.6360
G1 X49.245 Y75.716 E0.8472
G1 X49.245 Y75.100 E0.8657
G1 X42.066 Y79.245 E1.1138
G1 X40.999 Y79.245 E1.1457
G1 X49.245 Y74.484 E1.4307
G1 X49.245 Y73.869 E1.4492
G1 X40.755 Y78.770 E1.7426
G1 X40.755 Y78.154 E1.7611
G1 X49.245 Y73.253 E2.0545
G1 X49.245 Y72.637 E2.0730
G1 X40.755 Y77.539 E2.3664
G1 X40.755 Y76.923 E2.3848
G1 X49.245 Y72.021 E2.6783
G1 X49.245 Y71.405 E2.6967
G1 X40.755 Y76.307 E2.9902
G1 X40.755 Y75.691 E3.0086
G1 X49.245 Y70.789 E3.3021
G1 X49.245 Y70.174 E3.3205
G1 X40.755 Y75.075 E3.6140
G1 X40.755 Y74.459 E3.6324
G1 X49.245 Y69.558 E3.9259
G1 X49.245 Y68.942 E3.9443
G1 X40.755 Y73.844 E4.2378
G1 X40.755 Y73.228 E4.2562
G1 X49.245 Y68.326 E4.5496
G1 X49.245 Y68.109 E4.5561
G1 X49.030 Y67.834 E4.5666
G1 X40.755 Y72.612 E4.8526
G1 X40.755 Y71.996 E4.8711
G1 X48.699 Y67.409 E5.1457
G1 X48.395 Y67.020 E5.1604
G1 X48.373 Y66.982 E5.1618
G1 X40.755 Y71.380 E5.4251
G1 X40.755 Y70.764 E5.4435
G1 X48.097 Y66.525 E5.6973
G1 X47.822 Y66.068 E5.7133
G1 X40.755 Y70.149 E5.9575
G1 X40.755 Y69.533 E5.9760
G1 X47.553 Y65.608 E6.2109
G1 X47.333 Y65.119 E6.2270
G1 X40.755 Y68.917 E6.4543
```

```
G1 X40.755 Y68.301 E6.4728
G1 X47.114 Y64.630 E6.6926
G1 X46.923 Y64.204 E6.7065
G1 X46.902 Y64.136 E6.7087
G1 X41.357 Y67.338 E6.9003
G1 X41.605 Y67.020 E6.9124
G1 X42.012 Y66.344 E6.9360
G1 X46.740 Y63.614 E7.0994
G1 X46.577 Y63.092 E7.1158
G1 X42.527 Y65.430 E7.2558
G1 X42.900 Y64.599 E7.2831
G1 X46.429 Y62.562 E7.4050
G1 X46.327 Y62.005 E7.4220
G1 X43.199 Y63.811 E7.5301
G1 X43.432 Y63.060 E7.5536
G1 X46.225 Y61.448 E7.6501
G1 X46.165 Y61.119 E7.6601
G1 X46.150 Y60.875 E7.6674
G1 X43.612 Y62.341 E7.7552
G1 X43.738 Y61.652 E7.7761
G1 X46.114 Y60.280 E7.8583
G1 X46.078 Y59.685 E7.8761
G1 X43.844 Y60.975 E7.9534
G1 X43.882 Y60.337 E7.9725
G1 X46.070 Y59.074 E8.0481
G1 X46.070 Y58.458 E8.0665
G1 X43.921 Y59.699 E8.1408
G1 X43.930 Y59.546 E8.1454
G1 X43.930 Y59.078 E8.1594
G1 X46.070 Y57.842 E8.2334
G1 X46.070 Y57.226 E8.2518
G1 X43.930 Y58.462 E8.3258
G1 X43.930 Y57.846 E8.3442
G1 X46.070 Y56.611 E8.4182
G1 X46.070 Y55.995 E8.4367
G1 X43.930 Y57.230 E8.5106
G1 X43.930 Y56.614 E8.5291
G1 X46.070 Y55.379 E8.6030
G1 X46.070 Y54.763 E8.6215
G1 X43.930 Y55.999 E8.6954
G1 X43.930 Y55.383 E8.7139
G1 X46.070 Y54.147 E8.7878
G1 X46.070 Y53.531 E8.8063
G1 X43.930 Y54.767 E8.8802
G1 X43.930 Y54.151 E8.8987
G1 X46.070 Y52.916 E8.9726
G1 X46.070 Y52.300 E8.9911
G1 X43.930 Y53.535 E9.0650
G1 X43.930 Y52.919 E9.0835
G1 X46.070 Y51.684 E9.1574
G1 X46.070 Y51.068 E9.1759
G1 X43.930 Y52.304 E9.2499
G1 X43.930 Y51.688 E9.2683
G1 X46.070 Y50.452 E9.3423
```

```
G1 X46.070 Y49.984 E9.3563
G1 X46.079 Y49.831 E9.3609
G1 X43.930 Y51.072 E9.4351
G1 X43.930 Y50.456 E9.4536
G1 X46.118 Y49.193 E9.5292
G1 X46.156 Y48.555 E9.5483
G1 X43.922 Y49.845 E9.6256
G1 X43.886 Y49.250 E9.6434
G1 X46.262 Y47.878 E9.7256
G1 X46.388 Y47.189 E9.7465
G1 X43.850 Y48.655 E9.8343
G1 X43.835 Y48.411 E9.8416
G1 X43.775 Y48.082 E9.8516
G1 X46.568 Y46.470 E9.9481
G1 X46.801 Y45.720 E9.9716
G1 X43.673 Y47.525 E10.0797
G1 X43.571 Y46.968 E10.0967
G1 X47.100 Y44.931 E10.2186
G1 X47.473 Y44.100 E10.2459
G1 X43.423 Y46.438 E10.3859
G1 X43.260 Y45.916 E10.4023
G1 X47.988 Y43.186 E10.5657
G1 X48.395 Y42.510 E10.5893
G1 X48.643 Y42.192 E10.6014
G1 X43.098 Y45.394 E10.7930
G1 X43.077 Y45.326 E10.7952
G1 X42.886 Y44.900 E10.8091
G1 X49.245 Y41.229 E11.0289
G1 X49.245 Y40.613 E11.0473
G1 X42.667 Y44.411 E11.2747
G1 X42.447 Y43.922 E11.2908
G1 X49.245 Y39.997 E11.5257
G1 X49.245 Y39.382 E11.5441
G1 X42.178 Y43.462 E11.7884
G1 X41.903 Y43.005 E11.8044
G1 X49.245 Y38.766 E12.0582
G1 X49.245 Y38.150 E12.0766
G1 X41.627 Y42.548 E12.3399
G1 X41.605 Y42.510 E12.3412
G1 X41.301 Y42.121 E12.3560
G1 X49.245 Y37.534 E12.6306
G1 X49.245 Y36.918 E12.6490
G1 X40.970 Y41.696 E12.9351
G1 X40.755 Y41.421 E12.9455
G1 X40.755 Y41.204 E12.9520
G1 X49.245 Y36.302 E13.2455
G1 X49.245 Y35.686 E13.2639
G1 X40.755 Y40.588 E13.5574
G1 X40.755 Y39.972 E13.5758
G1 X49.245 Y35.071 E13.8693
G1 X49.245 Y34.455 E13.8877
G1 X40.755 Y39.357 E14.1812
G1 X40.755 Y38.741 E14.1996
G1 X49.245 Y33.839 E14.4930
```

```
G1 X49.245 Y33.223 E14.5115
G1 X40.755 Y38.125 E14.8049
G1 X40.755 Y37.509 E14.8234
G1 X49.245 Y32.607 E15.1168
G1 X49.245 Y31.991 E15.1353
G1 X40.755 Y36.893 E15.4287
G1 X40.755 Y36.277 E15.4472
G1 X49.245 Y31.376 E15.7406
G1 X49.245 Y30.760 E15.7590
G1 X40.755 Y35.661 E16.0525
G1 X40.755 Y35.046 E16.0709
G1 X49.001 Y30.285 E16.3559
G1 X47.934 Y30.285 E16.3879
G1 X40.755 Y34.430 E16.6360
G1 X40.755 Y33.814 E16.6545
G1 X46.867 Y30.285 E16.8657
G1 X45.801 Y30.285 E16.8977
G1 X40.755 Y33.198 E17.0721
G1 X40.755 Y32.582 E17.0905
G1 X44.734 Y30.285 E17.2280
G1 X43.667 Y30.285 E17.2600
G1 X40.755 Y31.966 E17.3606
G1 X40.755 Y31.351 E17.3791
G1 X42.601 Y30.285 E17.4429
G1 X41.534 Y30.285 E17.4748
G1 X40.755 Y30.735 E17.5017
G92 E0
G1 E-1.0000 F1800
; layer end
M104 S0 ; turn off extruder
M140 S0 ; turn off bed
M84 ; disable motors
; Build Summary
;   Build time: 0 hours 13 minutes
;   Filament length: 211.1 mm (0.21 m)
;   Plastic volume: 507.71 mm^3 (0.51 cc)
;   Plastic weight: 0.63 g (0.00 lb)
;   Material cost: 0.03
```